SINGLE-CELL FUNCTIONAL PROFILING OF LYMPHOCYTES FOR CANCER IMMUNOTHERAPY

A Dissertation

Presented to

the Faculty of the Department of Chemical and Biomolecular Engineering

University of Houston

In Partial Fulfillment

of the Requirements for the Degree

Doctor of Philosophy

in Chemical and Biomolecular Engineering

by

Xingyue An

August 2019

SINGLE-CELL FUNCTIONAL PROFILING OF LYMPHOCYTES FOR

CANCER IMMUNOTHERAPY

_____

Xingyue An

Approved:

_____

Chair of the Committee
Navin Varadarajan, Associate Professor,
Chemical and Biomolecular Engineering

Committee members:

_____

Patrick C. Cirino, Associate Professor,
Chemical and Biomolecular Engineering
Biology and Biochemistry

_____

Jeffrey D. Rimer, Professor,
Chemical and Biomolecular Engineering

_____

Weiyi Peng, Assistant Professor,
Biology and Biochemistry

_____

Harjeet Singh, Instructor,
Pediatrics
The University of Texas
MD Anderson Cancer Center

_____

Suresh K. Khator, Associate Dean,
Cullen College of Engineering

_____

Michael P. Harold, Professor and
Chair of Dept in Chemical and
Biomolecular Engineering

ACKNOWLEDGMENTS

- Dr. Navin Varadarajan for invaluable and continuous guidance through each stage of doctoral studies and related research, and extensive support of personal and professional development.
- Dr. Patrick C. Cirino, Dr. Jeffrey D. Rimer, Dr. Weiyi Peng and Dr. Harjeet Singh for serving as doctoral thesis defense committee members for their insightful comments and inspirations.
- Dr. Gila E. Stein for serving as a qualifier committee member.
- Dr. Naval G. Daver for collaboration and providing the clinical samples for experiments.
- Dr. Badrinath Roysam and Dr. Yanbin Lu for the collaboration and consultation on imaging process and data analysis.
- Dr. Patrick C. Cirino and Dr. Richard C. Willson and their labs for use and consultation of the lab equipment.
- Dr. Gabrielle Romain, Dr. Ankit Mahendra, Dr. Melisa Martinez-Paniagua, Dr. Vandana Kaul, Dr. Irfan Bandy, Dr. Ankita Leekha, Dr. Ivan Liadi, Dr. Balakrishnan Ramesh, Dr. Shaza Abnouf, Dr. Jay R T. Adolacion, Fatemeh Sadeghi, Mohsen Fathi, Conrad Hom, Ali Rezvan, Arash Saeedi, Rasindu Rajanayake, and Monish Kumar for assistance of experiment, stimulating discussion, and helpful feedback.
- Dr. Yufeng Shen and Dr. Bryan G. Alamani from Dr. Rimer's lab for assisting with the scanning electron microscopy.

- Staff in the Department of Chemical & Biomolecular Engineering for their kind assistance.
- Finally, yet importantly, I would thank my family, friends, and relatives who have supported me in pursuing this degree and never-ending inspiration.

SINGLE-CELL FUNCTIONAL PROFILING OF LYMPHOCYTES FOR CANCER IMMUNOTHERAPY

An Abstract

of a

Dissertation

Presented to

the Faculty of the Department of Chemical and Biomolecular Engineering

University of Houston

In Partial Fulfillment

of the Requirements for the Degree

Doctor of Philosophy

in Chemical and Biomolecular Engineering

by

Xingyue An

August 2019

ABSTRACT

Immunotherapy by harnessing patients' the immune system has changed the landscape of cancer therapeutics and shown promising and remarkable clinical responses. However, not all the patients would be beneficial from the treatment. Lymphocytes are a significant target in anti-tumor immunotherapy, and the functional assessment of lymphocytes will provide insights on their functional biology and will provide a direct path to the improvement of the treatment efficacy.

In the first part of this dissertation, we developed and implemented a methodology based on Timelapse Imaging Microscopy in Nanowell Grids (TIMING) platform that integrates phenotypic profiling and dynamic cytokine secretion with single-cell resolution. Analysis of hundreds of human peripheral nature killer cells (NK cells) suggested that $CD56^{dim}CD16^{+}$ NK cells are immediate interferon gamma (IFN-γ) secretor upon activation by phorbol 12-myristate 13-acetate (PMA) and ionomycin (< 3 h), and no evidence of cooperation between NK cells to synergistic activation or faster IFN-γ secretion. These results establish our technology as an investigational tool for cellular phenotyping and real-time protein secretion of individual cells in a high-throughput manner and demonstrate that the conventional phenotypic based functional annotation of NK cells might be overly simplistic.

In the second part of this dissertation, we performed whole transcriptomic profiling on T cells from acute myeloid leukemia patients (responders and non-responders) who were treated with combination therapy of a hypomethylating agent (5-azacytidine) and an immune checkpoint inhibitor (nivolumab, programmed cell death protein 1/PD-1 inhibitor). Sixty-four patient-derived T cells from peripheral blood or bone marrow (site of disease),

which were collected before the initiation of the therapy (baseline, T0) and after the first round of treatment (end of cycle one, EC1), were evaluated. Our results demonstrate (1) treatment-induced gene expression changes on circulating CD8 T cells, and (2) the ratios of effector and exhausted CD8 T cells has the potential to serve as a biomarker for patient stratification.

TABLE OF CONTENTS

LIST OF FIGURES

LIST OF TABLES

ABBREVIATIONS AND DEFINITIONS

ACT: adoptive cell transfer

AFU: arbitrary fluorescence units

AML: acute myeloid leukemia

APC: antigen-presenting cell

AZA: 5-azacitidine

BM: bone marrow

CAR: chimeric antigen receptor

CD: cluster of differentiation

CTLA-4: cytotoxic T-lymphocyte-associated protein 4

DEG: differentially expressed genes

ELISPOT: enzyme-linked immune absorbent spot

FBS: fetal bovine serum

FC: flow cytometry

FDA: enzyme-linked immune absorbent spot

FDR: false discovery rate

FI: fluorescent intensity

HLA: human leukocyte antigen

HMA: hypomethylating agents

ICAM-1: intercellular adhesion molecule 1

ICI: immune checkpoint inhibitors

IFN-γ: interferon gamma

LAG-3: intercellular adhesion molecule 1

LoD: Limit of detection

MC: Mass cytometry

MFI: Mean Fluorescence Intensity

MHC: major histocompatibility complex

NCR: natural cytotoxicity receptors

NK cells: natural killer cells

NSCLC: non-small cell lung cancer

PBMC: peripheral blood mononuclear cell

PBS: phosphate-buffered saline

PCA: principal component analysis

PD-1: programmed cell death protein 1

PD-L1: programmed death-ligand 1

PD-L2: programmed death-ligand 2

PDMS: polydimethylsiloxane

PLL-g-PEG: Poly-L-Lysine grafted with polyethylene glycol

PMA: phorbol 12-myristate 13-acetate

R10: RPMI-1640 media supplemented with 10% fetal bovine serum/FBS

RNA-seq: RNA-sequencing

SCBC: single-cell barcode chip

scRNA-seq: single-cell RNA-seq

scWB: single-cell Western Blot

SEM: scanning electron microscope, or the standard error of the mean

SHP-2: Src homology 2 domain-containing tyrosine phosphatase 2

T_{CM}: central memory T-cell

TCR: T-cell receptor

T_{EFF}: effector T-cell

T_{ex}: exhausted T-cell

T_H1: type 1 T help cell

TIL: tumor infiltrating lymphocytes

TIM-3: T cell immunoglobulin mucin-3

TIMING: Timelapse Imaging Microscopy in Nanowell Grids

$T_{Naïve}$: Naïve T-cell

TNF: tumor necrosis factor

Treg: regulatory T-cell

$t_{secrete}$: characteristic time of secretion of cytokine

Chapter 1

Single-cell technologies for profiling T cells to enable monitoring of immunotherapies

Note: This is a reformatted version of a paper published at Current Opinion in Chemical Engineering

An, Xingyue, and Navin Varadarajan. “Single-Cell Technologies for Profiling T Cells to Enable Monitoring of Immunotherapies.” *Current Opinion in Chemical Engineering* 19 (2018): 142–52.

1.1. Introduction

Immunotherapy has revolutionized the treatment of cancer and relies on utilizing the patients’ immune system and its anti-cancer properties for therapeutic benefit (Khalil et al., 2016; Lim,Wendell A. and June, 2017). This approach is fundamentally different from chemotherapy and even targeted therapy, both of which depend on the ability of the drug to kill the tumor cell directly (Zitvogel et al., 2013). Immunotherapeutic treatment is based on the recognition that there is a failure of the host immune system to control the tumor adequately, and that the goal of treatment is to facilitate resetting the dysregulated balance to enable eradication of the tumors via the host immune system (Shore, 2015; Tsai and Hsu, 2017; Zarour, 2016). In other words, the treatment does not work to kill the tumor cells directly but instead tries to reinvigorate the immune system to get rid of the tumors. One of the primary objectives of this approach, akin to vaccination, is the ability to

establish immunological memory of the tumor, thereby enabling the immune system to seek and destroy metastases anywhere in the body and enable long-term control (Sharma et al., 2017).

Although utilizing the immune system for therapeutic benefit has been around for quite some time, and proteins such as cytokines (e.g., interleukin-2) (Jiang, Zhou, and Ren, 2016; Rosenberg, 2014) and a suite of monoclonal antibodies (such as anti-CD20, anti-EGFR) (Lim,Sean H. et al., 2010; Nakai, Hung, and Yamaguchi, 2016) have been used clinically over the last two decades, two newer approaches to treatment — the inhibitors of checkpoint molecules (Topalian, Drake, and Pardoll, 2015), and the adoptive transfer of genetically modified T cells (Restifo, Dudley, and Rosenberg, 2012), have made substantial advances in the clinic. After decades of frustration with the 5-year survival rates of chemotherapy, these newer forms of immunotherapeutic treatment have altered the treatment landscape and have facilitated durable and lasting remissions in subsets of patients (Sharma and Allison, 2015b). Both classes of treatment, immune checkpoint inhibitors (ICI) and adoptive cell transfer (ACT), critically rely on the functionality of a particular subset of lymphocytes within the immune system — the T cells. ICI aims to reinvigorate T cells and activate them to attack tumor cells and has shown clinical efficacy in various tumors, albeit in only 20% of patients (Hodi et al., 2010; Weber et al., 2015). ACT, on the other hand, delivers *ex vivo* expanded (and/or genetically modified) T cells as the therapeutic and has shown complete responses in leukemias (response rate can be more than 70%) (Maude et al., 2014; Kalos et al., 2011; Turtle et al., 2016; Brentjens et al., 2013).

The introduction of immunotherapeutic molecules as drugs has facilitated new challenges and opportunities for engineers. While the potency of small-molecule-based

therapies can be mapped to their mechanism of action (binding/inhibiting appropriate proteins) facilitating tumor cell killing (Wu, Nielsen, and Clausen, 2015; Zhang et al., 2012), understanding the efficacy of ICI or ACT is a significant challenge since the mechanism of action is neither simple nor wholly defined (Topalian, Drake, and Pardoll, 2015; Sharma and Allison, 2015a; Wei,Spencer C. et al., 2017; Yu,Shengnan et al., 2017). The origin of this challenge can be mapped to our inability, to define comprehensively, all of the different T-cell functionalities that can contribute to their efficacy. T cells are essential players in the adaptive immune systems and can recognize cognate antigen through their T cell receptor (TCR) (Kuang et al., 2017). T cells bearing TCR specific for foreign or non-native peptides displayed in the context of human leukocyte antigens (HLA) get activated and can undergo a process of programmed differentiation depending on the availability of other accessory molecules including cytokines within the activating environment. Unlike antibodies, the TCR itself does not undergo somatic hypermutation subsequently, and hence can be considered a barcode to identify populations of clonally related T cells (Qi et al., 2014; Gong et al., 2017; Tirosh et al., 2016). T cells are capable of many different functions, including cytotoxicity, cytokine secretion, proliferation, and migration, which are determined by multiple cues from intrinsic properties of T cells and its environmental factors. The relative importance of these functions in defining clinical benefit is only partially understood and confounded by the differentiation status of the T cell (naïve, stem-cell-like central memory, central memory, effector memory, and effector) (Restifo and Gattinoni, 2013; Ahmed et al., 2016), or by their functional status (polyfunctional, anergic, or exhausted). It is thus apparent that the availability of methods that can map all of these properties onto the same T cell will advance our understanding of

the efficacy of immunotherapeutic treatments. From the perspective of the ACT, the availability of precise definitions on the properties that need to be engineered into the T-cell infusion product will facilitate consistent biomanufacturing of therapeutic products (Maus and June, 2016). It is thus clear that immunotherapeutic treatments stand to benefit from single-cell technologies that can map the complexity of T cells. While the vast majority of advances in immunotherapeutic treatment have focused on oncology, the principles of modulating the immune system are likely to find broad applicability in other infectious diseases and autoimmunity, as well.

Single-cell technologies have attracted researchers' attention for several decades, and there is an increasing trend to develop more accurate and sensitive, higher-throughput, and automated single-cell characterization tools. These approaches allow the detection of details that cannot be revealed using traditional population-level assays (Proserpio and Mahata, 2016). Generally, these single-cell technologies are designed to capture cellular information from either the genome, transcriptome, or more recently, the proteome level (Heath, Ribas, and Mischel, 2016). While some assays like flow cytometry (FC) have been standardized and used even in clinical settings (Barlogie et al., 1983), some of the more recent single-cell technologies like mass cytometry (MC) (Spitzer and Nolan, 2016), and single-cell RNA sequencing (scRNA-seq) (Haque et al., 2017) have been recently commercialized. Despite this, however, the vast majority of tools are designed in the research setting, and recent advances have enabled the integration of approaches from different omic dimensions to be able to quantify cell features simultaneously (Bock, Farlik, and Sheffield, 2016).

In this review, we briefly highlight several types of emerging single-cell technologies, mainly focusing on technologies that monitor multiple features (function, transcripts, phenotype, *etc*.) in the context of T-cell characterization (**Table 1-1**). We believe that analyzing T cells at single-cell resolution will provide valuable insights on both experimental and clinical investigations, and has the potential to improve the clinical outcomes of T-cell based therapy. Furthermore, the development of multiplexed single-cell interrogations tools to explore the phenotypical and functional correlations within heterogeneous T cells populations can reveal the underlying biological networks, eventually paving the way for both a better understanding of T cells and delivering surrogate T-cell biomarkers for immunotherapy.

Table 1-1 Summary of versatile single-cell technologies which allowing multi-feature characterization

	Technology	Throughput	Highlight	Reference
FC/ Microscopy & protein	scWB	Up to thousands of single cells	Combination of microwells and PAGE gel for protein detection based on mass or/and pI Can detect up to 11 proteins on the same cells by antibody stripping/re-probing Compatible with FACS sorting or cell imaging as pre-characterization Re-probing archival sample is possible	(Duncombe et al. 2016; Kang et al. 2014, 2016; J. J. Kim, Sinkala, and Herr 2017; Tentori, Yamauchi, and Herr 2016; Hughes et al. 2014)
Protein &mRNA	FC	Millions	Fusion of Flow-FISH & ICS Quantification of mRNA + protein of three cytokines simultaneously (IFN-γ, IL-2, and TNF-α)	(Nicolet, Guislain, and Wolkers, 2016)

Table 1-1 Summary of versatile single-cell technologies which allowing multi-feature characterization (continued)

	Technology	Throughput	Highlight	Reference
	MC	Millions	PLAYR Relies on MC (mass tag) or FC (fluorophore) for protein (antibody) and transcript (oligonucleotides) read-out The multiplexing capacity is determined by the available tags (~40 MC)	(Frei et al., 2016)
	Single-cell PCR	96 (using Fluidigm™ C1)	Leverages the DNA polymerase activity of reverse transcriptase to simultaneously perform proximity extension assays and complementary DNA synthesis in the same reaction Compatible with scRNA-seq platform Demonstrated detection of 96 RNA + 38 proteins	(Genshaft et al., 2016)
scRNA-seq & TCR-seq	TraCeR, scTCRseq, VDJPuzzle, TRAPeS	Depends on the throughput of scRNA-seq	Extract TCR information from scRNA-seq results Provide both transcriptional profiling and clonality of single T-cell	(Stubbington et al., 2016; Redmond, Poran, and Elemento, 2016; Eltahla et al., 2016; Afik et al., 2017)
	scRNA-seq	Thousands of single cells	CITE-seq (10 surface proteins), REAP-seq (82 proteins) Oligonucleotide with poly A tail as unique antibody barcode Use reverse transcriptase as DNA polymerase to extend antibody barcode and reverse transcription of mRNA simultaneously Compatible with current scRNA-seq platform	(Peterson et al., 2017; Stoeckius et al., 2017)
	Abseq	>10,000 cells	Detection protein via DNA-labeled antibody to increase multiplexing capacity Each antibody also has UMI sequence for PCR-bias correction Compatible with current scRNA-seq platform Theoretical limit of detected protein is determined by the sequencing depth and availability of antibody	(Shahi et al., 2017)
	Seq-Well	~15,000 cells	Co-capture cells and transcripts-capture beads within individual microwells On-chip lysis, reverse transcription in bulk Compatible with on-chip imaging cytometry Transcriptomic profiling is done by scRNA-seq	(Gierahn et al., 2017)

Table 1-1 Summary of versatile single-cell technologies which allowing multi-feature characterization (continued)

	Technology	Throughput	Highlight	Reference
Integration: cell-cell interaction, protein, *etc*	TIMING	20,000 cells	Co-culture lymphocyte and target cell on the same individual microwell Time-lapse microscopy live cell imaging Integrated with real-time cytokine secretion and cell retrieval for gene expression profiling	(Romain et al., 2014; Haymaker et al., 2015; Liadi et al., 2015; Sendra et al., 2013)
	Droplet	~1,000 events	Similar to TIMING Co-encapsulate two types of cells within a droplet Droplet docking into individual microwells	(Martinelli et al., 2009)
	SCBC	Up to several thousands of cells	Single cells or cell pairs are isolated in individual microchambers Cell-cell interaction can be investigated Detection antibody-coated surface is detachable for analysis Up to 45-plex protein detection including secreted proteins	(Kravchenko-Balasha et al., 2016; Wei et al., 2016; Zhou et al., 2017)
	BOBarray	Several thousands of cells	Similar to SCBC, but use antibody-coated beads as a protein sensor Miniaturized device achieved by a combination of bead size and fluorophore combination: 4 bead size x 3 color =12-plex	(Yang et al., 2016)

1.2. Protein detection from single-cell

1.2.1. Single-cell western blotting (scWB)

Similar to the standard western blotting methodology, this approach includes protein separation based on both the affinity between the antibody and the target protein, and the relative size of protein thus minimizing concerns about antibody-cross reactivity (**Figure 1-1**, adapted from reference (Duncombe et al., 2016). Closed-up false-color fluorescent images represent part of arrays (over 400 lanes)). By the application of open microwells on a polyacrylamide gel-coated glass slide, single cells were deposited into individual wells, subsequently lysed, subjected to gel electrophoresis, immobilized by UV-light, and the protein detected by immune-probing. By repetition of antibody-stripping and

re-probing, it could detect up to eleven different proteins across thousands of single cells in the same experiment (Duncombe et al., 2016; Kang et al., 2014, 2016). By utilizing a combination of lab-on-a-disk cell device and the scWB analysis, it was possible to quantify protein from less than one hundred cells (Kim, Sinkala, and Herr, 2017). The same group further developed an approach termed single-cell isoelectric focusing (scIEF) using isoelectric point (pI) difference to separate protein isoforms (Tentori, Yamauchi, and Herr, 2016). In this work, they reported ten cells were analyzed in the same chip as a proof-of-concept; however, the throughput can theoretically be scaled up. ScWB can be combined with flow sorting (Hughes et al., 2014) or on-chip cell phenotyping (Kang et al., 2014). This approach can be beneficial for direct measurement of proteins in a single cell, especially when the number of available cells is limited, allowing the validation of known biomarkers in a multiplexed fashion while maintaining single-cell resolution.

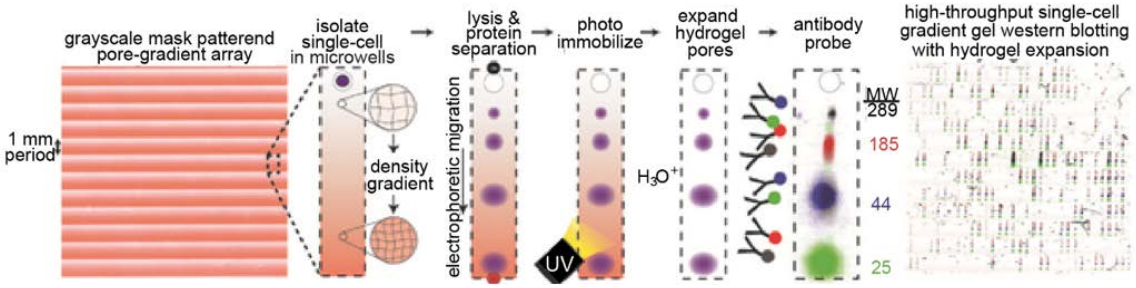

Figure 1-1 Workflow of scWB

1.3. Integration of protein detection and transcriptional profiling of single cell

1.3.1. Flow cytometry

FC has been widely adopted for several decades to characterize the phenotype of cells and the intracellular molecules across millions of cells. It can detect up to around 17 parameters simultaneously, which is determined by the availability of fluorescent dyes (Perfetto, Chattopadhyay, and Roederer, 2004). Recently, Nicolet et al. were able to

simultaneously profile the expression of primary human T-cell cytokines (IFN-g, IL-2, and TNF-a) at both the protein and mRNA transcript level via integration of fluorescence in situ hybridization (FISH) and flow cytometry-based platform (Nicolet, Guislain, and Wolkers, 2016). This work paved a road for finding the correlation between cytokine secretion and mRNA transcripts within the same single cell.

1.3.2. Mass cytometry

To improve the multiplexing capacity of cytometry, heavy-metal tagged antibodies are used in mass cytometry (MC). This strategy enables the quantification of more targets on a single cell simultaneously, including surface phenotypic marker characterization, intracellular protein detection, cytokine secretion, transcription factor expression, and mRNA transcripts expression (Wei et al., 2017; Bengsch et al., 2017; Chevrier et al., 2017; Frei et al., 2016; Huang et al., 2017; Lavin et al., 2017; Matos, Liu, and Ritz, 2017; Spitzer et al., 2017). Frei et al. developed a method called PLAYR (proximity ligation assay for RNA) and demonstrated that this approach was able to quantify multiplexed mRNA transcripts and protein via flow cytometry or mass cytometry simultaneously (Frei et al., 2016). The oligonucleotide labeled with fluorescence or metal tags were used to detect target transcripts. The authors validated this method by detection of 8 different mRNA transcripts and 18 proteins (cytokine + surface molecules) in LPS-stimulated PBMC for various stimulation times, and the results suggested the most LPS-responding cells were likely to be a $CD14^{+}$ phenotype. Frei and colleagues expected the theoretical upper limit in the number of detected targets could be as high as 40 if combined with MC. The disadvantage of MC is that unlike FC, it is sample destructive, and thus, it is not possible to sort single cells for downstream analyses like RNA-seq.

Both FC and MC are well-developed technologies and can directly detect proteins from millions of single cells but are restricted to providing snapshots since it is not possible to track the same cell longitudinally using these methods. Despite these disadvantages, however, FC and MC are robust knowledge-based methods to identify subsets of T cells directly from tumors and hence will play an essential role in tracking the efficacy of immunotherapies.

1.3.3. Single-cell PCR

Unlike the PLAYR method that utilized the mass tag or fluorescent tag to capture transcript or protein abundances, other studies relied on the usage of DNA as a label to detect proteins. Although initially the profiling of mRNA and protein was achieved by splitting the cell lysate to multiple parts and characterizing each of them separately (Bichsel et al., 2016; Darmanis et al., 2016), Genshaft et al. presented an approach that combined the detection of protein and mRNA from same mammalian cells in a single reaction chamber in a parallel manner (Genshaft et al., 2016). Modified proximity extension assays (PEA) method was used in this technology for protein detection. For each protein of interest, there were two different single-stranded oligonucleotides-labeled antibodies to detect the target protein. The 3' end of DNA labels of this antibody pair were complementary to each other; as a result, DNA labels would hybridize once both antibodies co-localized on the target protein. The extension of DNA label complex and reverse transcription of RNA from the same cell happened simultaneously by taking advantage of the DNA polymerase activity of the reverse transcriptase. qPCR (FluidigmTM C1 system) was used to quantify protein expression and RNA abundance. By applying this approach to study protein and mRNA abundances in the PMA-stimulated MCF7 cells, they found that the correlation of

mRNA and protein was variable among genes or time points: highly-expressed genes were more correlated with the corresponding protein expression in untreated cells, but after simulation the lowly-expressed genes with high cell-cell variance showed the most substantial correlation.

1.3.4. ScRNA-seq

ScRNA-seq, a rapidly-growing technology can provide unbiased, high-dimensional genome-wide transcriptomic profiling of individual cells, and has emerged as a robust method to facilitate the discovery of novel cellular status (Mahata et al., 2014), and provide biological insights (Tirosh et al., 2016; Kakaradov et al., 2017; Zheng et al., 2017). ScRNAseq has been extensively reviewed elsewhere, and we will only highlight combinations of scRNA-seq with other kinds of single-cell assays. Researchers have developed several algorithms to utilize scRNA-seq data to reconstitute T cell receptor information. One advantage of obtaining TCR information at the single-cell level is that the possibility to acquire the pairing detail of TCR chains (ab, gd). Computation approaches, such as TraCeR (Stubbington et al., 2016), scTCRseq (Redmond, Poran, and Elemento, 2016), VDJPuzzle (Eltahla et al., 2016), work quite well with transcriptomic profiling results obtained from full-length mRNA transcripts. More recently, the TRAPeS pipeline was reported to enable extraction of TCR sequence information from short-read (25–30 bp) sequencing data (Afik et al., 2017). Combining transcriptomic profiling and TCR profiling at single-cell resolution, the clonal expansion of exhausted or dysfunctional T cells was found in tumor sites, indicating the reinvigoration of T cell function may recover its anti-cancer functionality (Tirosh et al., 2016; Zheng et al., 2017). Owing to these emerging computational pipelines, developmental trajectories of diverse T cell population can be

deciphered, holding the promise of investigating the antigen-specific T cells functions in response to diseases, and also to identify the diversity of T-cell responses within the tumor microenvironment. Stoeckius et al. and Peterson et al. recently reported two closely related methods (CITE-seq and REAP-seq) for simultaneous detection of mRNA and protein (Peterson et al., 2017; Stoeckius et al., 2017) (**Figure 1-2**, adapted from reference (Peterson et al., 2017)). A droplet containing Ab-Barcodes (AbBCs) coated cells fuse to another discreet droplet which contains cell-barcode beads with primers. The cell is lysed once two droplets fuse, and polyadenylated mRNA and AbBC hybridize with poly(dT) primer, and the extension of AbBC and complementary synthesis of transcripts can be achieved by reverse transcriptase in the same reaction. AbBC sequences (~ 155 bp) and cDNA from mRNA (~> 500 bp) are separated based on the size difference, and protein and transcript libraries are constructed and sequenced. Both methods utilized a combination of unique oligonucleotide barcodes and poly (dA) sequence for indexing antibody (but using different linkers) thus enabling the detection of multiple proteins along with transcripts. Extension of DNA labels of antibodies and reverse transcription of mRNA transcripts could be achieved in the same reaction by taking advantage of the DNA polymerase function of reverse transcriptase. These two methods can be readily adapted to different high-throughput scRNA-seq platforms. Another similar technique that can be expanded to demonstrate the same capability is called Abseq (**Figure 1-3**, adapted from reference (Shahi et al., 2017)), which utilizes a combination of DNA-labeled antibody and droplet microfluidics (Shahi et al., 2017). Cells stained with DNA-conjugated antibodies are isolated in a droplet with unique cell barcoding information, and the linkage of antibody barcode and cell barcode is achieved via overextension PCR. The chimeric DNA products

from over 10,000 single cells can be pooled and sequenced in parallel. The single-cell protein information will be sorted by the cell barcoding. Unique molecular identifiers are utilized for PCR-bias correction. One disadvantage of all these approaches is that the information about the spatial distribution of proteins is lost. An orthogonal method, Seq-Well (**Figure 1-4,** adapted from reference (Gierahn et al., 2017)), takes advantage of arrays of microwells instead of droplets. The complex tissue is dissociated to single-cell suspension first, and then barcoded mRNA capture beads and cells are loaded onto microwell array by gravity. The device is sealed by a semipermeable membrane to allow lysis buffer change but confine mRNA within the well. Once the beads (contained poly(dT) primers, which including cell-specific barcodes and unique molecular identifiers for each transcript) capture liberated transcripts from an individual cell, the beads are recovered from the array. Reverse transcription of bead-bound transcripts is performed in bulk, followed by library preparation, sequencing, and *in silico* analysis. The cell lysis and reverse transcriptions of mRNA are accomplished on-chip by sealing single cells and individual barcoded capture beads (Gierahn et al., 2017). This assay is compatible with on-array imaging cytometry for resolving the phenotype of cells from complex samples and has the potential to obtain more information from a limited amount of samples using a single platform.

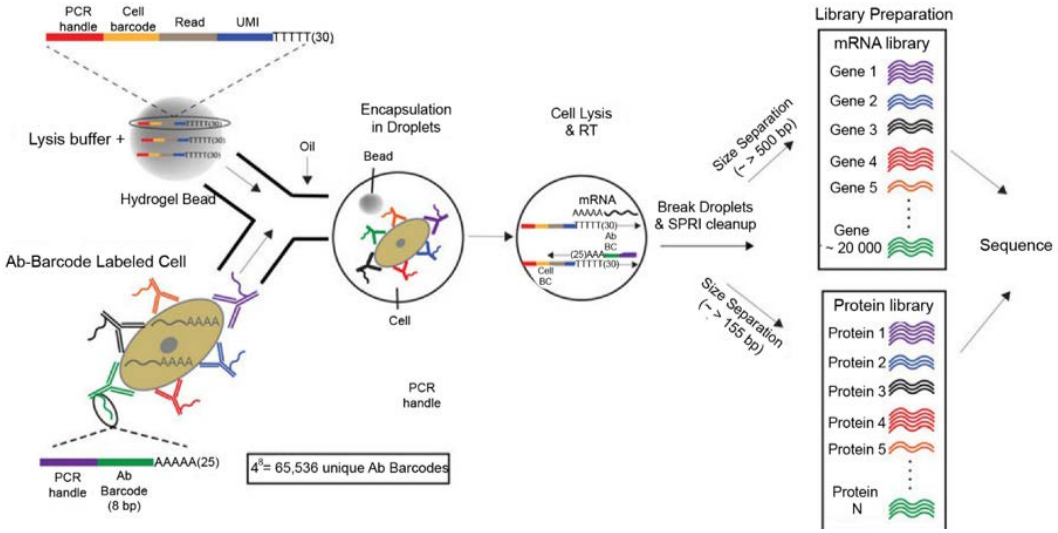

Figure 1-2 Workflow of REAP-seq.

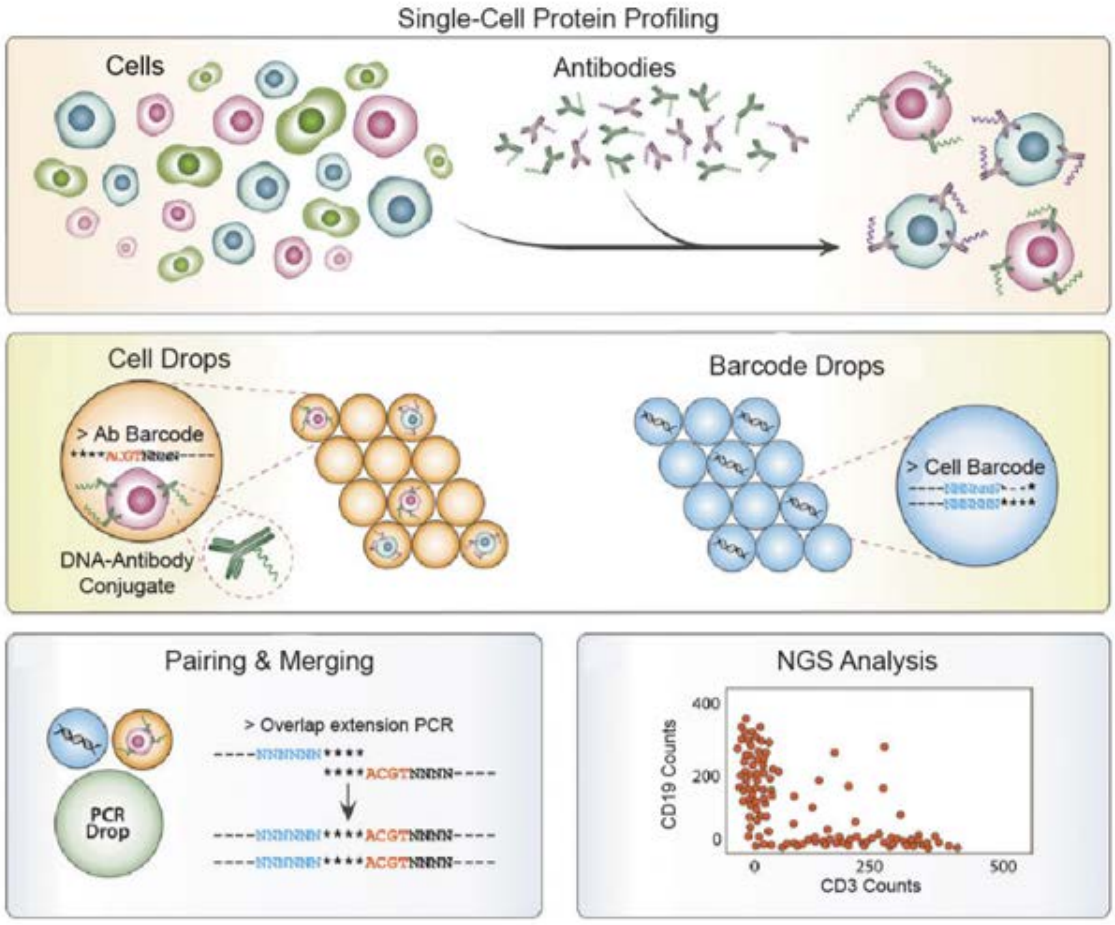

Figure 1-3 Abseq workflow.

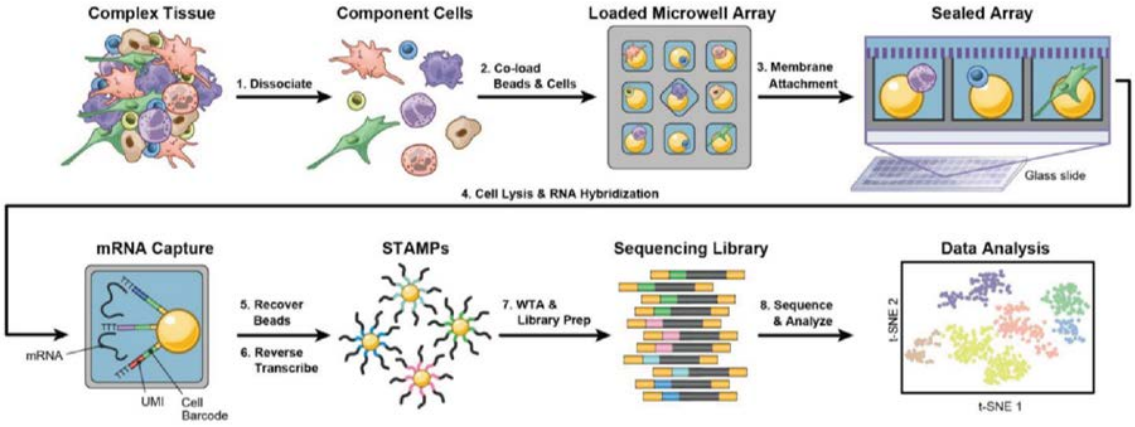

Figure 1-4 Workflow of Seq-Well

Unquestionably, the integration of transcriptomic and proteomic profiling on the same single cells can characterize cellular response to perturbations in a more accurate, unbiased way. However, these approaches require cell fixation or cell lysates, which exclude the possibility for tracking the dynamic transcriptomic and proteomic changes in the same cell. Although it has the advantage of being able to profile the complete transcriptome, the abundance of lowly expressed transcripts like transcription factors remains a challenge and requires pooling of data when the magnitude of change is also small. Recent reports have aimed to improve the analysis algorithms and to extract more information out of the data (Bacher et al., 2017; Bacher and Kendziorski, 2016; Poirion et al., 2016; Wu et al., 2017; Lee et al., 2017). Since the cells are lysed to retrieve the mRNA, scRNA-seq ideally provides a snapshot of the cell state, inferred by the transcript profile. Immune gene signatures could be obtained from sequencing results without prior knowledge, making it ideal for the discovery of candidate biomarkers in an unbiased manner. There are disadvantages of this approach, including the lack of correlation between mRNA and protein for some genes (Genshaft et al., 2016), the inability to directly

detect post-translational modification of proteins, and a complete lack of protein localization information. Thus, an ideal implementation of scRNA-seq would be in combination with another method that directly profiles biological function.

1.4. Integrated platforms to monitor dynamic T cell behavior and polyfunctionality

Immune cells, specifically T cells, demonstrate a variety of dynamic behaviors. From the standpoint of studying the therapeutic potential of T cells for adoptive transfer, or for identifying biomarkers of ICI, quantifying the functional status of the T cells will be essential.

1.4.1. Time-lapse imaging microscopy in nanowell grids (TIMING)

The characterization of the interaction between pairs of cells would benefit the understanding of how cells interact or cooperate with other cells, and help the discovery of underlying mechanisms of dynamic cell behavior. Microfluidic devices have the potential to dynamically monitor cell-cell interaction in a high-throughput manner in combination with live-cell microscopy. TIMING (**Figure 1-5,** adapted from reference (Romain et al., 2014)), a microwell-based platform, was reported to able to dynamically monitor cell-cell interaction, cytotoxicity, cell motility, and cell survival simultaneously (Lee,Chang-Han H. et al., 2017; Aschenbrenner et al., 2017; Liadi et al., 2015). Additionally, it can integrate real-time cytokine profiling by bead-based cytokine sensors (Romain et al., 2014) or gene expression profiling by single-cell retrieval via micromanipulator (Sendra et al., 2013) due to the non-destructive feature of this assay. Similarly, it has also been reported that droplets can be used to co-encapsulate the two types of cells before docking to the microwells (Walsh, Dodd, and Hautbergue, 2013); Martinelli et al., 2009). This microwell-based

device was compatible with live-cell imaging analysis, allowing the dynamic monitoring of cell morphology, behavior, and fate. Another new technology, DropMap, utilized droplets to dynamically profile antibody secretion from antibody-secreting cells (ASCs) (Eyer et al., 2017). Although the rate of secretion of cytokines is much lower than immunoglobulin secretion from ASCs, in principle, the DropMap technology can be adapted to monitoring cytokine secretion from T cells.

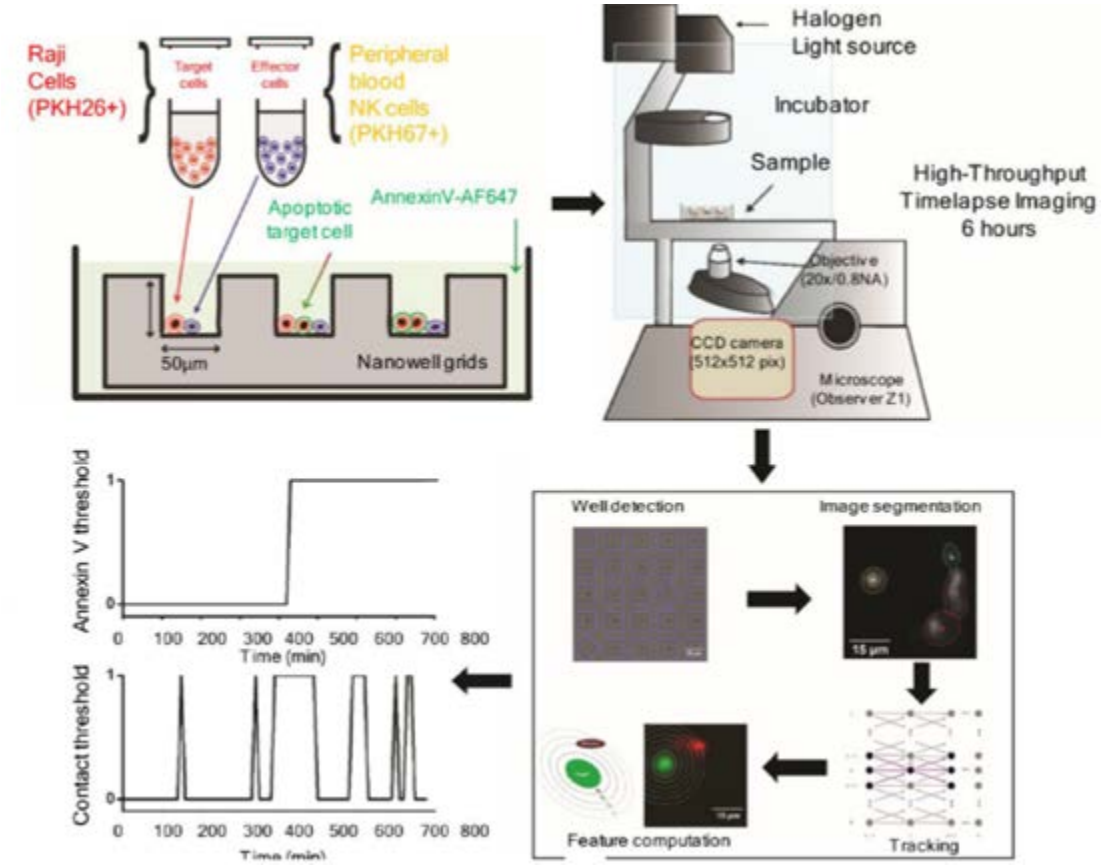

Figure 1-5 Workflow of TIMING (Time-lapse imaging in nanowell grids)

1.4.2. Single-cell barcoding chip (SCBC)

Single-cell barcoding chip, pioneered by the Heath and Fan groups, can quantify multiple proteins from the same cell, based on the fluorescence readout and on-chip calibration (**Figure 1-6,** adapted from reference (Kravchenko-Balasha et al., 2016)). Top

left of **Figure 1-6** is a schematic of an SCBC microchamber with valve and DEAL (DNA-encoded antibody library) barcodes. The bottom left panel of **Figure 1-6** is the schematic of immune sandwich formation that indicates protein detection. The top right is a representative time-lapse images of an SCBC microchamber containing two cells over 8 hours (scale bar = 100 μm). The bottom right is fluorescent images of patterned barcodes of 5 detected proteins, SCBC consists of a collection of microchambers on the microfluidic chip (from several hundred to several thousand) to confine single cell or two cells, and one of the surfaces of the microchamber contains barcode-like patterned antibody arrays for protein capture and further detection (Kravchenko-Balasha et al., 2016; Wei et al., 2016; Zhou et al., 2017). Apart from protein detection, this approach entitled the monitoring cell movement of the single-cell pair along with the protein secretion (Kravchenko-Balasha et al., 2016). Built on a similar concept, beads-on-barcode antibody microarray (BOBarray) was developed to quantify released proteins from a single cell confined in the individual well, but with modification of protein detection strategy: color-coded and size-coded functionalized microbeads were coated on the glass slide instead of patterned antibody arrays to minimize the size of the microfluidic device (Yang et al., 2016). SCBC technology is amenable of up to around 40-plex protein detection from a single cell and only need a small sample amount as an input; however, due to its intrinsic design, it was not designed to study dynamic or real-time protein secretion. The advantage of these function-based single-cell assays like TIMING and SCBC is that they have the potential to reveal heterogeneity of complex biologies like motility (reflection of the homing ability of T-cell to find tumor), cytotoxicity (representative of tumor-killing functionality) or cytokine secretion (communication with other immune cells), which are potential

predictive biomarker candidates of T cells-based immunotherapy, especially combined biomarkers that require simultaneous measurement of different perspectives of T-cell functionalities. One of the disadvantages of these approaches is that unlike FC/ MC that are available as part of core facilities, microfluidics often requires unique expertise and infrastructure to be able to execute these assays. As mentioned above, since the ability to retrieve cells of interest has been demonstrated for at least the TIMING assay, the ability to integrate functional and transcriptional profiling at single-cell resolution might provide the in-depth insight required for defining the efficacy of immunotherapies.

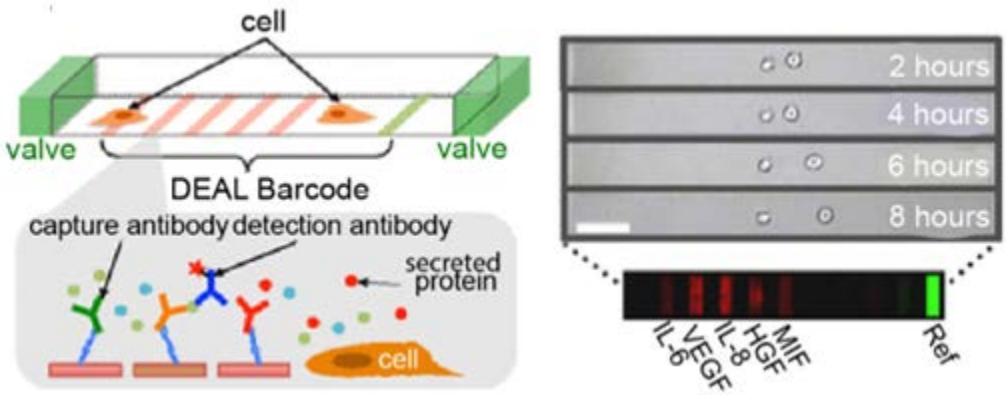

Figure 1-6 Schematic of a single-cell barcode chip (SCBC) and representative time-lapse images of an SCBC microchamber containing two cells.

1.5. Challenges

1.5.1. Identification and validation of biomarkers

A lot of effort has been devoted to obtaining the predictive biomarkers for ICI and ACT, and candidate biomarkers are showing promising results in multiple clinical trials. Biomarkers could be in various and different formats: tumor infiltrating lymphocyte density at tumor sites, immune checkpoint expression on tumor cells, neoantigen/mutation load of tumor cells, serum protein/antibodies, circulating tumor cells, lymphocyte counts, T cell clonality, *etc* (Maleki Vareki, Garrigós, and Duran, 2017; Rosenberg et al., 2016;

Vasaturo et al., 2016; Butterfield, 2018; Axelrod, Johnson, and Balko, 2018; Diggs and Hsueh, 2017). However, validated clinically actionable biomarkers for predicting the clinical outcomes of ICI/ACT are still lacking. The ligand of immune checkpoint expression of certain tumor samples is considered as one of the promising biomarkers for ICI; for instance, PD-L1 qualitative immunohistochemical assays were FDA-approved but with suboptimal sensitivity and specificity (Diggs and Hsueh, 2017). Many factors may contribute to the inconsistent performance of candidate biomarkers including the complexity of the anti-tumor response, the heterogeneity of tumor or/and patients, the inducible and non-static property of biomarkers, the suboptimal specificity, and accuracy of assays. It is evident that the discovery of biomarkers with high accuracy and sensitivity will enable better patient selection into the 3000+ immunotherapy clinical trials currently underway. Since T cells are considered as the primary effector cells in ICI and ACT, it is not surprising that some T-cell based predictive biomarkers have been discovered (Huang et al., 2017; Kamphorst, Pillai, et al., 2017). Although profiling T cells directly from the tumor site are more indicative of T-cell functional status within the tumor, peripheral blood is a more accessible compartment with limited inconvenience to the patients. For this reason, parallel efforts are devoted to studying T cell within the blood to determine if the changes within these T cells can be used to infer changes in T-cell functionality as a result of treatment (Huang et al., 2017; Kamphorst, Pillai, et al., 2017). Unfortunately, however, T cells demonstrate a variety of dynamic behaviors, and thus mapping these to the same T cells, at single-cell resolution is a challenging problem (**Figure 1-7**). T cells are capable of many different functions and integrate cues from both the cells and soluble factors from the microenvironment to facilitate decision-making. A complete understanding of T cells

can be only accomplished by tracking cell-cell interactions dynamically (e.g., synapse formation, cytotoxicity), intrinsic and chemokine guided motility, cytokine secretion, bioenergetics, transcriptome, morphology, differentiation status, and proliferation or survival. Assays that can provide insights into one or more of these features on the same cells, at single-cell resolution, can provide a deeper understanding of the underlying biology.

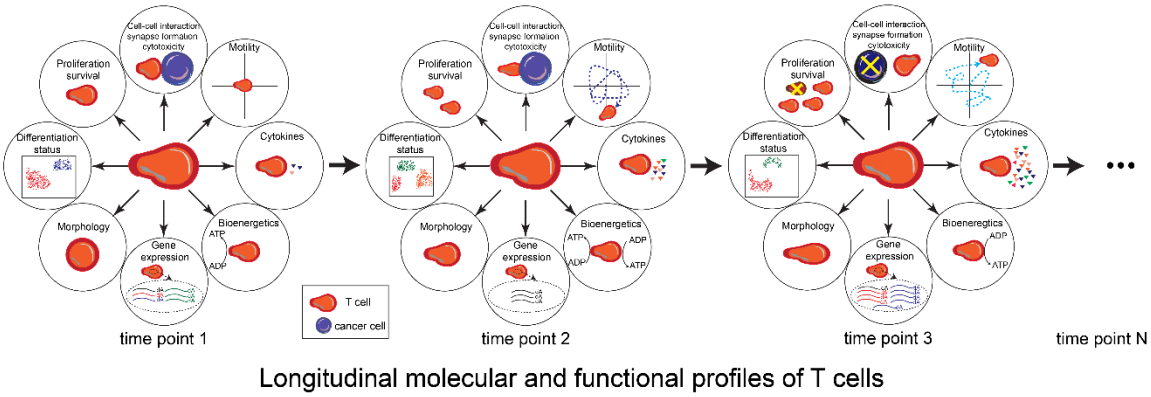

Figure 1-7 Integrated and dynamic profiling of T cells Integrated and dynamic profiling of T cells

1.5.2. Choice of assay

The choice of the appropriate assay to define T-cell functionality is defined by a combination of multiple factors including the number of T cells available, the depth of information being sought, ease of assay standardization, and cost. ScRNA-seq is an excellent choice for the discovery of biomarkers but is still rather expensive for routine implementation. At the other end of the spectrum, FC is considered standard, but it requires that the biomarkers have already been discovered using another assay. Presently, at least for monitoring ICI trials, there is no unique way to converge to a single assay, and the choice is often determined by one or more of factors listed above. ACT, on the other hand, should not be limited by cell numbers for at least the infusion product, and not surprisingly

more complex assays and dynamic assays have been used to evaluate T-cell functionality (Ma et al., 2013; Liadi et al., 2015). Spatial information All the techniques we have described work with homogenized single cells or single cells in suspension. These methods are ideal and relevant in tumor immunotherapy when profiling single T cells in peripheral blood. Thus, while the comprehensive documentation of the molecular profiles revealed by scRNA-seq is useful for identifying compositional frequencies of immune cell subsets, they cannot, however, reveal the link between the molecular profile and functional capacity, and how this impacted by space and time. The tumor microenvironment is a three-dimensional structure composed of different kinds of cells, and it is essential to document the spatial localization of immune cells within the tumor microenvironment (TME). A few in situ sequencing, proof-of-concept technologies have been demonstrated that can directly map spatial information and transcript profiles (Larsson et al., 2010; Ke et al., 2013; Lee,Je Hyuk et al., 2014), but it remains to be seen if they can match the depth of transcript profiling afforded by even scRNA-seq. Similarly, FISH-based methods that can preserve the spatial information and directly count RNA molecules down to the single-molecule level have been reported (Mellis et al., 2017; Shah et al., 2016; Moffitt et al., 2016). The drawbacks, however, are that even with repetitive cycles of probing different mRNA molecules, the total number of unique mRNA molecules that can be detected is smaller than scRNA-seq and that researchers have to pre-determine the transcripts that are being studied.

1.5.3. Bioinformatics

One of the significant and central challenges for realizing the potential and benefit of the next generation of single-cell technologies is matching advances in bioinformatics.

As outlined above, the low number of reads per single cell, the ability to differentiate technical and biological variation, amplification biases, batch-effect, all present significant challenges to systematic data analyses. Besides, the ability to integrate single-cell data acquired across different platforms analyzing different kinds of biomolecules and functions is a complex problem, which requires adequate normalization methods and the capability to investigate the correlation among different dimensions of single-cell data (Bacher et al., 2017; Tricot et al., 2015; Vallejos et al., 2017; Wang et al., 2017). The identification of conserved signatures of genes and dimension-reduction-based visualization are the most common methods to extract information from single-cell datasets with high-dimensionality (Wang et al., 2017; Kiselev et al., 2017). However, the algorithms for prediction of single-cell responses within heterogeneous cell populations, to perturbation is not well-defined (Su, Shi, and Wei, 2017). In other words, while the currently available analytic approaches are mainly focusing on descriptive analyses at single-cell resolution in vitro, it remains unclear how to utilize and integrate these single-cell data to accurately predict the behavior and fate of diverse cell populations in vivo, especially within TME, eventually serving as biomarkers to predict the clinical outcomes of cell-based therapeutics.

Chapter 2

Single-cell profiling of dynamic cytokine secretion and the phenotype of immune cells

Note: this is a reformatted manuscript, which was published in PLOS One.

Xingyue An, Victor G Sendra, Ivan Liadi, Balakrishnan Ramesh, Gabrielle Romain, Cara Haymaker, Melisa Marinez-Paniagua, Yanbin Lu, Laszlo G Radvanyi, Badrinath Roysam, and Navin Varadarajan, "Single-Cell Profiling of Dynamic Cytokine Secretion and the Phenotype of Immune Cells," ed. Golo Ahlenstiel, PLOS ONE 12, no. 8 (August 24, 2017): e0181904.

2.1. Introduction

Although natural killer (NK) cells were classically defined as pre-activated effector lymphocytes empowered with innate cytolytic functionality, more recent data suggest that NK cells are also endowed with complex functionalities including cytokine secretion and activation of antigen-presenting cells, and can thus act as a bridge between innate and adaptive immunity (Vivier et al., 2011). NK cells are of pivotal importance in the execution of antiviral and anti-tumor responses (Long et al., 2013). Human NK cells are identified as $CD3^{-}CD56^{+}$ cells and are typically classified into different subsets based on the relative expression of the cell surface markers CD56 (adhesion marker) and CD16 (FcγRIIIA, low-affinity Fc receptor) (Decocq et al., 2011; Poli et al., 2009). The majority of NK cells in peripheral blood (> 90%) are the $CD56^{dim}CD16^{+}$ phenotype, which is primarily believed to be responsible for cytolytic functionality including antibody-dependent cell-mediated

cytotoxicity (ADCC) mediated by CD16. By contrast, the $CD56^{bright}CD16^{-}$ phenotype is the minor population in peripheral blood and is described as primarily responsible for the secretion of cytokines like interferon gamma (IFN-γ) (Decocq et al., 2011; Poli et al., 2009).

The secretion of the pro-inflammatory cytokine IFN-γ is an essential mechanism of defense mediated by lymphocytes. Unlike cytotoxicity that only influences the target cell that is directly conjugated to the lymphocyte, IFN-γ secretion has a more profound influence on all cells within the microenvironment via multiple mechanisms including elevated expression of HLA-class I molecules (Zaidi and Merlino, 2011), induction of chemokines that can promote immune cell infiltration (Hu, Chakravarty, and Ivashkiv, 2008), mediation of angiostasis (Qin et al., 2003), and prevention of the outgrowth of antigen-loss variants (Gerbitz et al., 2012). From a clinical perspective, the secretion of IFN-γ by immune cells is likely an important contributor to the efficacy of immunotherapies, including treatment with antibodies against PD-1 and CTLA-4 (Zaretsky et al., 2016; Gao et al., 2016). Direct measurement of NK cell (or lymphocyte) functions at the single-cell level requires the simultaneous monitoring of multiple parameters including the cell's phenotype, its migration, and interaction with other cells, secretion of proteins, and its survival. These challenges have been tackled by measuring just a subset of these effector functions and relying on correlative studies to establish links among cellular functionalities. While multiphoton microscopy is useful for studying lymphocyte motility and cytotoxicity *in situ* or *in vivo* (Mempel, 2010; Breart et al., 2008; Roysam et al., 2008), the number of immune cells that can be simultaneously tracked is small and limited to the field-of-view, potentially leading to sampling bias. In contrast, *in vitro* dynamic imaging systems (Liadi et al., 2013; Romain et al., 2014; Zaretsky,Irina et al.,

2012; Liadi et al., 2015) may be better suited for studying the longitudinal interactions between lymphocytes and target cells at single-cell resolution and in a high-throughput manner. Microfabricated nanowell arrays are ideal for tracking both the motility and interaction between cells (Liadi et al., 2013; Zaretsky,Irina et al., 2012; Liadi et al., 2015). While elegant methods like microengraving (Varadarajan et al., 2012; Han et al., 2012) and the single-cell barcode chip (SCBC) (Ma,Chao et al., 2011; Lu et al., 2015; Son et al., 2016) have been reported for the analysis of cytokines secreted by single cells confined in such nanowell arrays, these systems require the capture of the secreted cytokine on a separate glass substrate via encapsulation thus precluding real-time dynamic measurements of cytokine secretion (Son et al., 2016).

Here, we have developed and validated an integrated methodology that combines nanowell arrays (Romain et al., 2014; Liadi et al., 2015) and bead-based molecular sensors (Son et al., 2016; Chokkalingam et al., 2013; Konry, Golberg, and Yarmush, 2013) for detecting cytokine secretion dynamically without the need for encapsulation of single T cells/NK cells. We used this methodology to link the phenotype of peripheral blood human NK cells with their dynamic cytokine secretion profiles. Our results demonstrate that contrary to the long-term secretion that has been routinely profiled, human NK cells bearing the $CD56^{dim}CD16^{+}$ phenotype are immediate secretors (< 3 h) of IFN-γ upon stimulation. Surprisingly, both the rate and total amount of IFN-γ secretion from individual NK cells were donor-dependent parameters.

2.2. Methods

2.2.1. Human subjects statement

All work outlined in this report was performed according to protocols approved by the Institutional Review Boards at the University of Houston and the University of Texas M.D. Anderson Cancer Center (IRB# LAB06-0755).

2.2.2. TILs, PBMCs, primary T cells, NK cells, and reagents

Tumor infiltrating lymphocytes (TILs) from melanoma patients were isolated and expanded as previously described (Haymaker et al., 2015). Briefly, initial TIL expansion was performed in 24-well plates from either small 3-5 mm^2 tumor fragments or from enzymatic digestion, followed by centrifugation with Ficoll-Paque PLUS (GE Healthcare Life Sciences, USA). TILs were then allowed to propagate for 3-5 weeks in TIL-complete media containing 6000 IU/ml human recombinant IL-2 (Nestlé Health Science, Switzerland). Once the desired number of TILs was achieved, Rapid Expansion Protocol (REP) was performed in which TIL was cultured together with PBMC feeder cells (1 TIL: 200 feeders) preloaded with anti-CD3 (OKT3, eBioscience) in a G-REX 100M flask until the desired number of cells was achieved and harvested. PBMC isolation from buffy coat was performed by density gradient centrifugation using either Ficoll-Paque PLUS or Lymphoprep™ density gradient medium (Stemcell Technologies, Canada). Immunomagnetic isolation of T cells from PBMC was then conducted using the EasySep™ Human T Cell Enrichment Kit (Stemcell Technologies, Canada). NK cell isolation from PBMC was accomplished using the RosetteSep™ Human NK Cell Enrichment Cocktail (Stemcell Technologies, Canada), as described previously (Somanchi et al., 2011). **Table 2-1** provides a complete listing of important reagents used in this study.

Table 2-1 List of reagents described in this manuscript.

Reagents	Manufacturer	Reference
Alexa Fluor® 488 NHS Ester (A-20000)	Thermo Fisher Scientific Inc.	https://tools.thermofisher.com/content/sfs/manuals/mp10168.pdf
Brilliant Violet 421™ mouse anti-human CD4 (317433)	BioLegend	http://www.biolegend.com/pop_pdf.php?id=7775
Brilliant Violet 421™ streptavidin (405226)	BioLegend	http://www.biolegend.com/pop_pdf.php?id=7297
BCIP/NBT substrate	Sigma-Aldrich	http://www.sigmaaldrich.com/catalog/product/sigma/b1911?lang=en&region=US
CEF-MHC Class I Control Peptide Pool "Classic" (CTL-CEF-001)	Cellular Technology Limited	http://www.immunospot.com/includes/pdfs/PDSs/PDS_CEF-MHC-Class-I-Control-Peptide-Pool-Classic.pdf
ExtrAvidin-alkaline phosphatase	Sigma-Aldrich	http://www.sigmaaldrich.com/catalog/product/sigma/e2636?lang=en&region=US
LumAvdin® microsphere 115 (L100-L115-01)	Luminex	N/A
Mouse anti-human CD56 HCD56 biotinylated (318319)	BioLegend	http://www.biolegend.com/pop_pdf.php?id=4076
Mouse anti-human IFNγ mAb 1-D1K (3420-3-250)	Mabtech	https://www.mabtech.com/sites/default/files/datasheets/3420-3-250.pdf
Mouse anti-human IFNγ mAB 7-B6-1 biotinylated (3420-6-250)	Mabtech	https://www.mabtech.com/sites/default/files/datasheets/3420-6-250.pdf
PE Mouse anti-human CD16 3G8 (560995)	BD Pharmingen™	http://www.bdbiosciences.com/ds/pm/tds/560995.pdf
Poly(L-lysine) grafted with poly(ethylene glycol) [PLL(20)-g[3.5]- PEG(2)]	Susos AG	N/A
ProMag™ 3 Series • Goat anti-Mouse IgG (Fc) beads (PMM3N)	Bangs Laboratories, Inc.	http://www.bangslabs.com/sites/default/files/imce/docs/PDS%20723%20Web.pdf
R-Phycoerythrin Streptavidin (Strep – PE) (016-110-084)	Jackson ImmunoResearch Laboratories, Inc.	https://www.jacksonimmuno.com/catalog/products/016-110-084
SU-8 3050	MicroChem Corp.	http://microchem.com/pdf/SU-8%203000%20Data%20Sheet.pdf
SU-8 developer	MicroChem Corp.	N/A
Sylgard® 184 silicone elastomer kit	Dow Corning, Corp.	http://www.dowcorning.com/DataFiles/090276fe80190b08.pdf
Tridecafluoro-1, 1, 2, 2-Tetrahydrooctyl)-1-Trichlorosilane	UCT Specialties	N/A

2.2.3. Functionalization of beads

One microliter of ProMag™ 3 Series goat anti-mouse IgG-Fc beads (Bangs Laboratories, Inc., USA) (~2.3×10^5 beads) in solution was washed with 10 µl of PBS and resuspended in 19.6 µl PBS (~0.05% solids). Mouse anti-human IFN-γ (1-D1K, Mabtech) was added to the beads at a final concentration of 10 µg/ml, followed by incubation for 30 min at room temperature (RT), and then washed and resuspended in 100 µl PBS.

Forty microliters of LumAvidin® 115 microspheres (Luminex Corp., USA) (~10^5 microspheres) in solution was washed with the same volume of PBS and resuspended in 80 µl of PBS. Biotinylated mouse anti-human IFN-γ (7-B6-1, Mabtech) was added to the microspheres at a final concentration of 10 µg/ml, followed by incubation for one hour at RT, and was subsequently washed and resuspended in 40 µl PBS.

2.2.4. PLL-g-PEG solution preparation

Poly(L-lysine) (20 kDa) grafted with poly(ethylene glycol) (2 kDa) (PLL-g-PEG) (SuSoS, Switzerland) was dissolved in 10 mM HEPES buffer at RT (final PLL-g-PEG concentration is 0.1 mg/ml). The PLL-g-PEG solution was filtered using a 0.2 µm pore size syringe filter, kept at 4 ^{o}C for use within two weeks of dissolution.

2.2.5. ELISPOT assays

ELISPOT assays were performed with fresh PBMC and TIL as previously described (Varadarajan et al., 2012; Martinon et al., 2009). Briefly, microwell plates (Merck Millipore, USA) were coated with capture antibody anti-human IFN-γ (1-D1K, Mabtech) at 10 µg/ml overnight at 4 °C. The next day, the plates were washed twice with PBS and blocked with complete culture medium RPMI + 10% FBS (R10) for 45 min at 37 °C. Cells were prepared as follows in triplicates: (1) 4,000 PBMCs stimulated with 10

ng/ml phorbol 12-myristate 13-acetate (PMA) and 1 µg/ml ionomycin per well; (2) 4,000 TILs derived from a melanoma patient stimulated with 10 ng/ml PMA and 1 µg/ml ionomycin per well; (3) 200,000 PBMCs stimulated with 2 µg/ml CEF peptide (CEF peptide is a peptide pool consisting of 23 MHC I-restricted 8-11 mer epitopes from influenza virus, cytomegalovirus, and Epstein-Barr virus; it has been shown to elicit IFN-γ release from $CD8^+$ T cells in human PBMCs of the majority of randomly selected healthy donors); and (4) 200,000 corresponding non-stimulated cells. Next, cells were incubated at 37 °C/5% CO_2 for 18 h, followed by successive washes and incubation with biotinylated anti-human IFN-γ (7-B6-1, Mabtech), extravidin-alkaline phosphatase (Sigma-Aldrich, USA) and BCIP/NBT (Sigma-Aldrich, USA) substrate. The plate was subsequently read with an ELISPOT reader (C.T.L. counter) while taking into account background measurement.

2.2.6. Thin bottom nanowell array fabrication

Standard soft lithography techniques were applied for fabrication of PDMS nanowell arrays. The nanowell pattern was designed using AutoCAD (Autodesk, USA), as described previously (Liadi et al., 2013; Romain et al., 2014; Liadi et al., 2015). The dimensions of the square well were 50 µm×50 µm, while the pitch between two adjacent wells was set to 100 µm.

The master template of the nanowell array was fabricated by standard photolithography, using SU-8 3050 (MicroChem Corp., USA) spin-coated on a 4-inch silicon wafer (WRS Materials, USA) to yield 60 µm thickness, according to manufacturer's directions. Silanization was achieved by vapor deposition of (Tridecafluoro-1, 1, 2, 2-

Tetrahydrooctyl)-1-Trichlorosilane (UCT Specialties, USA) in a vacuum desiccator chamber overnight.

PDMS (Sylgard 184, Dow Corning, USA) was mixed in 10:1 (base-to-curing agent, weight ratio), then degassed in a vacuum desiccator chamber for 1 h. 10 ml degassed PDMS mixture was poured onto the master and spun at 1000 rpm for 30 s with an acceleration of 500 rpm/s. The silicon master with PDMS thin layer was baked in a convection oven at 80 ^{o}C for 3 hours. After curing, the nanowell arrays in PDMS were peeled and cut to fit standard 50 mm Petri dishes.

The nanowell array was air plasma-oxidized and bonded to the bottom of 50 mm Petri dish (Ted Pella Inc., USA). Immediately before use, the nanowell array was re-oxidized with air plasma and then incubated with 1.5 ml PLL-g-PEG solution for 20 min at 37 ^{o}C. The PLL-g-PEG solution was aspirated from the nanowell array, and the array was subsequently rinsed with R10 before use in cell-based assays.

2.2.7. Finite element simulations

The system of partial differential equations to model the variation of analyte concentrations, C (in liquid media) and C_s (on bead surface), with time, was solved using the Transport of diluted species interface, Chemical reaction engineering module in COMSOL Multiphysics 4.1. The mass balance equation involving C_s was solved using its weak form. The relative distance between the bead and the cell within the nanowell was varied systematically across simulations. Changes in cell and bead positions, convective transport, surface diffusion on the bead ($D_s = 10^{-25}$ m^2/s), non-specific adsorption on walls and analyte degradation were neglected to simplify numerical simulations.

2.2.8. TIMING assays for the study of NK cells phenotypes and IFN-γ secretion

Functionalized beads and pre-stained NK cells (anti-CD16-PE, 3G8, BD Pharmingen™; anti-CD56-biotin, HCD56, BioLegend; streptavidin-Brillant Violet™ 421, BioLegend) were loaded sequentially onto a nanowell array. The nanowell array was incubated in 1.5 ml R10 that contained one microgram per microliter detection antibody against IFN-γ (1-D1K, Mabtech) conjugated with Alexa Fluor® 488 (AF488), 10 ng/ml PMA and one microgram per microliter ionomycin. The nanowell array was imaged using a Zeiss fluorescent microscope with 20× 0.8 NA objectives and a scientific CMOS camera (Orca Flash 4.0). The phenotype of the cells was imaged with three channels (brightfield, CD16, CD56) at the initial time point and all beads-related channels (brightfield, AF488, beads) were imaged at subsequent time points for the duration of 6 h with 10 min intervals.

2.2.9. Automated image segmentation.

Images at the initial time point were analyzed through in-house algorithms to acquire fluorescent intensities (FIs) of all channels (brightfield, CD16, CD56, beads) and the frequencies of cells and beads within each well. Nanowells containing single beads were chosen for further analysis. Analysis of time-lapse for beads was processed by a modified pipeline for FIs from IFN-γ channel at each time point (Liadi et al., 2015). Access and Excel (Microsoft, USA) were used for matching data between cell phenotyping and FI change of beads.

As time increased, the beads FI (IFN-γ channel) followed a sigmoidal trend. Thus, we plotted and fit FI versus time using GraphPad Prism 6 (GraphPad Software Inc., USA) using a four-parameter logistic curve fit model (log [agonist] – the concentration model [variable slope]) whose formula was rewritten in order to include all the available data

points for fitting, allowing quantification of the EC50 that reflected the critical secretion time:

$$\text{MFI} = \text{Bottom} + \frac{(\text{Top}-\text{Bottom})\times t^h}{t^h+\text{EC50}^h}. \quad (2\text{-}1)$$

Bottom and Top are the corresponding values of the low plateau and high plateau, respectively; *t* is the time when the imaging was recorded during the time-lapse experiment (*t* = 0 min represents the first time point); EC50 is the time when the MFI reaches halfway between Bottom and Top; *h* is the Hill slope.

2.3. Results

2.3.1. Thin bottom nanowell arrays.

As we and others have previously reported, nanowell arrays fabricated in PDMS offer a convenient route to track the dynamic functional behavior of immune cells but might not be amenable to high-resolution imaging due to the thickness of the bottom of the PDMS array (Romain et al., 2014; Liadi et al., 2015). In order to overcome this limitation, we fabricated nanowell arrays in PDMS by spin-coating that enabled control over the thickness of the bottom of the PDMS nanowells (Zaretsky et al., 2012; Schneider et al., 2009).

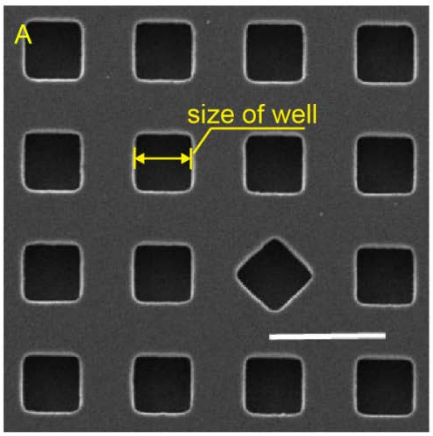

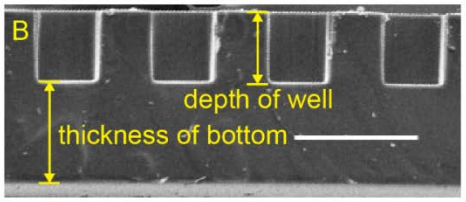

C

	size of wells (μm)	depth of wells (μm)	thickness of bottom (μm)
mean±SD	51±1	63±2	84±2
# of measurements	39	136	205

Figure 2-1 Thin bottom nanowell arrays fabricated by spin-coating.

Figure 2-1A shows SEM top-view images of the nanowell array obtained by spin-coating (scale bar = 100 μm). The depth of the well was measured across multiple regions of a 10 mm×2 mm chip and confirmed by optical microscopy to be 63±2 μm (N = 136, **Figure 2-1B**, scale bar = 100 μm). Similarly, the bottom thickness of the PDMS was uniform across the chip (84±2 μm, N = 205, **Figure 2-1C**) and this facilitated adaptation of the nanowell array to high-resolution microscopy.

To demonstrate proof-of-principle that the thin bottom nanowell arrays were compatible with high-resolution imaging, human NK cells were isolated from peripheral blood by immunodensity separation, stained with antibodies directed against the phenotypic markers CD16 and CD56, and then ~50,000 of these cells were loaded onto the nanowell array. Imaging was accomplished using a Nikon confocal microscope using a 100× objective (**Figure 2-2**).

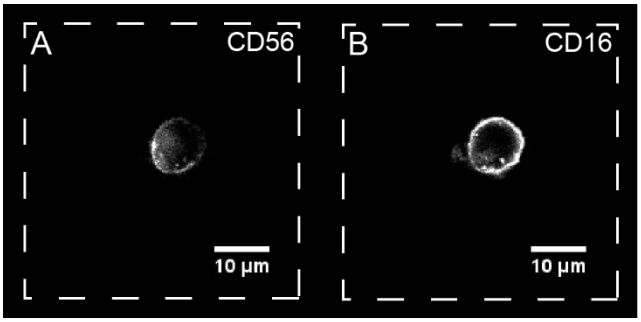

Figure 2-2 Fluorescence microscopy images of a labeled human NK cell (CD56 and CD16) were recorded using a 100× objective.

Despite the fact that PDMS is widely adopted for the fabrication of microfluidic devices, PDMS tends to display a high level of non-specific protein adsorption. Although a partial reduction in this effect can be accomplished by the oxidation with air plasma that renders PDMS hydrophilic, a better strategy had to be implemented since we were interested in the dynamic secretion of proteins from single cells in PDMS nanowell arrays.

In order to reduce the non-specific adsorption of proteins, we explored the utility of PEG treatment of PDMS. The ability of PEG and its derivatives to passivate surfaces is well described, and a graft copolymer of PEG with poly-L-lysine (PLL-g-PEG) has been previously reported for use in PDMS microchannels (Marie et al., 2006).

PDMS nanowell arrays were oxidized using air plasma to render the surface hydrophilic with silanol groups and incubated with a 100 μg/ml solution of PLL-g-PEG in HEPES. Subsequent to washing, human T cells isolated by immunomagnetic separation from PBMCs were loaded onto two separate nanowell arrays and stained with mouse anti-human CD4 antibody conjugated to Brilliant Violet™ 421 (OKT4, BioLegend). In the absence of surface modification, the signal from the cells was obscured by the background fluorescence from the nanowell edges (**Figure 2-3A, s**cale bar = 50 μm, exposure time = 500 ms). By contrast, even a short 20 min treatment with PLL-g-PEG demonstrated excellent surface passivation leading to clearly distinguishable cells and very little background staining of the nanowell edges (**Figure 2-3B, s**cale bar = 50 μm, exposure time = 500 ms). In order to quantify the differences arising from the signal against the background, the background-corrected mean fluorescence intensities (MFI) were computed for at least 30 single cells using ImageJ (NIH, USA). Regardless of the exposure time used (100–500 ms), PLL-g-PEG-treated nanowell arrays showed consistently enhanced cell-specific labeling, and an increase in the signal with increasing exposure times, confirming effective surface passivation (**Figure 2-4,** p-value < 0.0001. Each dot represents a single T cell. Non-parametric tests were performed for comparison of populations corrected fluorescent intensities of $CD4^+$ T cells. ****: p-value < 0.0001; ns: not significant; mean±SEM is shown).

These results confirmed that even a short treatment with PLL-g-PEG was sufficient to reduce non-specific adsorption and thus all our nanowell arrays were passivated using this method.

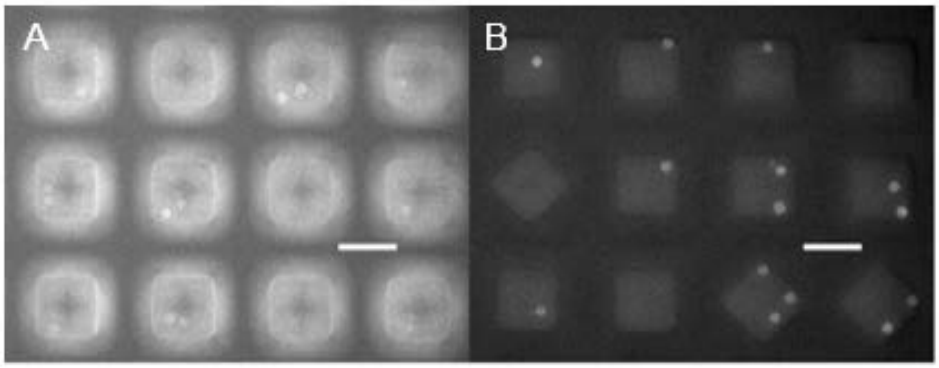

Figure 2-3 PLL-g-PEG treatment of PDMS nanowell arrays reduce non-specific binding.

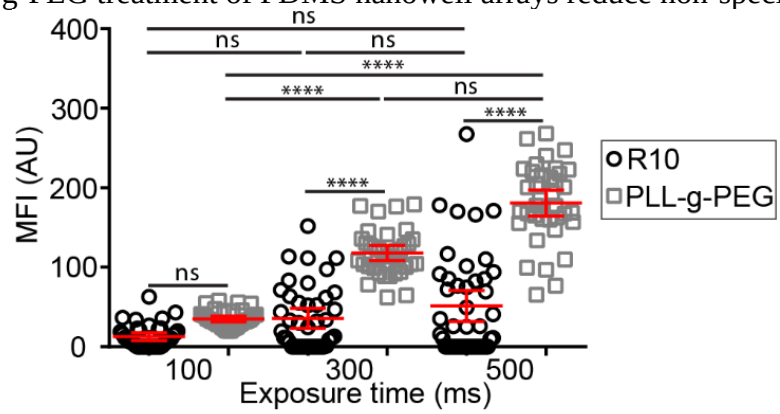

Figure 2-4 Background corrected mean fluorescent intensities of individual cells in either PLL-g-PEG or R10 passivated nanowell arrays.

2.3.2. The frequency of IFN-γ-secreting T cells enumerated by functionalized beads within nanowell arrays is correlated to the same responses determined using ELISPOT.

We first tested the ability of functionalized beads to efficiently capture proteins secreted by single cells after incubation in individual nanowells by measuring the limit of detection (LoD) of functionalized beads at different analyte concentrations. Antibody-coated beads were incubated with varying concentrations of IFN-γ (0.25–5 ng/ml) for a

period of 2 h at 37 °C, loaded onto glass-bottom Petri dish, and subsequently detected with a fluorescently labeled secondary antibody. The background-corrected mean fluorescent intensity (MFI) quantified across a minimum of 30 beads confirmed that IFN-γ was detectable at a concentration of 2.5 ng/ml (**Figure 2-5**, error bar: standard deviation). Next, the correlation between the nanowell-encapsulated bead assay and ELISPOT for quantifying frequencies of single immune cells secreting IFN-γ upon activation was determined. To account for variations in stimulus and the diversity of T cell populations, the frequency of IFN-γ secreting single T cells was enumerated under three sets of conditions: (1) stimulation of PBMCs with PMA/ionomycin; (2) stimulation of *in vitro* expanded, melanoma TILs with PMA/ionomycin; and (3) incubation of PBMCs with HLA-class I peptide pools derived from common viral antigens (CEF peptide pool). An aliquot of 10^6 cells was stimulated for a period of 3–5 h, from which an aliquot of ~100,000 cells was loaded onto a nanowell array. A suspension of 200,000 beads pre-coated with anti-IFN-γ (1-D1K, Mabtech) was subsequently loaded onto the nanowell array and incubated for a period of 2 h at 37 °C. By analyzing an average of 10,182±8,589 (mean±SD) nanowells containing single cells matched to one or more beads, the frequency of the activated T cell IFN-γ response was determined to be 0.40–7.8%. The magnitude of these responses was similar to those recorded by ELISPOT [0.20–11.2%], and results of both assays were significantly correlated ($R^2 = 0.87$, *p*-value = 0.0008), demonstrating that beads can be utilized to capture cytokine secretion from single cells (**Figure 2-6,** *p*-value = 0.0008). In the absence of stimulation, the frequency of IFN-γ beads detected when incubated with immune cells was < 1 in 10,000, and this result sets the limit of detection of our assay at 0.01%. In summary, these results established that functionalized beads

within nanowell arrays were capable of detecting IFN-γ secretion from single immune cells at frequencies correlated with those from conventional ELISPOT assays.

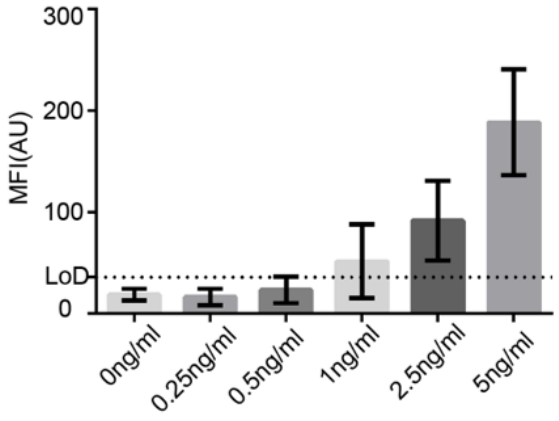

Figure 2-5 Background-corrected mean fluorescence intensity (MFI) detected from a minimum of 30 IFN-γ-positive beads, as a function of IFN-γ analyte concentration with functionalized LumAvidin® beads.

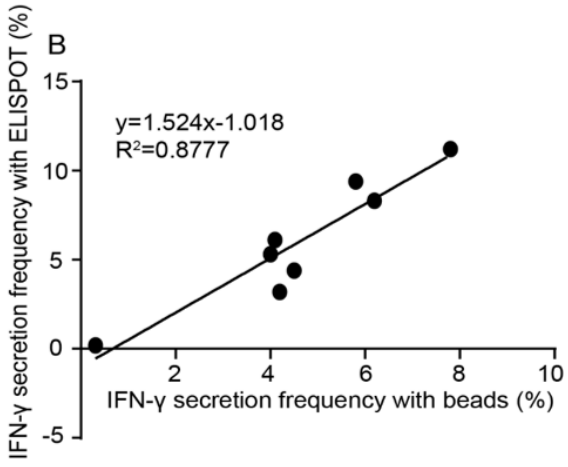

Figure 2-6 Linear regressions show that bead assay and ELISOPT for detection of single effector cells secreting IFN-γ at varying level of antigenic stimulation are significantly correlated.

2.3.3. In open-well systems, analyte capture density increases linearly with time.

As opposed to encapsulated systems, open-well configurations can be advantageous for the long term monitoring of cell fate and function since they allow a

continuous exchange of gases and nutrients. Furthermore, they avoid potential alterations of cellular behavior that can arise from the artificially high local concentrations of analytes commonly found in closed systems (Torres, Hill, and Love, 2014). A disadvantage of open-well systems is that the analyte secreted by an individual cell within a nanowell is subjected to persistent diffusion into the bulk medium, potentially lowering the sensitivity. Therefore, we sought to quantify the efficiency of analyte capture on beads by modeling a simplified open-well system using finite element simulations (**Figure 2-7**). The concentration of the analyte in liquid media (C) can be described using Fick's 2nd law,

$$\frac{\partial C}{\partial t} = D\nabla^2 C, \tag{2-2}$$

where D represents the diffusion coefficient of the analyte. Since the walls of the PDMS can be assumed to be largely impermeable to proteins (Han et al., 2010), the flux at these boundaries was set to zero. At a constant rate of analyte secretion from the cell (10 molecules/sec), the mass balance of analyte concentration on bead surface (C_s) was determined by the equation

$$\frac{\partial C_s}{\partial t} = D_s\nabla^2 C_s + k_{on}C(\theta_0 - C_s) - k_{off}C_s, \tag{2-3}$$

where D_s represents diffusivity of the analyte on the bead surface, k_{on} and k_{off} represent kinetic binding constants determined by the strength of capture antibody-analyte interaction, and θ_0 represents the number of capture antibodies available per unit surface area of the bead. The choice of values for the parameters (**Figure 2-7**) was based on commercially available antibody binding affinities, the known rates of cytokine secretion from lymphocytes, and previously reported numerical simulations of closed systems (Han et al., 2010). Initial concentrations of analyte in liquid media and bead surface were set to zero and the increase in fractional occupancy ($\oiint \frac{C_s}{\theta_0}$) on the bead with time as the cell

secretes the analyte was modeled. Upon validating the model with previously published data (Han et al., 2010), we sought to optimize the density of capture antibody molecules, one tunable variable to maximize captured cytokine density (and therefore the fluorescent pixel intensity). For a set bead diameter, the simulations showed that the fractional occupancy (fraction of antibodies bound by cytokines) increased when the total number of binding sites was decreased (**Figure 2-8,** mean±SEM is shown. Error bars are shown only if SEM is higher than 2.5%), which is consistent with ambient analyte theory that predicts that higher sensitivity can be achieved by lowering the number of antibodies used to capture the analyte (Ekins, 1998). Ultimately however, the overall fluorescent signal is proportional to the density of antibody-cytokine pairs. This density is determined by both the fractional occupancy of captured cytokine and binding site density of capture antibodies. As expected, captured cytokine density increased with time (0–6 h) regardless of the density of capture antibody molecules (1×10^{-9}–1×10^{-7} mol/m^2); during short-term assays ($\leq$ 2 h), there was not a significant difference in the various cytokine capture densities profiled. During longer assays (2–6 h), as expected, beads with a smaller density of capture antibody molecules (1×10^{-9} mol/m^2) tend to saturate cytokine capture quicker. This saturation was only observed at the lowest density of antibody molecules and subsequent increases in antibody density (1×10^{-8}– 1×10^{-7} mol/m^2), did not significantly increase the density of cytokines being captured (**Figure 2-9**, mean±SEM is shown. Error bars are showen if SEM is lower than 1800 molecules/μm^2). In summary, the results of these simulations suggested that within the short window of experimental interrogation (0–6 h), the captured cytokine density (and hence fluorescence intensity on the beads) increased linearly as a function of time. Furthermore, since the captured cytokine density was not

significantly altered by increasing the antibody density on the bead, we chose to experimentally utilize beads with binding site capacities in this density range (1×10^{-8}–1×10^{-7} mol/m^2).

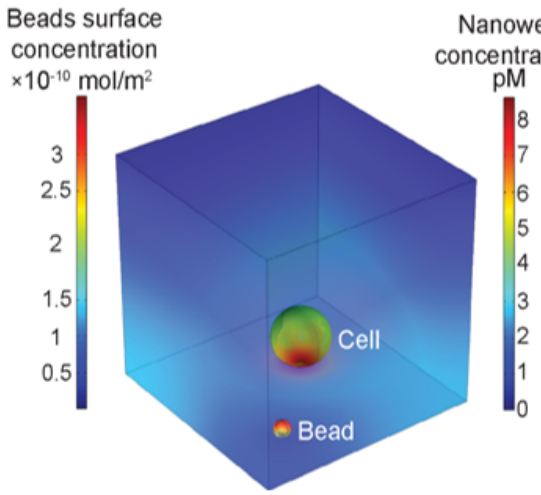

Simulation parameters

Variable	Symbol	Value	Unit
Forward rate constant	k_{on}	10^5	$M^{-1}s^{-1}$
Backward rate constant	k_{off}	10^{-3}	s^{-1}
Binding site density	θ_0	10^8	mol/m^2
Diffusivity	D	10^{-10}	m^2/s
Well size	W	4×10^{-5}	m
Cell size	D_c	10^{-5}	m
Secretion rate	N_s	10	molecules/s

Figure 2-7 Snapshot of heat maps showing analyte concentration in the liquid phase across the well and on the bead surface after five hours of secretion in a 40 μm nanowell.

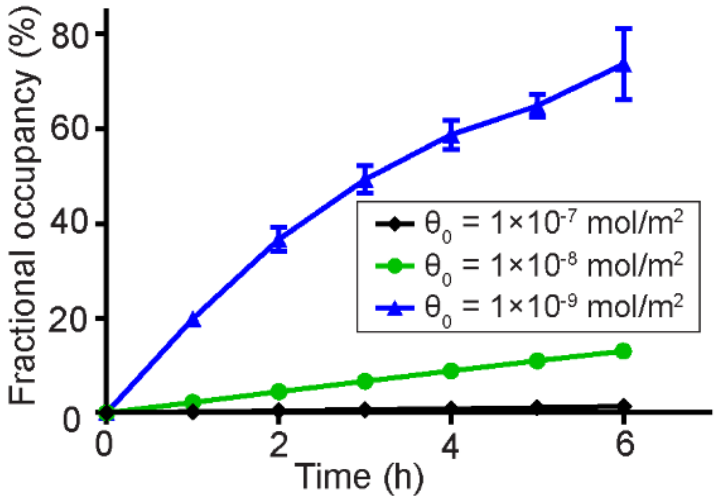

Figure 2-8 Fractional occupancy of 5 μm beads as a function of incubation time when the binding site density was varied across three orders of magnitude.

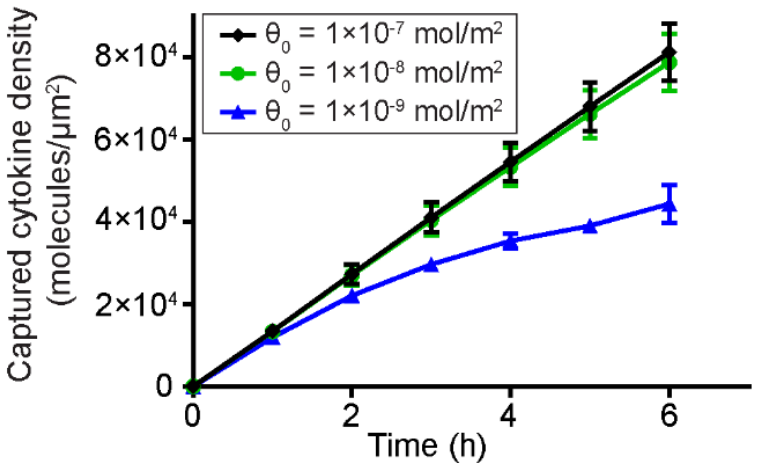

Figure 2-9 The variation in captured cytokine density obtained by varying the density of capture antibodies on the surface of the bead.

2.3.4. An open-well system can be used to profile the dynamic secretion of cytokine molecules from individual NK cells.

Since the end-point experiments confirmed the ability to detect IFN-γ from single immune cells upon activation, and the modeling suggested that the beads should work well in an open-well system, we next wanted to investigate if dynamic secretion of IFN-γ could be detected from individual NK cells upon activation. Human NK cells isolated *ex vivo* were stained and loaded into individual wells of a nanowell array and were incubated in R10 containing the mitogenic activators PMA/ionomycin; cytokine secretion was quantified by the formation of immuno-sandwiches on beads (**Figures 2-10** and **2-11**). We modified our previously-reported image analysis algorithms to not only enable the automated segmentation and tracking of cells but also to facilitate the identification of fluorescence intensity on the beads monitoring the secretion of IFN-γ (Liadi et al., 2015). Dynamic tracking of the AF488 fluorescence demonstrated that these bead-based sensors could report IFN-γ secretion from individual NK cells incubated within the same nanowell (**Figure 2-12**, $t_{Secrete}$ is 90 min. Scale bar = 10 μm). Individual NK cells could be identified

as secretors and non-secretors based on simple thresholding, and the fluorescence intensity of beads incubated with secretors showed a characteristic sigmoidal response that could readily be fit to a standard dose-response curve to identify the characteristic time of secretion ($t_{Secrete}$, **Figure 2-13**). The best-fitting response curve is overlaid on top of the raw data (triangles). The $t_{Secrete}$ (red), Hill slope and MFI ratio are shown.

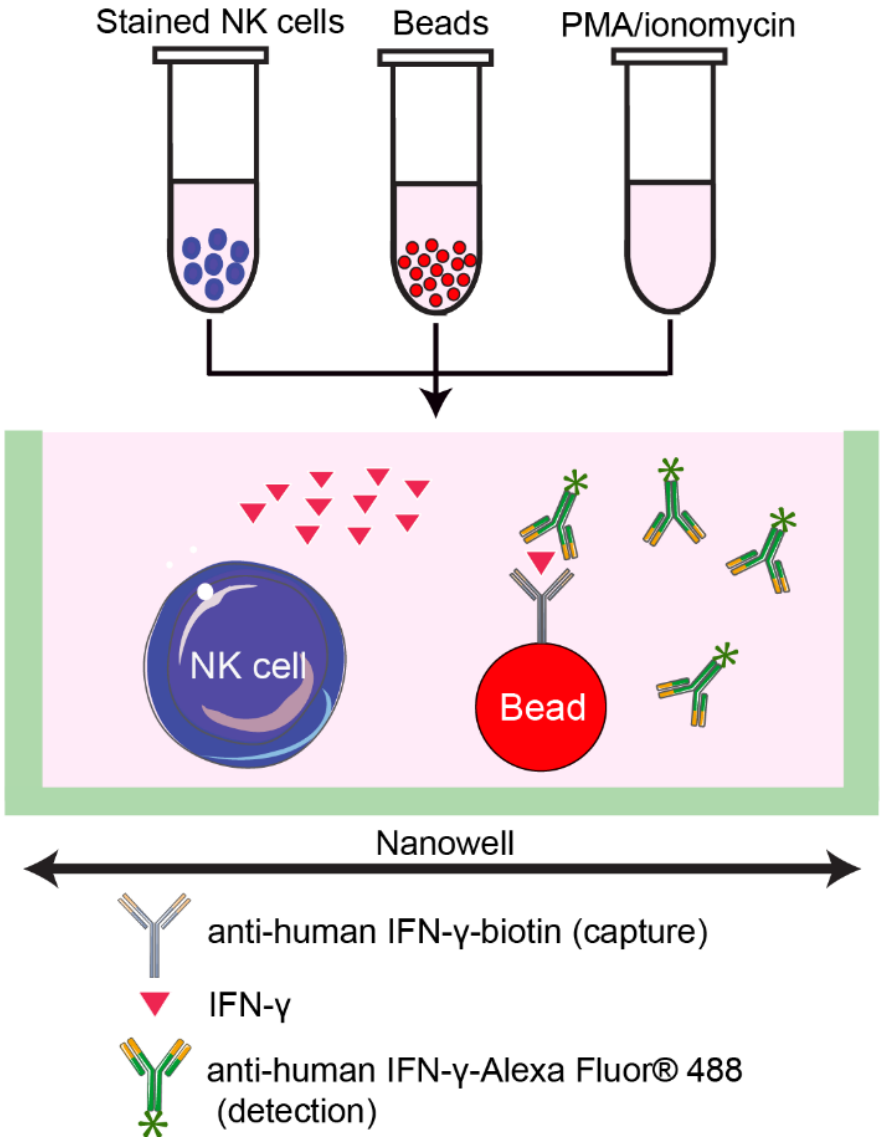

Figure 2-10 Schematic of immuno-sandwich design for detecting IFN-γ secretion from single NK cells using nanowell arrays.

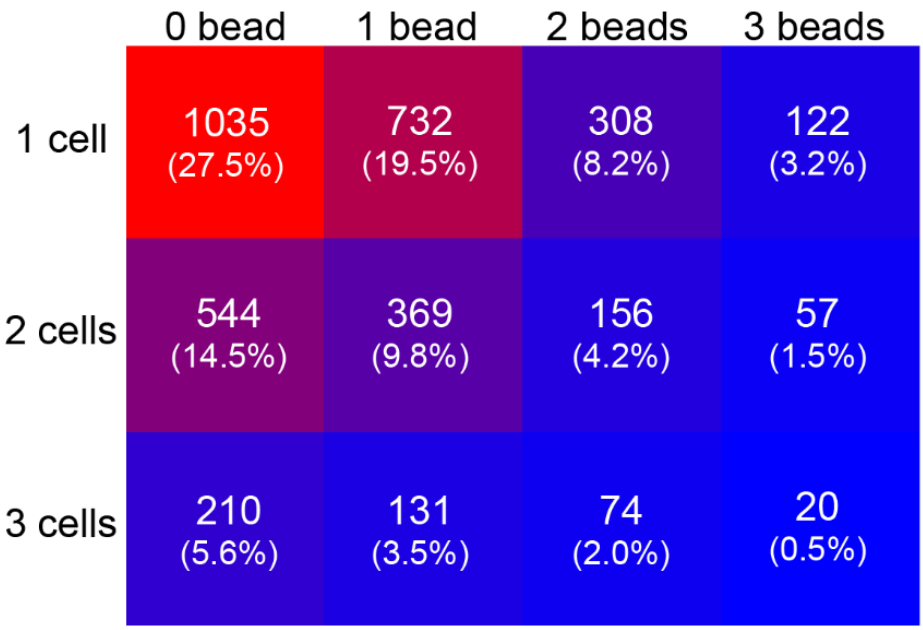

Figure 2-11 Distribution of functionalized beads and pre-stained NK cells in individual nanowell.

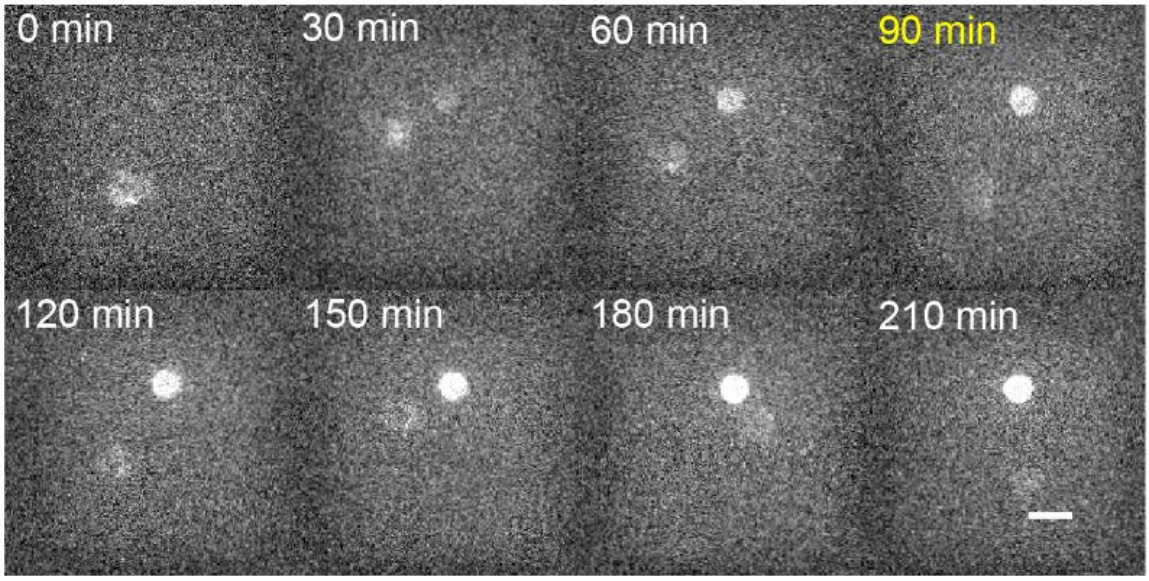

Figure 2-12 Dynamic tracking of the IFN-γ secretory activity of an NK cell within the same nanowell.

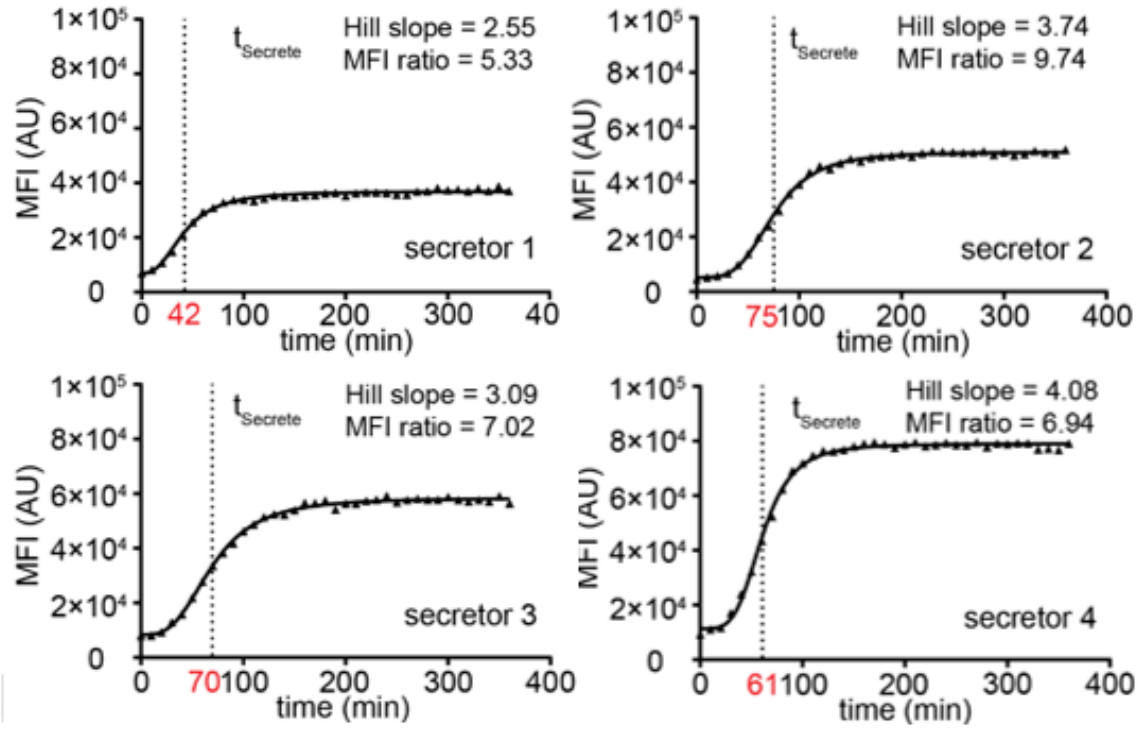

Figure 2-13 Four representative examples of dynamic fluorescence intensity (MFI) of the beads upon activation of individual NK cells.

2.3.5. CD56^{dim} CD16^{+} NK cells are immediate secretors of IFN-γ.

Having established the feasibility of our method to detect both the phenotype and the dynamic cytokine secretion profile of individual NK cells, we next sought to define the subset of human NK cells that were immediate secretors of IFN-γ upon stimulation. Towards this objective, NK cells isolated *ex vivo* from fresh blood were enriched by immunodensity sorting, labeled with antibodies against CD16 and CD56, and loaded onto a PDMS nanowell array along with pre-functionalized beads coated with IFN-γ capture antibodies as cytokine sensors. Our phenotypic classification of NK cell subsets determined by imaging cytometry was consistent with known NK cell subsets determined by flow cytometry as previously reported (**Figure 2-14**) (Poli et al., 2009). Control nanowell arrays were set up with stained NK cells and IFN-γ sensor beads, which were

imaged dynamically for a period of 6 h to confirm that the CD16 and CD56 antibodies used for immunostaining did not enable NK cells activation.

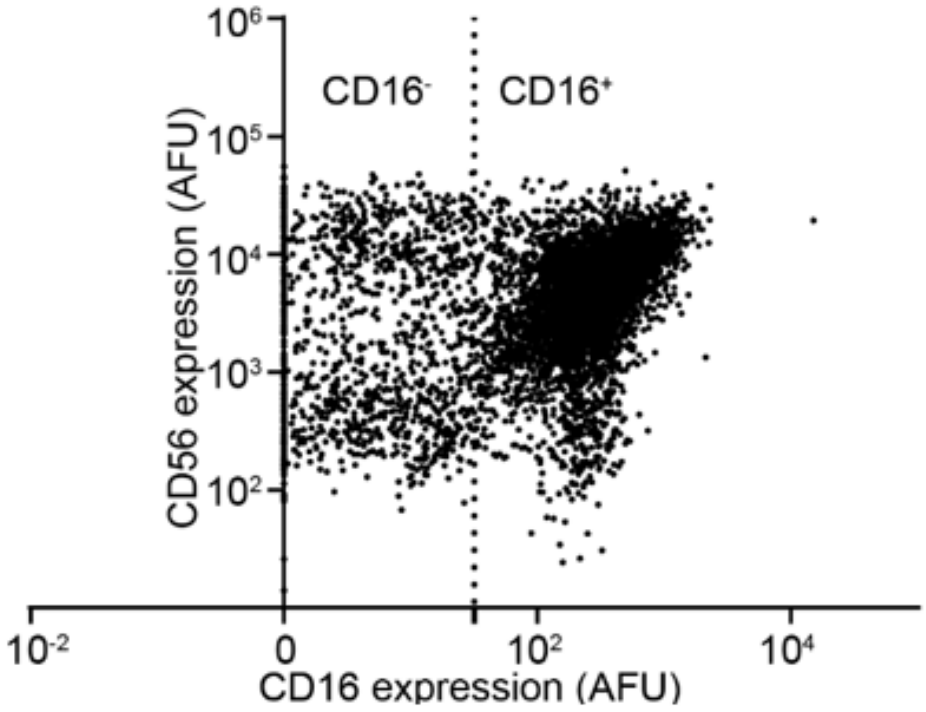

Figure 2-14 Representative phenotypic classification determined by imaging cytometry of NK cells based on CD16 and CD56 staining.

Immediately subsequent to recording the phenotype of the NK cells, the entire nanowell array was immersed in cell culture media R10 containing PMA/ionomycin to enable mitogenic stimulation. As anticipated, individual NK cells demonstrated a heterogeneous dynamic IFN-γ secretion profile, as reflected by the distributions of $t_{Secrete}$ (**Figure 2-15**). IFN-γ secretion was detected as early as 30 min from a small subset of NK cells, and the peak of the distribution of $t_{Secrete}$ for individual IFN-γ secreting NK cells was around 50–60 min; this behavior was conserved across at least two separate donors (**Figure 2-15**).

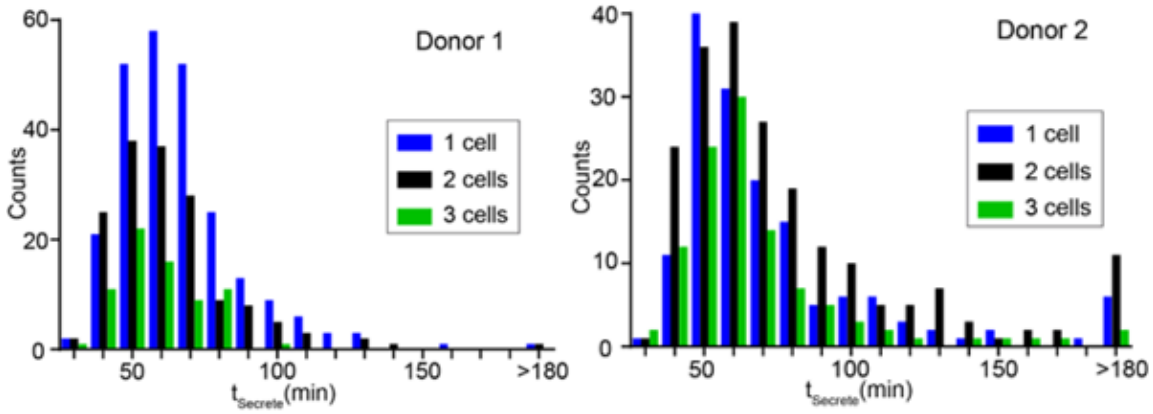

Figure 2-15 Histograms of $t_{Secrete}$ showed a conserved pattern of distribution across two different donors.

Comparison of the phenotype of single NK cells that were immediate secretors ($t_{Secrete} \leq 180$ min) to the entire parent population showed a significant enrichment of the $CD16^+$ population (p-value < 0.0001 for donor 1 and p-value = 0.0034 for donor 2, **Figure 2-16**, p-value < 0.0001). Since the distribution of $t_{Secrete}$ (**Figure 2-17**, the distribution is in black and the corresponding normal distributions (same mean and standard deviation of $t_{Secrete}$ of single-NK cells. Left: donor 1, right: donor 2) suggested the potential existence of early secretors subpopulations within the immediate secretors, we defined early secretors and late secretors based on the mean of $t_{Secrete}$ (donor 1: 62 min; donor 2: 70 min), and further investigated the differences in CD16 and CD56 expression of these two subpopulations. There was a trend that early secretors NK cells from both donors tended to express a higher level of CD16 on the surface (**Figure 2-18**. (Left): CD16 expression; (right): CD56 expression. Error bar: mean±95% CI. Mann-Whitney test was performed, ns: not significant, ***: p-value < 0.001, ****: p-value < 0.0001); while no similar trend was found in the comparison of expression of CD56 of early secretors and late secretors (**Figure 2-18**).

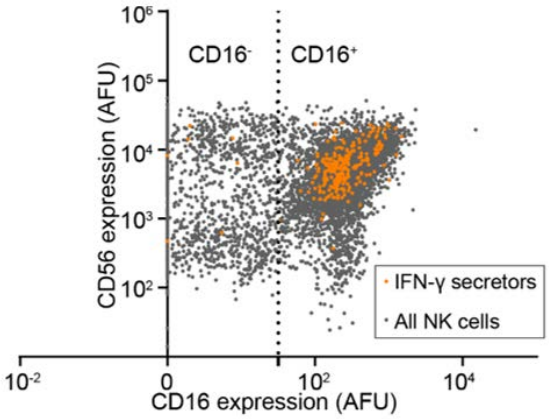

Figure 2-16 In comparison to the parent population, NK cells that were immediate secretors of IFN-γ were predominantly the $CD16^{+}$ phenotype.

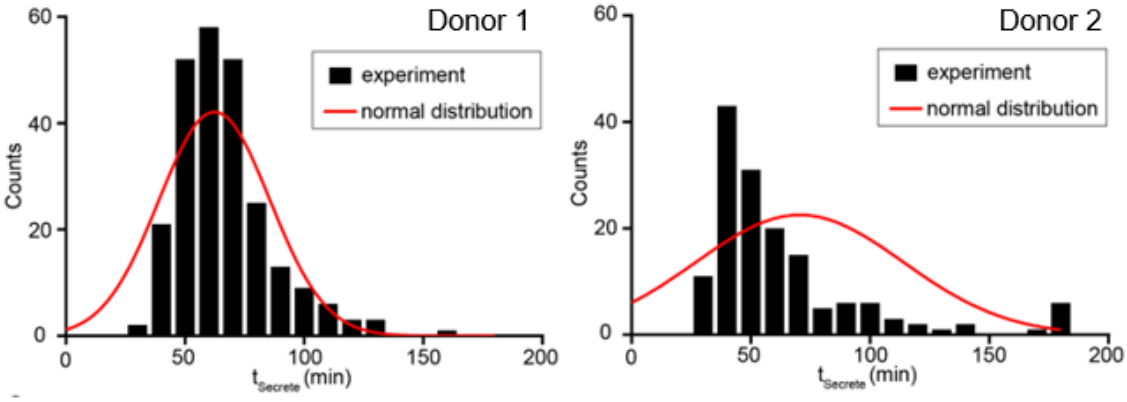

Figure 2-17 The distributions of $t_{Secrete}$ of single-NK cells.

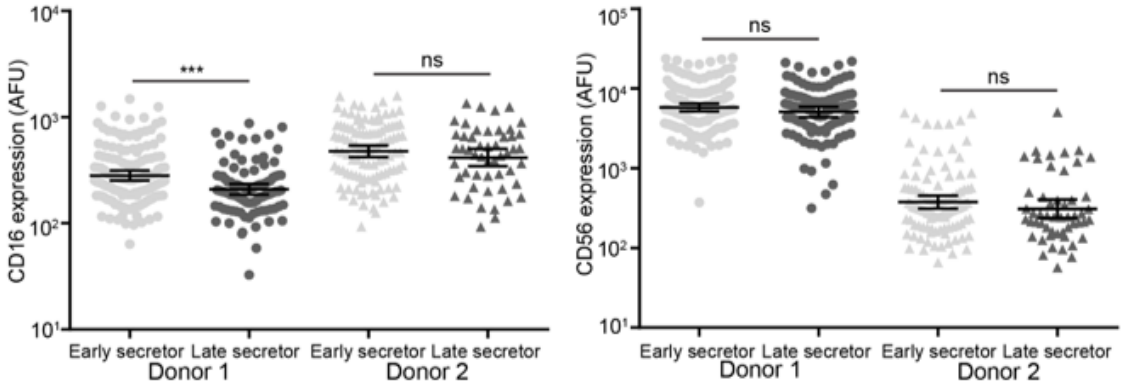

Figure 2-18 The relative comparison of CD16 or CD56 surface expression of early secretors and late secretors.

To investigate other parameters besides $t_{Secrete}$, we also compared the total amount and the rate of IFN-γ secretion from individual NK cells. Consistent with the $t_{Secrete}$, NK cell populations from a single donor tended to have individual NK cells with heterogeneous amounts and rates of secreted IFN-γ. Surprisingly, the donor with the collective population of NK cells secreting higher amounts of IFN-γ also had individual NK cells with lower rates of IFN-γ secretion (**Figure 2-19**. Error bar: mean±95% CI. Mann-Whitney test, ns: not significant, ***: *p*-value < 0.001, ****: *p*-value < 0.0001). Collectively, these results suggest that human NK cells isolated from different donors display differences in both the rate of IFN-γ secretion, likely reflective of their activation/memory state; and the total amount of IFN-γ secreted, likely reflective of the number of preformed granules containing the cytokine.

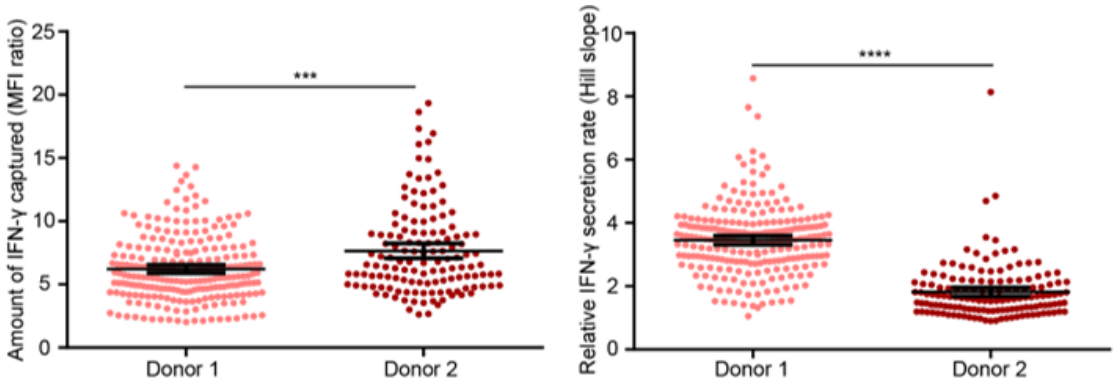

Figure 2-19 The amount of IFN-γ secreted and the relative IFN-γ secretion rate by NK cells during the six hours period.

Next, the frequencies of IFN-γ secretion in nanowells that contained one, two, or three NK cells were quantified to determine whether increasing NK cells density could lead to synergistic activation and faster IFN-γ secretion. Not surprisingly, increasing the number of NK cells within the nanowell increased the frequency of nanowells with IFN-γ^+ beads (**Table 2-2**). In order to investigate evidence of cooperation, we utilized the

probability of single IFN-γ secreting NK cells upon activation (regardless of $t_{Secrete}$), based on the nanowells containing exactly one NK cell. The experimentally computed frequencies for nanowells containing both 2 and 3 NK cells were lower than the theoretically computed frequencies, indicating that there was no significant evidence of cooperation or synergistic activation (**Table 2-2**). As the cell density in the nanowell increased, frequencies of IFN-γ secreting NK cells also increased as expected; however, there was no evidence for significant cooperation or synergistic effect.

Table 2-2 The frequency of IFN-γ secreting NK cells under various cell density conditions.

Donor	Number of cells per well	Number of single beads	Number of cells that were IFN-γ positive	IFN-γ secretion frequency (experimental)	IFN- γ secretion frequency (expected)
Donor 1	1 cell	732	246	0.34	0.34
	2 cells	369	159	0.43	0.56
	3 cells	131	71	0.54	0.71
Donor 2	1 cell	420	153	0.36	0.36
	2 cells	490	204	0.42	0.59
	3 cells	231	106	0.46	0.74

In summary, these results obtained by tracking the phenotype and dynamic secretion of IFN-γ from individual NK cells demonstrated that the NK cells classically defined as cytolytic ($CD16^+$) were also immediate secretors of IFN-γ, at least upon mitogenic stimulation.

2.4. Discussion

We have demonstrated a high-throughput assay for profiling the dynamic secretion of cytokines from individual immune cells while preserving high imaging resolution that was made possible by the fabrication of thin-bottom (<100 μm) PDMS-based nanowell arrays. This single-cell assay uses nanowell arrays for co-incubating cells with functionalized beads and thus can be readily integrated with our reported TIMING

platforms to enable tracking of the key functional attributes of immune cells including phenotype, motility, cytotoxicity, and cytokine secretion; it can also serve as a front-end screen for identifying functional attributes that can be interrogated at the molecular level using multiplexed transcriptional profiling (Romain et al., 2014; Liadi et al., 2015). Although we have demonstrated the application of this method in the context of NK cell IFN-γ secretion, the method can be adapted to other immune cells as well as other cell types for monitoring combined cellular behaviors, protein secretion, and transcriptional profiling. Furthermore, since the multiplexing of beads based on the Luminex platform (Elshal and McCoy, 2006; Cao et al., 2015) is extensively documented, it should be straightforward to expand the number of analytes secreted by individual cells simultaneously.

PDMS is widely used in microfluidics primarily because it is low-cost, optically transparent, biocompatible, and gas permeant. Despite these advantages, one of the major drawbacks of PDMS is the non-specific adsorption (NSA) of proteins onto its surface (Yu, Xiao, and Dang, 2015; Dundua, Franzka, and Ulbricht, 2016; Liu et al., 2016). In dynamic imaging applications akin to what we have outlined, the NSA of both the secreted proteins and the labeled detection antibodies severely impacts both the detection limit and assay reliability/reproducibility. PEG, likely because of hydration, behaves as a hydrogel that is effective in preventing NSA (Heyes et al., 2007; Nie et al., 2014; Wong and Ho, 2009). We sought to take advantage of this property of PEG by employing a simple protocol that enables the rapid modification (20 min) of oxidized PDMS by commercially available PLL-g-PEG, in aqueous environments. We demonstrate that this simple step dramatically decreases the NSA of antibody-dye conjugates onto the surface of PDMS. Furthermore,

since biotin-derivatized PEG (PLL-g-PEG-biotin) is also commercially available, this provides an avenue for surface modifying the PDMS to introduce adhesion molecules like biotinylated ICAM-1, or antibodies against the natural cytotoxicity receptors (NCRs) or CD3 to study lymphocyte activation. We have utilized our platform to profile the phenotype of human NK cells that respond quickest to stimulation. Although NK cells have been divided into two separate subsets with reciprocal functionalities — $CD56^{dim}CD16^{+}$ associated with cytotoxicity and $CD56^{bright}CD16^{-}$ with cytokine secretion — our data (tracking individual cell phenotypes with their ability to secrete IFN-γ) demonstrate that the $CD16^{+}$ NK cells are the early secretors of IFN-γ upon activation. Our results are consistent with other correlative studies that have also suggested that the $CD56^{dim}$ population might, in fact, be the early cytokine secretors upon activation through natural cytotoxicity receptors (NCRs) (Maria et al., 2011). Since it has also been shown that the secretion pathway for cytokines, like tumor necrosis factor (TNF) and IFN-γ in NK cells, is distinct from the pathway used for the secretion of perforin (Reefman et al., 2010), the existence of an elite population of $CD16^{+}$ NK cells capable of both lytic and rapid cytokine secretion fits with the pivotal role of NK cells in innate immunity.

NK cells also present a clinically appealing avenue for the treatment of tumors. Since the activation of NK cells is mediated by a panel of activating and inhibitory receptors, they offer clear translational advantages. First, unlike T cells, NK cells do not require HLA typing or peptide-epitope presentation. Second, NK cells directly recognize and lyse transformed cells either due to missing HLA expression or due to the elevated expression of stress ligands (Lanier, 2008). Third, the translation of NK cells as drugs does not require *a priori* identification of tumor-associated antigens (Becker et al., 2016).

Additionally, the infusion of NK cells has been proven to be largely safe with no significant toxicity concerns (Becker et al., 2016; Rezvani and Rouce, 2015). The biggest disadvantage of NK cell therapies, however, has been the disappointing persistence of NK cells. With newer methods of expansion *ex vivo* (Romee et al., 2016; Sakamoto et al., 2015), and the ability to propagate cytokine-induced memory NK cells, these cells are poised to join the immunotherapeutic arsenal in our fight against cancers. As our work suggests, the existence of subpopulations of NK cells that are polyfunctional ($CD16^+$ [cytotoxic] and IFN-γ secreting) are likely to be of keen interest in immunotherapy.

Chapter 3

T-cell correlates of response to PD-1 blockade treatment in AML

3.1. Introduction

Immunotherapy, utilizing the immune system to eliminate cancer cells, has revolutionized the landscape of cancer treatment and contributed to a durable, long-lasting response in the clinic. Unlike traditional cancer treatment, immunotherapy is based on the understanding of how and where the immune system fails to control tumor growth and facilitate the reinvigoration of the immune system to attack tumor cells (An and Varadarajan, 2018). T cells are considered as the central players in the anti-tumor army (Galon and Bruni, 2019). The classical paradigm of T cell activation and development depends on the engagement of dual signals: (1) antigen presented by major histocompatibility complex (MHC) on antigen-presenting cells (APC) to the T cell receptor (TCR), and (2) the interaction between positive regulator molecule (CD80 or CD86) on APC and CD28 expressed on T cells. The second signal can be either co-stimulatory or co-inhibitory signaling receptors that positively or negatively modulate the TCR signaling, thus determines the fate of the T cells (Chen and Flies, 2013). This regulatory mechanism of T cells usually maintains the immune balance between mounting T cell-mediated immune response and attenuating T cell activity; however, the malignantly transformed cells can take advantage of this mechanism to escape from immune surveillance by presentation of ligand of co-inhibitory receptors or immune checkpoint molecules thus providing immunosuppressive environment and attenuation of T cell activity. Physically blocking immune checkpoint molecules can prevent the interaction between immune checkpoint molecules and their ligands, resulting in suppression of the negative signal of

T cells received from cancer cells and initiation of an immune response against tumor cells. Immune checkpoint inhibition via monoclonal antibody has been translated to clinical setting and demonstrated successful, promising, durable clinical responses as monotherapy or combination cancer therapy, and FDA has approved multiple immune checkpoint inhibitors for treating in various types of cancers (such as melanoma, non-small-cell lung cancer, renal cell carcinoma, and bladder cancer) (Topalian, Drake, and Pardoll, 2015; Sharpe and Pauken, 2018; Wei, Duffy, and Allison, 2018).

The programmed cell death protein-1(PD-1)-PD-1 ligand (PD-L1)-axis is one of the dominant immune checkpoint pathways associated with the tumor microenvironment (Topalian et al., 2016). PD-1 (encoded by *PDCD1*) is a surface protein expressed on multiple cells, including activated and exhausted T cells (Simon and Labarriere, 2017). PD-L1 is found on a broad range of cells, including T cells, B cells, dendritic cells, macrophages, endothelial cells, and also cancer cells (Sharpe and Pauken, 2018). Upon the interaction of PD-1 and PD-L1, tyrosine residue of PD-1 cytoplasm region gets phosphorylated and recruits SHP-2 (a protein tyrosine phosphatase, Src homology 2 domain-containing tyrosine phosphatase 2), which suppresses the TCR signaling via dephosphorylation of proximal signaling molecules, eventually attenuating the function of T cells and dampening the immune response. Recent studies have indicated that the CD28 rather TCR might be the preferable target subjected to SHP-2 induced-dephosphorylation resulted from PD-1-PD-L1 interaction (Krueger and Rudd, 2017; Mellman et al., 2017), and CD28 costimulatory signal was necessary for effective PD-1 blockade therapy in a mouse model and lung cancer patients (Kamphorst, Wieland, et al., 2017). Mechanistically, the antibody against PD-1 invigorates T cell function and reverse T exhaustion to restore

anti-tumor response. Currently, there are five FDA-approved PD-1 or PD-L1 inhibitors for the treatment of certain cancer patients (Gong et al., 2018), and a large number of clinical trials underway involve anti-PD-1 or anti-PD-L1 drugs (Tang,Jun et al., 2018; Tang,J., Shalabi, and Hubbard-Lucey, 2018); nevertheless, only a fraction of cancer patients benefit from such treatments (Hellmann, Friedman, and Wolchok, 2016; Singh et al., 2019). Many studies focus on the exploration of prognosis or predictive biomarkers to help patient stratification, maximize the patient benefit, and help avoid unnecessary toxicity and cost to patients (Topalian et al., 2016). Previous studies showed that the PD-L1-expression in baseline tumor specimen was associated with response to PD-1 blockade treatment, and FDA has approved four immunohistochemistry-based tests for detection of PD-L1 expressions in solid tumors, such as non-small cell lung cancer (NSCLC) and melanoma (Ancevski Hunter, Socinski, and Villaruz, 2018; Garon et al., 2015; Borghaei et al., 2015; Larkin et al., 2015; Brahmer et al., 2015), as a guide for patient selection. However, this method comes with biological and technical variables (e.g., the intra-tumoral or inter-tumoral heterogeneity (Phillips et al., 2015), and the difference in protocols (Ancevski Hunter, Socinski, and Villaruz, 2018)) which can hinder the accurate evaluation of PD-L1 expression. It was reported that a fraction of PD-L1 negative patients with squamous-NSCLC and metastatic melanoma response to the treatment, which suggested PD-L1 expression in tumor tissue could not serve as a general biomarker regardless of the cancer type (Ancevski Hunter, Socinski, and Villaruz, 2018; Motzer et al., 2015; McDermott et al., 2016; Ma,Weijie et al., 2016; Gandini, Massi, and Mandalà, 2016; Larkin et al., 2015). Other parameters have been investigated as potential predictive and prognostic biomarkers, including tumor-related factors (tumor mutational burden (Yarchoan, Hopkins, and Jaffee,

2017), neoantigen (Yi et al., 2018), micro-satellite instability of tumor cells (Le et al., 2015)), and immune system related components, mainly associated to T cell (immune cell infiltration (Hamid et al., 2011; Tumeh et al., 2014; Chen et al., 2016; Gide et al., 2019), peripheral immune cell frequency (Manjarrez-Orduño et al., 2018; Krieg et al., 2018), circulating T cells cytotoxicity (Iwahori et al., 2019), treatment-induced certain subset peripheral T cell proliferation (Kim,Kyung Hwan et al., 2019; Kamphorst, Pillai, et al., 2017), TCR clonality (Hogan et al., 2018; Sade-Feldman et al., 2018), combination of T cell proliferation and tumor burden (‘reinvigoration score) (Huang et al., 2017), integration of tumor mutation burden and T cell-related genes (Cristescu et al., 2018)), and gut microbiome composition (Matson et al., 2018; Gopalakrishnan et al., 2018; Routy et al., 2018).

Acute myeloid leukemia (AML) is a type of cancer, which involves the uncontrolled growth of myeloid progenitor cells, and is the most common leukemia in adults. This aggressive disease is with a higher incidence in elderly patients, who show very poor clinical outcomes: less than 10% elder patients (≥ 60 years old) survive more than five years since diagnosis (Alibhai et al., 2009; Menzin et al., 2002). Hypomethylating agents (HMA) is often used as a frontline treatment for senior AML patients and is also considered as one of the potential therapies for relapsed/refractory AML patients (Stahl et al., 2018). It was reported that HMA demonstrates dual but antagonistic effects on anti-tumor response (Daver, Boddu, et al., 2018): (1) increasing the expression of cancer-related antigen to improve the immunogenicity of tumor (Goodyear et al., 2010), activation of tumor suppressor genes (Bewersdorf, Stahl, and Zeidan, 2019), upregulation of the MHC-I and co-stimulatory receptors (Chiappinelli et al., 2015; Coral et al., 1999); (2)

upregulation of PD-1 on T cells and PD-L1 on tumor cells which promote T cell exhaustion (Daver, Boddu, et al., 2018). Thus, not surprisingly, recent data suggested that HMA and PD-1 inhibitor have synergistic effects by providing additional stimulation and reverse the immune-suppressive environment to T cells (Daver, Boddu, et al., 2018; Bewersdorf, Stahl, and Zeidan, 2019). However, only a fraction of patients showed favorable clinical response (overall response rate = 33%) (Daver, Garcia-Manero, et al., 2018), which suggests the urgent need for predictive biomarkers to stratify the patient before the initiation of the treatment. There is no doubt that tumor biopsy is the gold standard to assess the progress of the disease and provide a spatial resolution of the tumor microenvironment, nevertheless, it is less convenient to acquire tumor biopsy multiple time for the longitudinal study. Peripheral blood is a highly accessible biological material allowing repeated sampling and long-term follow-up due to its non-invasive property (Quandt et al., 2017; Kamphorst, Pillai, et al., 2017; Huang et al., 2019). Although tumor-infiltrating T cells (T cells in bone marrow, in the context of AML) can reflect the status of the disease more accurately and appropriately, recent studies indicated that circulating T cells might correlate with response to checkpoint blockade therapy in solid tumor (Hogan et al., 2018; Huang et al., 2017, 2019; Manjarrez-Orduño et al., 2018). Additionally, more evidence indicated that tumor-reacting T cells were also found in peripheral blood of melanoma patients even without metastasis, suggesting peripheral blood T cell holds the promise to reflect T cells at tumor sites (Gros et al., 2016; Cohen et al., 2015; Huang et al., 2017; Baitsch et al., 2011).

To explore predictive biomarkers and to quantify the impact of treatment-induced immune response at both the site of disease and the peripheral compartment, we evaluated gene expression profile of 64 AML patient-derived T cell populations (bone marrow and

peripheral blood) by RNA-sequencing (RNA-seq) which were collected before the initiation of treatment (baseline, T0) and after the first round of treatment (end of cycle one, EC1). We hypothesized that the comprehensive profiling gene expression signature of T cells would provide insights on the treatment-induced effects on T cells and enable the identification of putative biomarkers for immune checkpoint blockade therapy.

3.2. Methods

3.1.1. Human subjects statement

All work outlined in these documents was performed according to protocols approved by the Institutional Review Board at the University of Houston and the University of Texas M.D. Anderson Cancer Center.

3.1.2. Clinical trial

All patients were enrolled in phase II clinical trial (NCT02397720), which was designed for older patients (>65 years) with newly diagnosed AML or relapsed/refractory AML patients using a combination treatment of 5-azacitidine (AZA) and Nivolumab (anti-PD-1 monoclonal Ab). **Figure 3-1** illustrated the design of this clinical trial and the sample collection time.

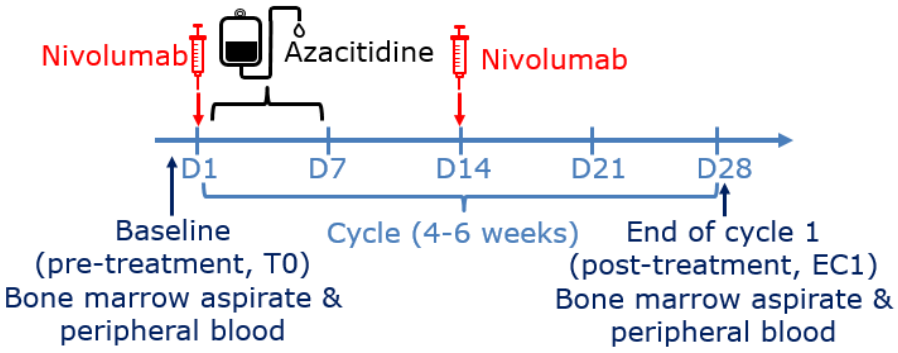

Figure 3-1 Design of the clinical trial

Peripheral blood mononuclear cell (PBMC) and bone marrow aspirate (BMA) samples from AML patients were collected, either before the beginning of treatment or after the 1st cycle of treatment.

3.1.3. Cells and antibodies

The peripheral mononuclear blood (PBMC) and bone marrow aspirate (BMA) from patients were collected as previously described (Daver, Garcia-Manero, et al., 2018). Briefly, PBMCs or BMAs isolated the blood or bone marrow from patients by density centrifugation, washed with PBS+10% fetal bovine serum (FBS), then froze in FBS+10%DMSO and stored in the vapor phase of liquid nitrogen.

All antibodies used were purchased from BioLegend (San Diego, CA): mouse anti-human CD3-FITC (catalog #: 300306, clone: HIT3a), mouse anti-human CD4-APC (catalog #: 317415, clone: OKT4) and mouse anti-human CD8a-PE (catalog #: 301008, clone: RPA-T8).

3.1.4. Fluorescence-activated cell sorting (FACS)

Thawed cryopreserved PBMC or BMA rapidly at 37 ^{o}C till the ice was about 5 mm in diameter, then transferred the cells to pre-warmed media (RPMI1640 media supplemented with 10% FBS; R10) to wash away cryopreserved reagent. Washed PBMC or BMA with 20 ml pre-warmed R10 at 400 × g for 5 min. Re-suspended cells at 1 million/ml in a T25 flask and kept it in a 37^{o}C incubator with 5% CO_2 overnight. On the next day, collected cells from T25 flask and pelleted down cells at 400 × g for 5 min. Cells were kept on the ice for the following steps. Washed cells pellet with 2 ml ice-cold PBS+2% FBS at 4 ^{o}C, then re-suspended in 0.5 ml PBS+2% FBS. PBMC or BMA cells were stained for T cell surface markers with fluorochrome-labeled antibodies: CD3, CD4 and CD8 (15

uL antibody per 10 million cells), followed by incubation for 20 min at 4 ^{o}C in the dark. Washed cells with 2 ml PBS+2%FBS twice at 400 x g for 5 min, and re-suspended cell at 10 million/ml in PBS+2%FBS. Sytox Blue, as the live/dead cell marker, was added at 1 uL per 10 million cells.

All sortings were done at flow cytometry and cellular imaging core facility at the University of Texas MD Anderson Cancer Center, on FACSAria Fusion, or FACSAria IIIu. Single live (Sytox Blue negative) $CD3^{+}CD4^{+}CD8^{-}$ cells (CD4 T cell) or $CD3^{+}CD4^{-}CD8^{+}$ cells (CD8 T cell) were sorted directly to lysis buffer (100 uL Buffer RA1 and 2 uL TCEP from MACHEREY-NAGEL NucleoSpin® RNA XS kit). The targeted number was set as 100,000 for both CD4 and CD8 populations.

3.1.5. Total RNA extraction from sorted cells

The cell lysate was snap-frozen using liquid nitrogen and kept at -80 ^{o}C until processed. RNA isolation was achieved using the NucleoSpin® RNA XS kit (MACHEREY-NAGEL, 740902) (Mahendra et al., 2019). Briefly, chaotropic ions and RNase-inhibitor containing lysis buffer lysed cells, inactivated RNases, and adjusted condition for silica membrane-based RNA binding. The membrane-bound DNA was removed by on membrane DNase treatment. Unwanted molecules, such as salt, metabolites, and macromolecular cellular components were removed by washing. RNA was eluted in RNase-free water. To further eliminate the potential remaining DNA contamination in RNA samples, another round of DNase treatment using NucleoSpin® RNA Clean-up XS kit (MACHEREY-NAGEL, 740903) was performed, and DNA-free RNA was eluted RNase-free water and stored at -80 ^{o}C.

3.1.6. Quantification and quality assessment of RNA/cDNA

Agilent 2100 BioAnalyzer with Agilent RNA 6000 Pico chip was used for quantification and integrity check of RNA samples. Qubit 2.0 Fluorometer with Qubit dsDNA HS assay kit, Agilent 2100 BioAnalyzer with Agilent High Sensitivity kit was applied for measurement of concentration of cDNA library and library size distribution evaluation. All quality control experiments were performed at UH Seq-N-Edit Core (SNEC).

3.1.7. Preparation of cDNA library

SMART-Seq® v4 Ultra® Low Input RNA Kit for Sequencing (Takara, 634891) was used for cDNA library preparation per manufacturer protocol, and the PCR cycle number depends on total RNA quantity (one nanogram of total RNA was used if applicable). One nanogram cDNA was used as input for tagmentation and barcoding, using Nextera XT DNA Library Preparation Kit (Illumina, FC-131-1096) and Nextera XT Index Kit v2 Set A (Illumina, FC-131-2001). The cDNA library was kept at -20 ^{o}C.

3.1.8. RNA-sequencing and gene expression analyses

75-bp paired-end RNA-sequencing (RNA-seq) was done through Illumina NextSeq 500 sequencer using a High output flow cell at UH SNEC. RNA-seq data (fastq.gz format) of CD4 T cells and CD8 T cells from healthy donors were obtained from GSE74310 (Corces et al., 2016) and GSE60424 (Linsley et al., 2014). Sequencing data quality was checked using FastQC tool (“Babraham Bioinformatics - FastQC A Quality Control Tool for High Throughput Sequence Data,” 2019), followed 5’ and 3’ trimming and transcript alignment to reference genome using HISAT2 package (Kim,Daehwan, Langmead, and Salzberg, 2015). The annotation of the mapped gene was obtained using R package

"GenomicAlignments" and "TxDb.Hsapiens,USCS.hg38,knownGene". Differentially expressed genes (DEGs) were recognized using DEseq2 (Love, Huber, and Anders, 2014), and the differential expressed pathways were identified using Gene Set Enrichment Analysis (GSEA) software provided by Board Institute (Subramanian et al., 2005; Mootha et al., 2003). Pathway enrichment analyses were done in Cytoscape (Shannon et al., 2003) using Enrichment Map (Merico et al., 2010; Reimand et al., 2019).

3.1.9. Deconvolution of bulk RNA-sequencing

The bulk RNA-seq data of T cells from healthy donors and AML patients were processed using kallisto package (Bray et al., 2016) to acquire transcript per million reads (TPM). Prebuilt indices (Homo-sapiens.GRCh38.cdna.all.release-94.k31.idx.gz) was downloaded from kallisto transcriptome indices sites. The transcripts (ensemble transcript ID with version) were converted to gene symbol using the biomaRt package in R (Durinck et al., 2005), and for multiple transcripts mapped to the same gene, only the transcript with maximum TPM of the same gene was kept. We use bseq-sc packages (Baron et al., 2016) to deconvolute bulk RNA-sequencing data to estimate the cell type composition (Newman et al., 2015). This method utilized sc-RNA sequencing data to build up a matrix containing cell type-specific gene expression as the signature, which will be used as a reference for estimation of the subpopulations in bulk RNA-seq samples mathematically. We used previously published T cell subset-specific signature from colorectal cancer patient as our reference matrix, which including 20 identified T cell subsets (CD4: 12 subsets, CD8: 8 subsets) (Zhang, Lei et al., 2018).

3.3. Results

3.3.1. Quality control of sorted CD4 T cells and CD8 T cells

Stained PBMC or BMA were sorted using the simple strategy indicating by **Figure 3-2**. Single live $CD3^+CD4^+CD8^-$ cells (CD4 T cells) or single live $CD3^+CD4^-CD8^+$ cells (CD8 T cells) were collected into lysis buffer for RNA-isolation.

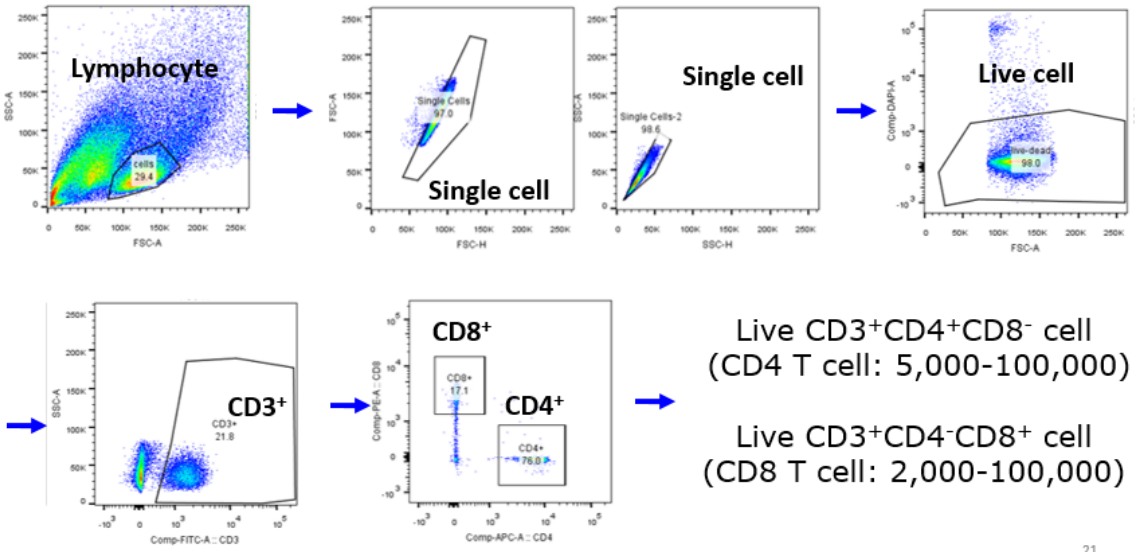

Figure 3-2 Density plot and gating strategy of a representative example.

We examined the frequency of T cells (single, live, $CD3^+$ cells), CD4 T cells, CD8 T cells, and also the ratio of CD4 T cells frequency and CD8 T cells frequency to see if (1) there was a conserved pattern in responder or non-responder samples and (2) if the treatment led to T-cell frequency changes.

For both baseline or post-treatment PBMC samples, there was no significant difference between the responder and non-responders in terms of the T cell frequency, CD4 T cells frequency, CD8 T cells frequency and the ratio of CD4 and CD8 (**Figures 3-3** and **3-4**. Wilcoxon matched pairs test, n.s.: not significant). Comparison paired baseline and post-treatment sample did not show a significantly consistent change in the T cell

frequency, CD4 T cells frequency, CD8 T cells frequency and the ratio of CD4 and CD8, due to the treatment effect (**Figures 3-3** and **3-4**).

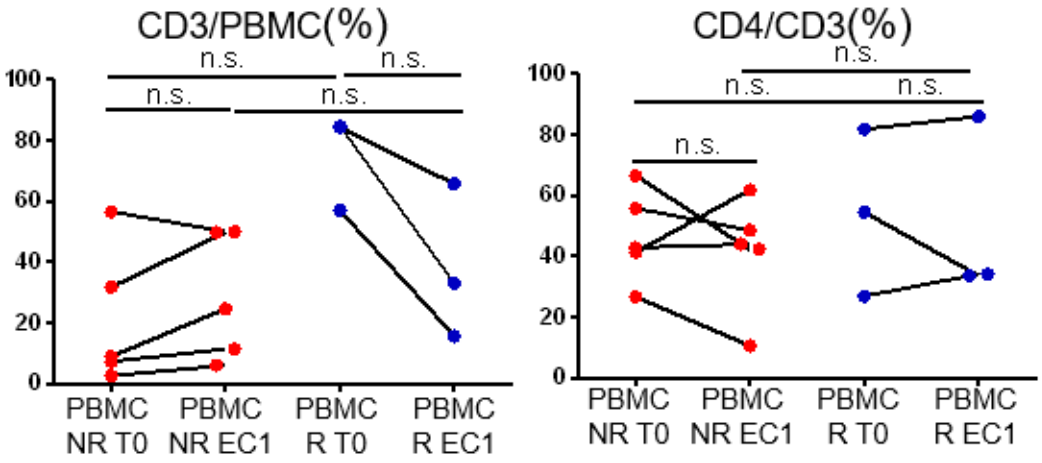

Figure 3-3 Cell frequency change after treatment in PBMC (CD3, CD4).

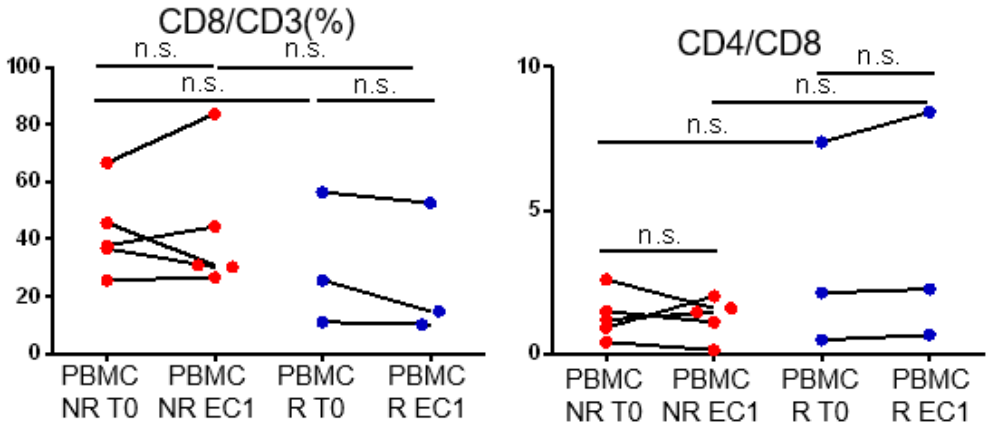

Figure 3-4 Cell frequency change after treatment in PBMC (CD8, CD4/CD8).

For bone marrow T cells, similar trends were observed: (1) no significantly difference between the T cells, CD4 T cells, CD8 T cells frequency, and CD4/CD8 cell ratio in comparison of responder and non-responder; (2) no consistent and very significant change of cell frequency due to the treatment (**Figures 3-5** and **3-6**. Wilcoxon matched pairs test, n.s.: not significant).

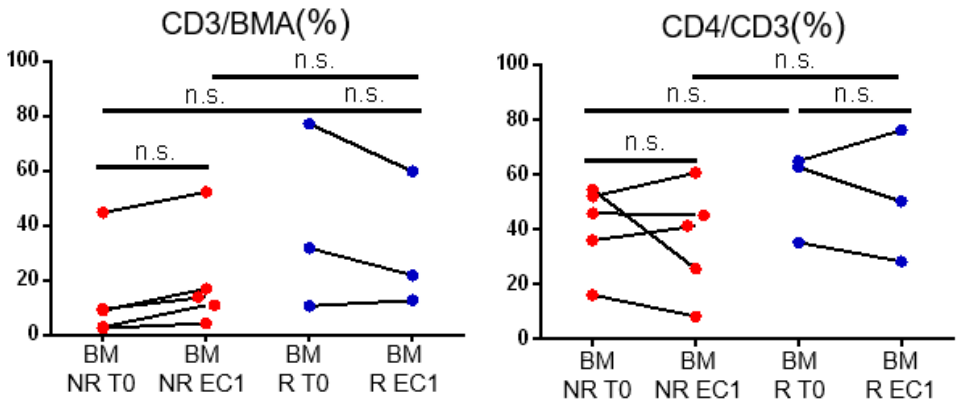

Figure 3-5 Cell frequency change after treatment in BMA (CD3, CD4).

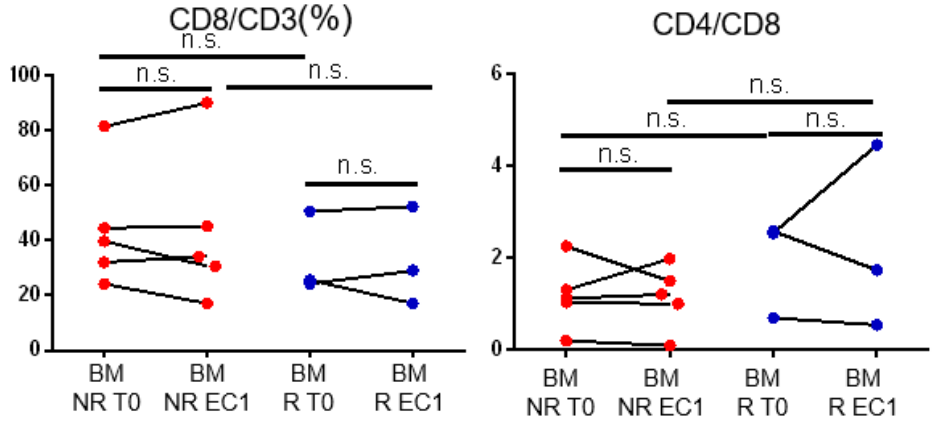

Figure 3-6 Cell frequency change after treatment in BMA (CD8, CD4/CD8).

After sorting, a total of 2000-100,000 CD4 (median cell number 72,000) or CD8 (median cell number 70,000) T cells from 64 peripheral blood or bone marrow patient-derived samples were used directly for the cDNA library preparation *ex vivo* to minimize perturbations to transcriptomic profiles of these cells. The cDNA library of 63 samples was constructed *ex vivo* successfully, followed by barcoding, pooling, and sequencing using 75-bp paired-end, and yield a minimal of 17 million reads per BM T cell library and 2.6 million reads per PBMC T cell library. **Tables 3-1** describes the reads depth of each sample.

Table 3-1 RNA-sequencing reads depth of CD4 T cell samples

Source	Response	Patient	Sampling time	Reads/million	
				CD4	CD8
BM	NR	NR_1	T0	17.6	19.7
		NR_1	EC1	19.2	17.9
		NR_2	T0	19.4	20.1
		NR_2	EC1	19.3	20.1
		NR_3	T0	18.9	19.0
		NR_3	EC1	17.7	20.0
		NR_4	T0	19.5	18.7
		NR_4	EC1	22.1	21.5
		NR_5	T0	19.7	22.5
		NR_5	EC1	22.5	22.0
	R	R_1	T0	19.9	17.7
		R_1	EC1	21.5	22.9
		R_2	T0	23.8	19.1
		R_2	EC1	20.5	22.4
		R_3	T0	19.4	17.2
		R_3	EC1	22.8	21.1
PBMC	NR	NR_1	T0	14.5	5.2
		NR_1	EC1	4.5	7.8
		NR_2	T0	4.9	5.8
		NR_2	EC1	5.0	8.4
		NR_3	T0	4.6	4.6
		NR_3	EC1	5.1	4.5
		NR_4	T0	6.4	6.3
		NR_4	EC1	7.0	6.0
		NR_5	T0	7.8	8.5
		NR_5	EC1	5.8	7.8
	R	R_1	T0	4.9	5.6
		R_1	EC1	2.6	N/A
		R_2	T0	6.0	6.0
		R_2	EC1	8.1	5.7
		R_3	T0	5.9	6.3
		R_3	EC1	6.6	6.4

We compared the normalized gene counts to confirm the purity of sorted T cells. The majority of sorted CD4 T cells from PBMC or BMA (**Figure 3-7**) were

$CD3^+CD4^+CD8^-$ cells, and the majority of sorted CD8 T cells from PBMC or BMA (**Figure 3-8**) were $CD3^+CD4^-CD8^+$ cells. These results suggested that our sorting strategy worked as expected.

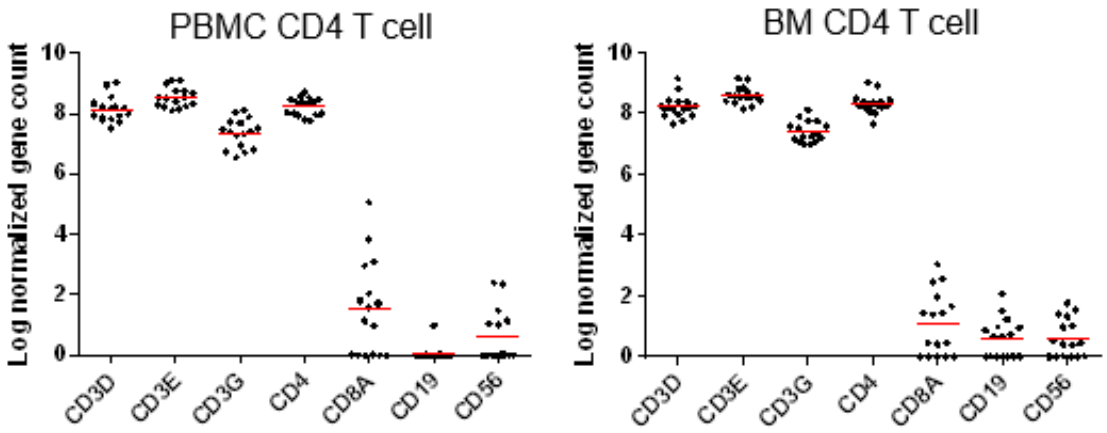

Figure 3-7 Quality control of RNA sequencing (CD4).

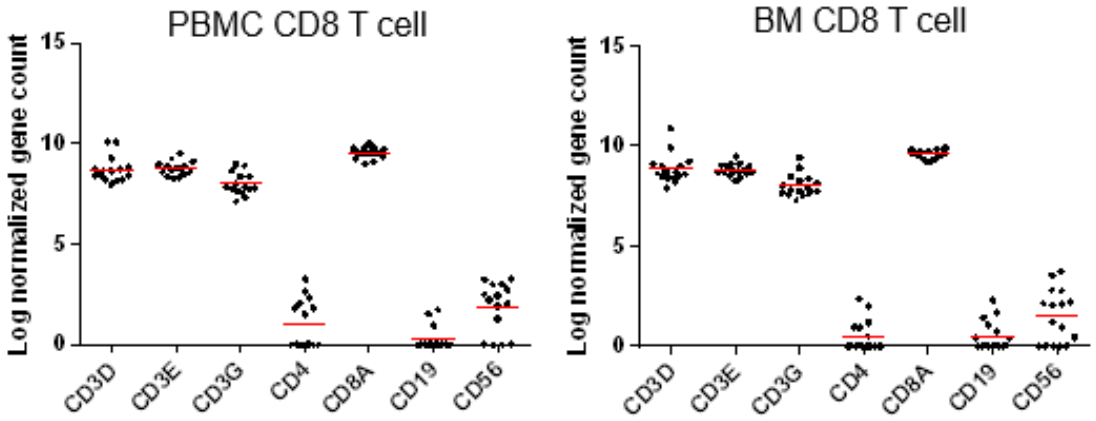

Figure 3-8 Quality control of RNA sequencing (CD8).

3.3.2. AML circulating T cells were more activated and differentiated compared to healthy donor peripheral blood T cells

First, we explored the difference between peripheral T cells from healthy donors and AML patients to see if the circulating AML T cells were more activated and exhausted due to the potential long-term exposure to tumor cells. RNA-seq data of healthy donor (HD)

circulating T cells were obtained from previously published studies (Corces et al., 2016; Linsley et al., 2014). **Table 3-2** depicts the T cells information from healthy donors.

Table 3-2 Information on healthy donor T cells (peripheral)

Donor	Donor	Sex	Age	Reads/million	
				CD4	CD8
HD_A	HD_1	Female	32	15.8	13.4
	HD_2	Female	29	25.4	18.2
	HD_3	Female	22	21.3	17.8
	HD_4	Female	30	19.1	21.0
HD_B	HD_5	Male	28	22.8	18.0
	HD_6	Female	53	36.2	33.5
	HD_7	Female	27	65.6	60.3
	HD_8	Male	28	25.6	21.8

All the samples involving the downstream analyses are summarized as **Figure 3-9**. In this work, we profiled CD4 T cells and CD8 T cells in PBMC and BMA samples from four responder patients (R) and four non-responder (NR) patients. Although there might be multiple cycles of treatments, we only included samples collected at two of early time points: before the initiation of the treatment (baseline, T0), and after the first round of treatment (end of cycle one, EC1), because we would like to focus on the early-stage predictive marker. The cDNA libraries were constructed successfully for 63 out of 64 samples (one PBMC CD8 T cell sample from a responder at the end of cycle one was failed, **Table 3-1** and **Figure 3-9**). Considering the functional differences, CD4 T cells and CD8 T cells were analyzed separately.

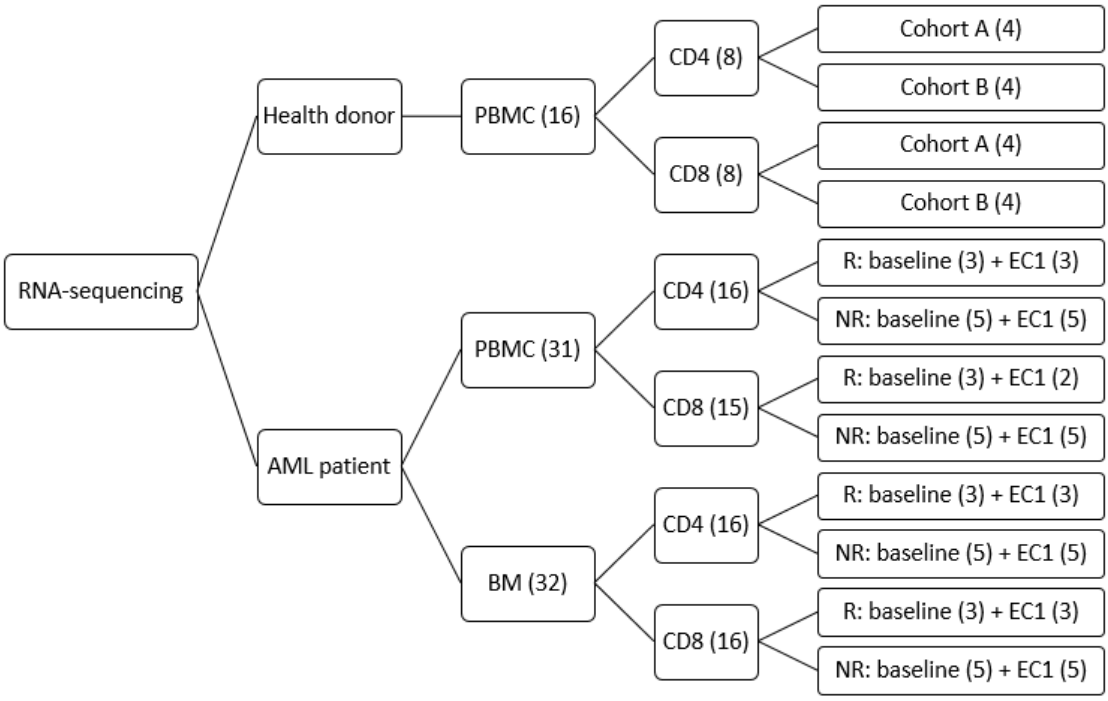

Figure 3-9 Samples used in the RNA-sequencing analyses

To get a better sense of the high-dimensional RNA-seq data, we implemented principal component analysis (PCA), a statistical method to reduce the dimensionality by transform potentially correlated variables into a smaller set of uncorrelated principal components and maintain the majority of variance information from the original dataset. We used using DEGs (**Table 3-3**) as the input of PCA to plot the differential gene profiles for each comparison. In the PCA plots (**Figure 3-10**), each dot stands for a T cell sample: the T cells from HD were labeled in green, T cells from NR were labeled in red, and T cells from R were labeled in blue. As expected, all AML T cells populations (red and blue) clustered away from peripheral blood T cells from healthy donors. We observed two separate clusters of HD T cells; this might because two cohorts (HD_A and HD_B) were independent, and the sample processing protocol was not the same. The distance on the PCA plot indicates the similarity of gene expression profiles of samples. As shown in the

PCA plot (**Figure 3-10**), the gene expression profile of AML T cells was more similar, no matter for CD4 or CD8 T cells, compared to any of the HD T cell clusters; thus we included both HD cohorts for the further analyses to avoid bias.

Table 3-3 DEGs list (T cells from AML against T cells from healthy donors).

T cells (FDR =0.05)	AML PBMC against HD PBMC	
Subset	CD4	CD8
DEGs	9054	8707

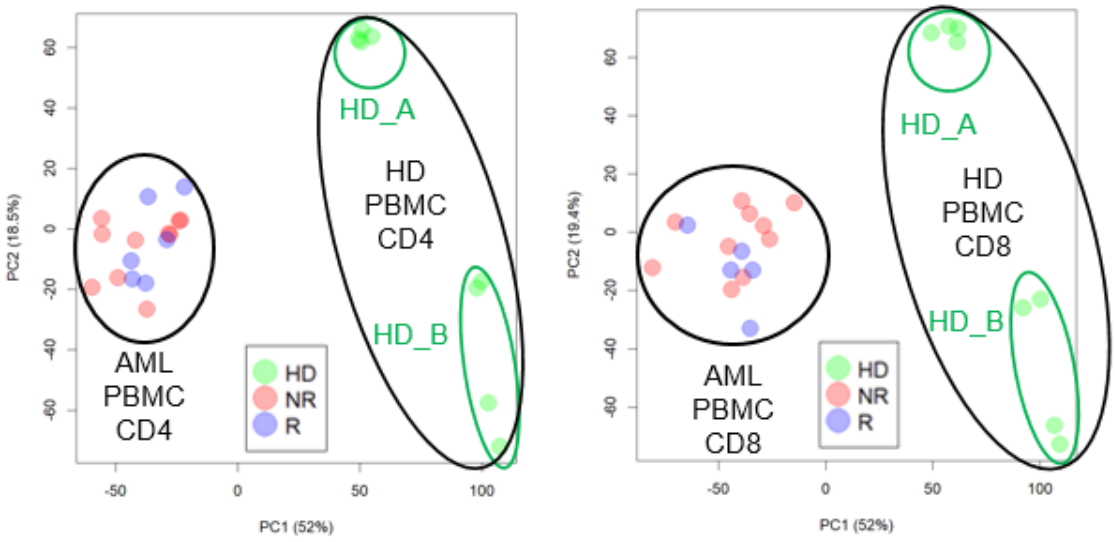

Figure 3-10 PCA plot for AML PBMC T cells and HD PBMC T cells.

To discover what might cause the separation, we performed the pathway enrichment analysis using established gene sets (c7 curated gene sets) related to T cells phenotype and functions (**Figures 3-11** and **3-12**), and we plotted the enrichment pathway using the Enrichment Map application in Cytoscape using a cutoff q-value = 0.10. Nodes (circles colored red or blue) represent pathways, and the edges (red or blue connecting lines) represents the overlapping gene among pathways. The size of nodes represents the number of genes enriched within the pathway, and the thickness of edges represents the number of the overlapping gene. The shades of the color indicated the normalized enrichment score

(NES) from GSEA result, and the higher the NES/darker the color was, the more enrichment of the pathway was observed. Red/blue indicated pathways were enriched in the AML PBMC/HD PBMC. AML T cells were more differentiated and more active compared to the healthy donor T cell while HD T cells displayed more naïve-like phenotype, for both CD4 T cells and CD8 T cells.

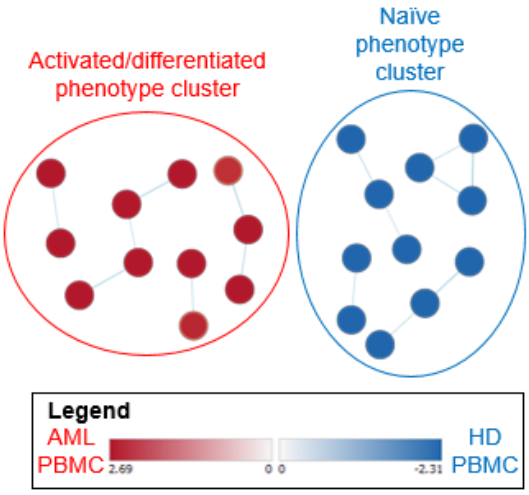

Figure 3-11 The GSEA-derived enriched c7 curated pathways of enriched by PBMC CD4 T cells were plotted using the enrichment map application in Cytoscape.

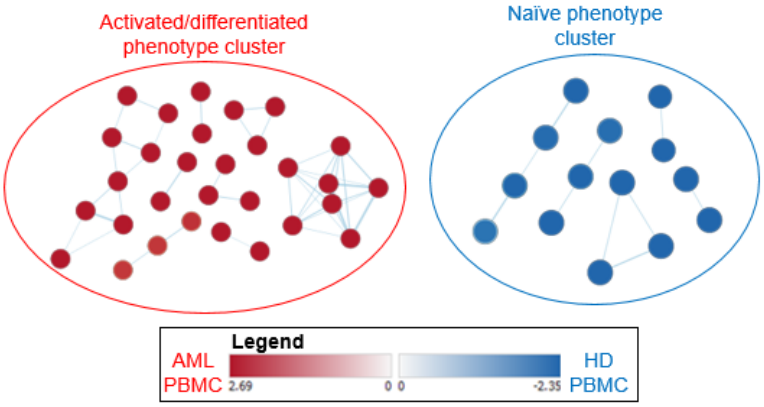

Figure 3-12 The GSEA-derived enriched c7 curated pathways of enriched by PBMC CD8 T cells were plotted using the enrichment map application in Cytoscape.

The GSEA results of the comparison of AML peripheral T cells and HD peripheral T cells suggested the transcriptomic profile difference might due to the phenotype and

differentiated status of the T cells. Thus we deconvoluted T cell subset composition from the bulk RNA-seq data using benchmark gene derived from scRNA-sequencing results mentioned earlier. Not surprisingly, CD4 T cells from HD had a higher percentage of naïve T cells and a lower percentage of differentiated subsets (T_{CM}: central memory T cell, T_H1: type 1 T helper cell, and T_{reg}: regulatory T cell), comparing to PBMC CD4 T cells from AML patients (**Figure 3-13**. Mann-Whitney test. ****: *p*-value ⩽ 0.0001, ***: *p*-value ⩽ 0.001, **: *p*-value ⩽ 0.01). Previous studies showed that the frequency of T_{reg} in CD4 T cells from AML patient peripheral blood were higher than the healthy donor (Wang, Xingbing et al., 2005; Williams et al., 2018; Shenghui et al., 2011; Szczepanski et al., 2009). We found a similar trend for CD8 T cells as well: HD CD8 T cells contained more naïve phenotype but less effector (T_{EFF}) and exhausted (T_{ex}) phenotypes (**Figure 3-14**, Mann-Whitney test. ****: *p*-value ⩽ 0.0001, ***: *p*-value ⩽ 0.001, **: *p*-value ⩽ 0.01.).

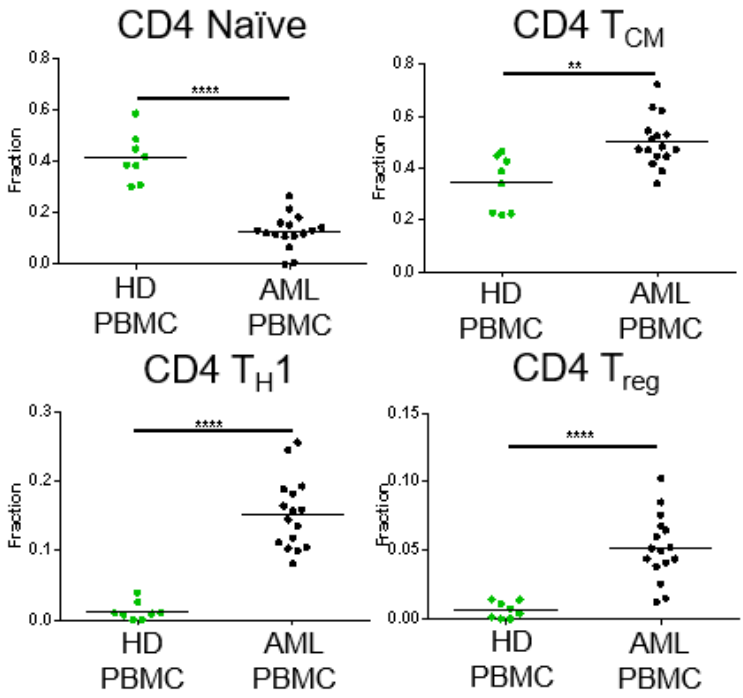

Figure 3-13 Cell subset composition of peripheral CD4 T cells.

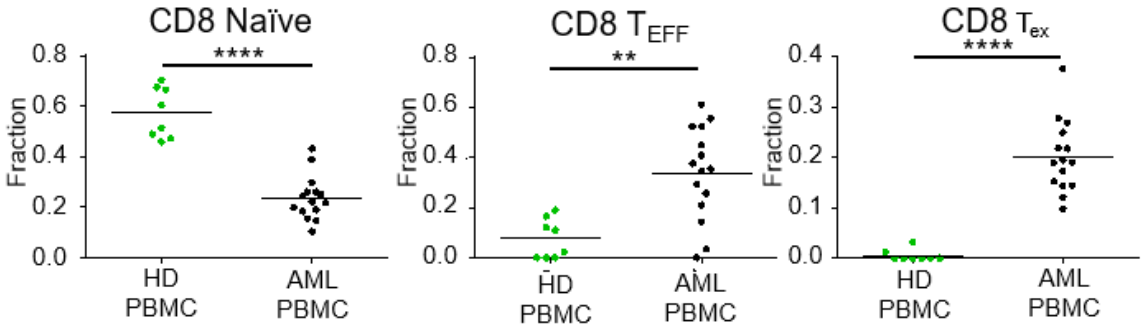

Figure 3-14 Cell subset composition of peripheral CD8 T cells.

Collectively, our pathway enrichment analysis and T cell phenotype composition data consistently revealed that T cells from AML patients were more active and differentiated compared to HD PBMC T cells, in line with the previous study, suggesting the pre-existing immune response of peripheral T cells towards to tumor cell (Dieu,Le et al., 2009).

3.3.3. BM marrow CD8 T cells might contain more T_{EFF} compared to peripheral T cells in pre-treatment samples

We compared the gene expression profile of AML T cells from PBMC or BM compartments and found little DEGs between two groups (BM vs. PBMC, CD4 or CD8, T0 or EC1; DEGs <5, FDR < 0.25). The GSEA-derived analysis results indicated that the CD8 T cells from BM were more activated/differentiated compared to the cells in the PBMC compartment before the start of treatment (Kaech et al., 2002) (**Figure 3-15**: enrichment pathways cluster, cutoff q-value = 0.10).

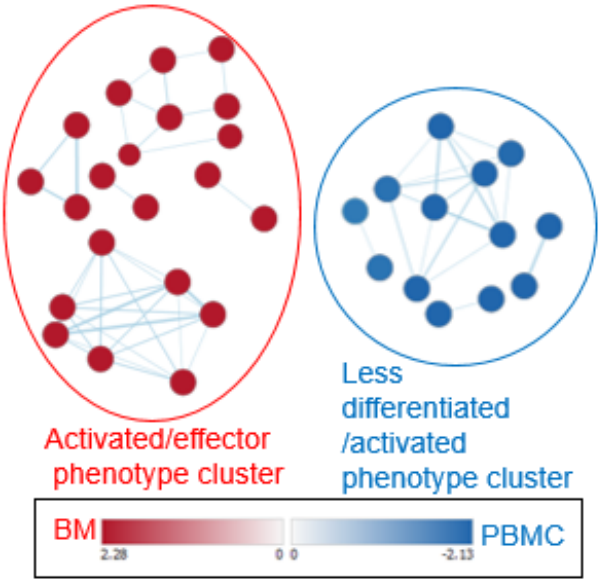

Figure 3-15 The GSEA-derived enriched c7 curated pathways of enriched by CD8 T cells from PBMC and BM were plotted using the enrichment map application in Cytoscape.

Then we examined the T cell composition from the deconvolution result and found for CD8 T cells sampled at baseline and found that the BM compartment might have a higher percentage of T_{ex} compared to PBMC CD8 T cells regardless of the clinical response (**Figure 3-16**, Mann-Whitney test. N.s.: not significant, *p*-value > 0.05).

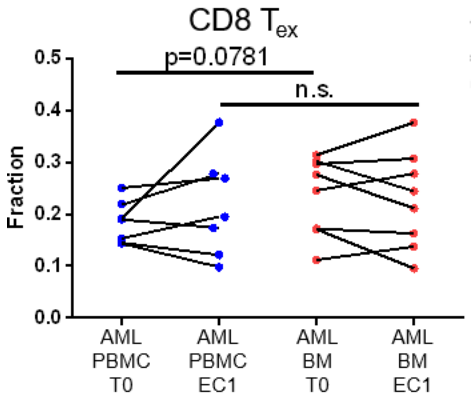

Figure 3-16 Fraction of T_{ex} subset in CD8 T cells from PBMC and BM of AML patients at different time points.

3.3.4. PBMC CD8 T cells showed treatment-induced activation and proliferation after one cycle of treatment

To investigate the treatment effect on T cells, we compared the gene expression profile of T cells (PBMC CD4, PBMC CD8, BM CD4, and BM CD8) collected before the treatment and after the first cycle of treatment. The DEG analysis only yielded with few genes, indicating the possible changes in the individual genes were not able to resolve the difference due to the treatment. **Figure 3-17** represented one of the enriched pathways (Agarwal et al., 2009) in the post-treatment PBMC CD8 sample, comparing the pre-ranked gene list of gene signatures of the baseline against after one cycle of treatment, which suggested treatment-induced activation of circulating CD8 T cells.

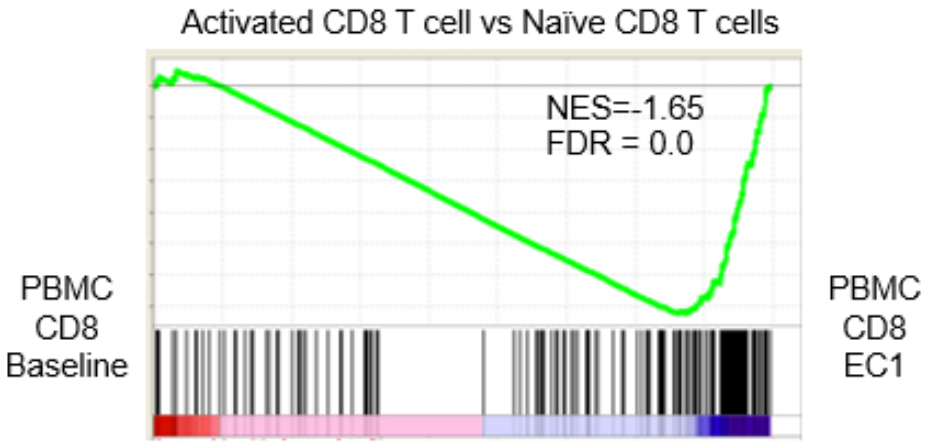

Figure 3-17 GSEA enrichment plot derived from the pre-ranked gene list comparing PBMC CD8 T cells collected at the baseline and after one cycle of treatment.

Considering the integration of the subtle gene expression change from a set of genes rather than individual genes, GSEA facilitated the discovery of systematic and subtle changes. Our GSEA result implied the noticeable treatment-induced activation/differentiation/proliferation of PBMC CD8 T cells, regardless of the patients' response to the treatment (**Figures 3-18, 3-19**, cutoff q-value = 0.10).

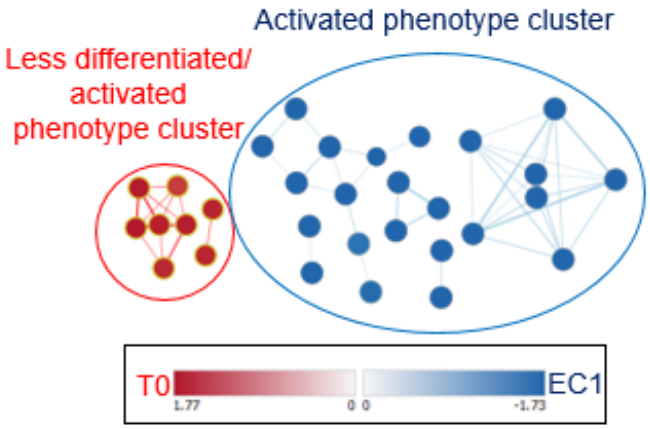

Figure 3-18 The GSEA-derived enriched c7 curated pathways of enriched by CD8 T cells from PBMC collected at baseline were plotted using the enrichment map application in Cytoscape.

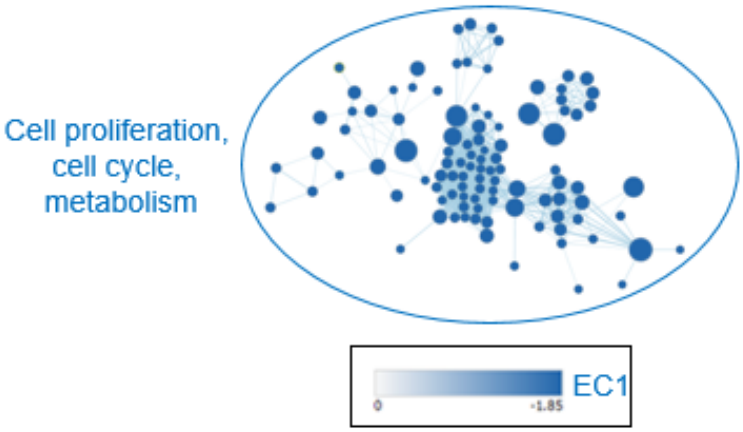

Figure 3-19 The GSEA-derived enriched c2 curated pathways of enriched by CD8 T cells from PBMC collected at baseline were plotted using the enrichment map application in Cytoscape.

3.3.5. Exhausted CD8 T cells frequency in PBMC and BM is a potential actionable biomarker of favorable clinical outcome to PD-1 inhibitor treatment

To explore the potential biomarker to predict the response to the treatment, we compare CD8 T cells from R and NR at the different time point (T0, EC1) and from different compartments (PBMC, BM). The number of DEGs indicated that the difference

of gene expression profile existed between T cells from R and NR (**Table 3-4**), and the PCA plots showed clear separation of T cell cluster from R and NR (**Figure 3-20**), indicating the distinct transcriptomic expression pattern between T cells of responder and non-responder.

Table 3-4 DEGs list (T cells from NR against R).

T cells (FDR = 0.25)	PBMC		BM	
Sampling time	T0	EC1	T0	EC1
DEGs	1655	14	32	7

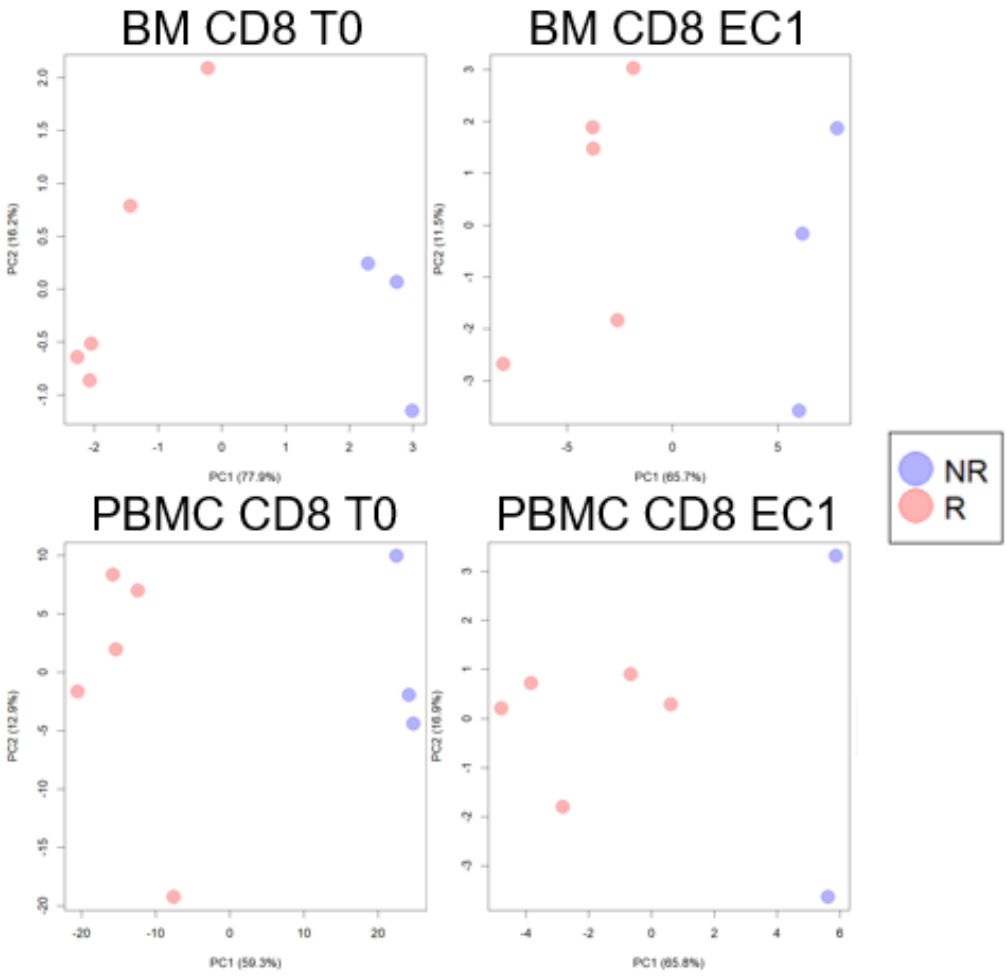

Figure 3-20 The PCA plots demonstrated identified DEGs from CD8 T cells were able to resolve two distinct populations.

The enriched pathway analysis result showed that before the initiation of the therapy, PBMC CD8 T cells from NR tended to be more PD-1^{hi} CD8 T cells-like phenotype, while circulating CD8 T cells from R were more similar to naïve CD8 T cells (Duraiswamy et al., 2011) (**Figure 3-21**).

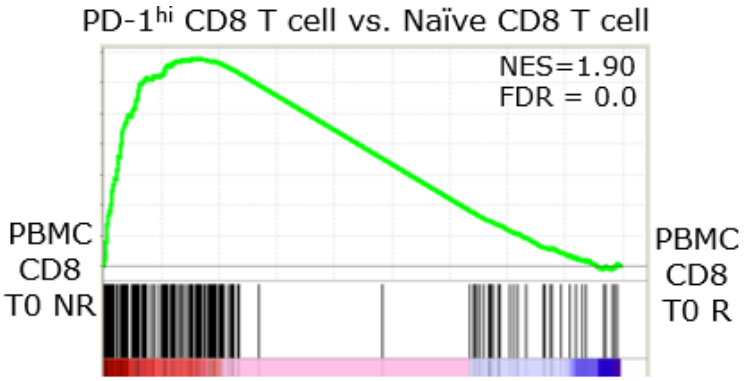

Figure 3-21 GSEA enrichment plot derived from the pre-ranked gene list comparing PBMC CD8 T cells from NR and R collected before the treatment.

We further inspected the relative abundance of exhausted CD8 T cells (T_{EFF}) to the functional CD8 T cells (T_{ex}) of circulating T cells and bone marrow T cells. CD8 T cells from non-responders showed a higher ratio of effector-like/exhausted-like CD8 T cells (**Figures 3-22, 3-23**. Paired sample: Wilcoxon matched pairs test; unpaired sample: Mann-Whitney test. N.s.: not significant, *p*-value < 0.05). This finding suggested the relative abundance of effector and exhausted CD8 T cells (plasticity) could serve as subpopulations relevant for clinical response and patient stratification of PD-1 blockade therapy.

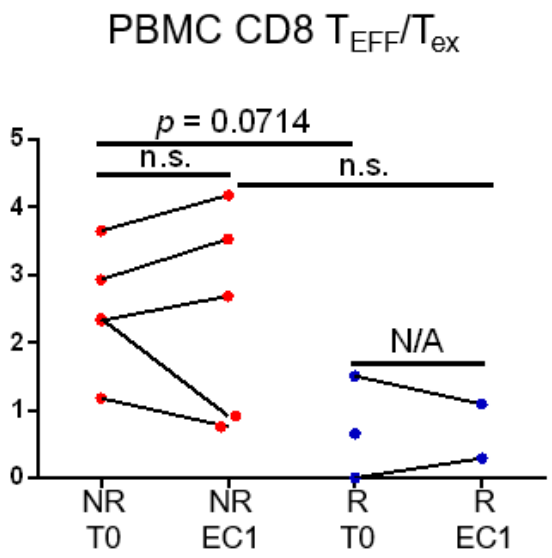

Figure 3-22 PBMC of NR has a higher ratio of T_{ex}/T_{EFF} in comparison to R.

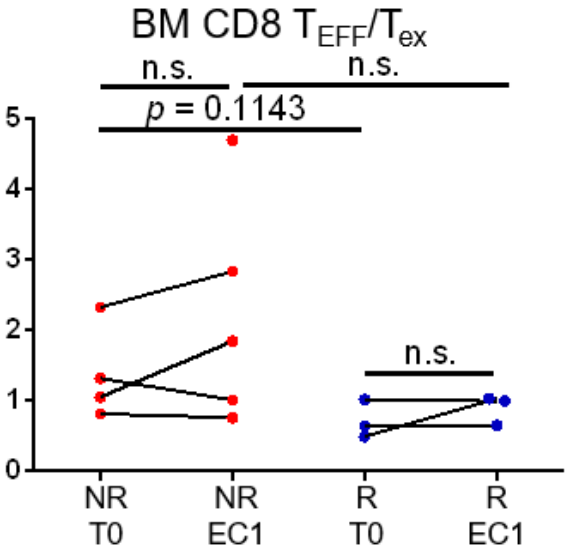

Figure 3-23 BM of NR has a higher ratio of T_{ex}/T_{EFF} in comparison to R.

3.4. Discussion and future direction

3.4.1. Discussion

In this work, we leveraged RNA-sequencing on patients' CD4 and CD8 T cells from blood and bone marrow to understand the biological process changes induced by HMA-PD-1 inhibitor treatment and explore the potential predictive biomarker to clinical outcome. By comparing the gene expression profile of peripheral CD4 and CD8 T cells

from AML patients against to circulating T cells from healthy donors, it was not surprising to observe that the gene expression patterns of T cells from patients were different from healthy control, indicating by the DEGs number and the PCA plots (Dieu, Le et al., 2009). The pathway enrichment analysis revealed that the T cells from HD were more naïve-like and less activated/differentiated, and this finding was in line with our deconvolution data, which suggested that AML peripheral T cells had a significantly higher percentage of CD4 $T_{CM,}$ T_H1, T_{reg}, CD8 T_{EFF} and CD8 T_{ex}, compared to healthy controls (Knaus et al., 2018). A recent study showed that peripheral T cells from new-diagnosed AML patients contained an increased percentage of terminated differentiated effector CD8 cells and a lower percentage of naïve CD8 T cells (Knaus et al., 2018). A limitation of this study is the size of the patient and healthy donor cohort (no age-matched elder healthy donor), and the findings should be tested on a larger cohort in the future.

Then we compared the patients T cells from peripheral blood and bone marrow, and our results indicated that the bulk gene expression profile of T cells from peripheral blood and bone marrow were not very different to each other, applicable for both CD4 and CD8 compartments. However, the pathway enrichment analysis of bulk RNA-sequencing data implied that for BM CD8 T cells were more activated than PBMC CD8 T cells. The deconvolution data revealed that the BM CD8 T cells might have a higher fraction of CD8 T_{ex} subpopulation compared to PBMC compartment. Before the start of treatment, bone marrow T cells seems like to be with more differentiated/activated that might be due to they were in closer proximity to malignant cells and exposed to chronic, long-term antigen stimulation, likely indicating an ongoing immune response against AML.

However, we did not find that this difference between bone marrow and circulating CD8 T cells was conserved after the one round of treatment, and we speculated the underlying reason might be that PBMC CD8 T became activated after the treatment, leading to less difference compared with already activated BM CD8 T cells. In order to test our hypothesis, we further examined the gene expression changes of PBMC CD8 T cells, and the pathway enrichment analysis indicated that PBMC CD8 T cells displayed a more activated phenotype, including the higher degree of differentiation, cell proliferation, and more active metabolism after one round of treatment. This result was consistent with the previous study, which showed that the proliferation of PBMC CD8 T cells was noticeable as early as seven days or three weeks in circulating CD8 T cells after the initiation of the anti-PD-1 treatment in solid cancers (Kamphorst, Pillai, et al., 2017; Huang et al., 2017, 2019; Kim,Kyung Hwan et al., 2019). Collectively, although the BM CD8 T cells suggested more differentiated and activated phenotype than paired peripheral CD8 T cells at baseline, this difference was not apparent at EC1, which indicated activation of PBMC CD8 T cells induced by treatment might be more profound than BM T cells at the end of cycle one. Inspired by the previous melanoma study (Huang et al., 2019), we cannot exclude the possibility that the treatment could induced gene expression profile change of bone marrow T cells, but the change might happen early and rapid and faded away when the samples were collected at the end of cycle one. Unlike the relatively more durable systematic T cell activation of circulating T cells, the treatment-induced immune response at bone marrow was transient and less sustainable.

Lastly, we found the upregulated or downregulated genes between T cells from responders and non-responders were able to clearly distinguish two groups, cell collected

at baseline or after one cycle of treatment. Our GSEA analysis revealed that at the pre-therapy stage, the gene expression pattern of circulating CD8 T cells from non-responders was more close to the PD-1^{hi} CD8 T cells than to naïve phenotype. Further investigation is required for a comprehensive understanding of the PD-1^{hi} CD8 T cells, especially how to distinguish PD-1^{+} activated or PD-1^{+} exhausted T-cell subsets, which may requires including co-expressing markers for more accurate subset definition. It was reported that the relative abundance of $CTLA^{hi}PD\text{-}1^{hi}$ $CD8^{+}$ TILs from melanoma patient was associated with PD-1 inhibitor therapy (Daud et al., 2016) and the relative abundance of PD-1 expression on T cells was associated with the response to PD-1 blockade therapy. However, the PD-1 expression level should be lower than a certain threshold, or in other words, the T cells were partially exhausted and could be restored (Singh et al., 2019). The T_{ex} phenotype we defined here might be different from the phenotype characterized by the previous study (Zhang, Lei et al., 2018). The deconvolution of T cell subset distribution results indicated that the non-responders seemed to have a high ratio of T_{EFF}/T_{ex} compared to the responders CD8 T_{ex} cells, no matter circulating T cells or bone marrow T cells, indicating the relative abundance of two phenotypes could serve as sub-populations relevant for patient stratification, predicting the favorable clinical outcome of HMA-PD-1 combination therapy in AML patients. The bone marrow T cell will be the more accurate reflection of the interplay between the immune system and leukemia cells, but peripheral blood is more accessible material compared to the bone marrow aspirate. The peripheral blood-based biomarker is preferable, and further verification is required to validate if circulating T_{ex} or T_{ex}/T_{EFF} can be reflective of the tumor-resident T_{ex} cells without loss of prediction power.

Collectively, the analyses of RNA-seq of CD8 T cells from AML patients on the azacytidine with nivolumab trial revealed that (1) the PD-1 blockade-based treatment-induced gene expression profiling changes (increased cell proliferation and metabolism) of CD8 T cells are detectable as early as the end of cycle one in the peripheral blood; (2) specific subpopulations of plastic CD8 T cells (relative abundance of T_{EFF} and T_{ex}) identified may have the potential to serve as an actionable biomarker to select AML patients most likely to benefit from such immune checkpoint therapies. These findings need to be confirmed in larger studies, planned or currently being conducted, with αPD-1 based therapies in AML.

3.4.2. Future direction

RNA-sequencing is a useful tool to for exploratory study at gene-level, and independently test should be performed to validate the findings. Since our findings were mainly focusing on the proliferation and difference in the subset distribution of CD8 T cells, we want to validate: (1) if the treatment-induced proliferation of circulating CD8 T cells is detectable after one cycle of treatment in AML patients who underwent anti-PD-1-based treatment; (2) if T_{EFF}/T_{ex} CD8 ratio difference between responders and non-responders are consistent with the independent assay, also if this parameter can be an actionable marker to predict the patient response towards to this HMA-PD-1 combination immunotherapy at the protein level.

Based on the questions we would like to study, we plan to study a list of protein markers related to cell proliferation (Ki-67) and T-cell phenotype and differentiation status of T cells (Table 3-5).

Table 3-5 Candidate markers to define the T_{ex} CD8 T cells ($CD3^+CD8^+$ cells)

Phenotype	Protein	Gene	Description
T_{ex}	PD-1	*PDCD1*	Co-inhibitory molecule (Chen, Lieping and Flies, 2013)
	TIM-3	*HAVCR2*	Co-inhibitory molecule (Chen,Lieping and Flies, 2013)
	CTLA4	*CTLA4*	Co-inhibitory molecule (Chen,Lieping and Flies, 2013)
	Granzyme B	*GZMB*	Secreted protein involving in T cell cytotoxicity (Barry and Bleackley, 2018)
	Interferon-gamma	*IFNG*	Cytokine involving in anti-cancer response (Zaidi and Merlino, 2011)
	CCL4	*CCL4*	Chemokine involving in inflammation process (Mortarini et al., 2003)
	CXCL13	*CXCL13*	Chemokine, recruiting immune cells (Mertz et al., 2018)
	CXCR6	*CXCR6*	Chemokine receptor, upregulated on activated T cells (Sato et al., 2005)
T_{EFF}	CX3CR1	*CX3CR1*	Chemokine receptor (Yan et al., 2018; Imai et al., 1997)
	KLRG1	*KLRG1*	Co-inhibitory receptor (Henson and Akbar, 2009)
	Granzyme H	*GZMH*	Immune effector protein, serine proteases (Chowdhury and Lieberman, 2008)
	Perforin	*PRF1*	Responsible for pore formation in cell membranes of target cells (Osińska, Popko, and Demkow, 2014)
	T-bet	*TBX21*	Transcription factor controls T-cell differentiation (Huang et al., 2017)
	Granulysin	*GNLY*	Antimicrobial protein (Zheng et al., 2017)
	Granzyme M	*GZMM*	Immune effector protein, serine proteases (Chowdhury and Lieberman, 2008)
	Eomesodermin	*EOMES*	Transcription factor controls T-cell differentiation (Huang et al., 2017)

Ki-67 protein is an intracellular protein maker associated with cell proliferation, and Ki-67 staining has been applied in previous studies to evaluate T cell proliferation upon treatment-induced activation (Huang et al., 2017; Kim, Kyung Hwan et al., 2019). Since the definition of CD8 T_{EFF} and T_{ex} cells was obtained from scRNA-seq data (Zhang,Lei et al., 2018) at transcript-level, which includes more than several hundreds of genes as cell-

type-specific gene signature, we propose to validate our finding using flow cytometry or mass cytometry (which allows higher multiplexity of detection protein at single-cell level) on a small set of highly-upregulated gene/protein in this phenotype for the sake of convenience. Although mass cytometry (CyTOF) enables high-dimensional characterization of targeted protein simultaneously with a single-cell resolution, the flow cytometry may be more advantageous: it can provide higher throughput capability and better cost-effective than mass cytometry, and it has been widely used in the clinical setting for decades as a more mature technology.

Furthermore, we hypothesize that T_{EFF}/T_{ex} can be a candidate biomarker to predict the clinical outcome, and there is redundancy of these candidate markers to define the T_{EFF} and T_{ex} phenotypes; thus it is possible to shrink the number of required protein markers for prediction while also maintain the predictive power.

Apart from phenotype and transcriptomic profiling, the TCR clonality and diversity is another crucial factor that should be considered for a comprehensive study of T cells anti-tumor effect. Previously published data suggested that PD-1 blockade might induce decreasing TCR clonality of tumor-infiltrating T cells from responders, which indicated the possible selective propagation of tumor-specific T cells after reinvigoration by PD-1 inhibitor (Cloughesy et al., 2019; Tumeh et al., 2014). A separate study demonstrated that lack of TCR diversity in peripheral blood T cells correlated to a better response in melanoma patients treated with anti-PD-1 (Hogan et al., 2018). The reason for the responder had lower TCR diversity might be that only a restricted number of TCRs contributed to the anti-tumor response (Hogan et al., 2018; Manne et al., 2002; Willhauck et al., 2003). Profiling of TCR repertoire of T cells from tumor site or peripheral blood can

provide insights on T cell developmental trajectories and migratory behaviors (Zhang, Lei et al., 2018). Harmonizing multifaceted characterizations of T cells will yield a more accurate assessment of T cell landscape in cancer patients.

Given the modest success of potential predictive and prognostic biomarkers have been proposed, a combination of multiple perspectives of immune system-tumor interplay may be helpful for improved predictive profiles (Singh et al., 2019). The interplay between the T cells or the immune system and tumor cells is complicated, and the study of tumor cells is a necessary part of drawing a comprehensive picture of the tumor microenvironment (Nishino et al., 2017). The immune checkpoint blockade therapy also strongly relies on how suppressive the tumor microenvironment is (Galon and Bruni, 2019). Except for PD-1, overexpression of other immune checkpoint molecules such as T cell immunoglobulin and mucin domain-3 (TIM-3), Cytotoxic T lymphocyte antigen-4 (CTLA-4), and Lymphocyte-activation gene 3 (LAG-3), also facilitate the tumor escape from immune surveillance (Blank et al., 2016; Anderson, Joller, and Kuchroo, 2016). The unfavorable clinical outcome may be overcome by combination therapy rather than monotherapy (Wei, Spencer C. et al., 2017; Sharma and Allison, 2015b). A previous preclinical study suggested the combination of PD-1/PD-L1 and TIM-3/galectin-9 blockade showed synergistic anti-tumor effects compared to individual blockade in AML mouse model (Zhou,Qing et al., 2011). The immunosuppression may also result from the genetic alteration in tumor cells to overexpression multiple oncogenic signaling pathways, eventually, lead to suppression T cells recruitment to the TME (Spranger, Bao, and Gajewski, 2015; Kato et al., 2017) and dysfunction of T cells and failure in tumor growth control (Thommen and Schumacher, 2018). Tumor mutational burden (Zhao et al., 2019;

Le et al., 2015; Rizvi et al., 2015), immunosuppressive molecule expression (e.g., PD-L1 (Topalian et al., 2012)), neoantigen burden (McGranahan et al., 2016), and the ratio of T-cell reinvigoration and tumor burden (Huang et al., 2017) were showed that have an impact on the performance of immune-modulating drugs.

REFERENCES

Afik, Shaked, Kathleen B. Yates, Kevin Bi, Samuel Darko, Jernej Godec, Ulrike Gerdemann, Leo Swadling, Daniel C. Douek, Paul Klenerman, Eleanor J. Barnes, Arlene H. Sharpe, W Nicholas Haining, and Nir Yosef. 2017. "Targeted Reconstruction of T Cell Receptor Sequence from Single Cell RNA-Seq Links CDR3 Length to T Cell Differentiation State." *Nucleic Acids Research* 45 (16): e148.

Agarwal, P., A. Raghavan, S. L. Nandiwada, J. M. Curtsinger, P. R. Bohjanen, D. L. Mueller, and M. F. Mescher. 2009. "Gene Regulation and Chromatin Remodeling by IL-12 and Type I IFN in Programming for CD8 T Cell Effector Function and Memory." *The Journal of Immunology* 183 (3): 1695–1704.

Ahmed, Raya, Laureline Roger, Pedro Costa Del Amo, Kelly L. Miners, Rhiannon E. Jones, Lies Boelen, Tinhinane Fali, Marjet Elemans, Yan Zhang, Victor Appay, Duncan M. Baird, Becca Asquith, David A. Price, Derek C. Macallan, and Kristin Ladell. 2016. "Human Stem Cell-like Memory T Cells Are Maintained in a State of Dynamic Flux." *Cell Reports* 17 (11): 2811–2818.

Alibhai, Shabbir M. H., Marc Leach, Mark D. Minden, and Joseph Brandwein. 2009. "Outcomes and Quality of Care in Acute Myeloid Leukemia over 40 Years." *Cancer* 115 (13): 2903–2911.

An, Xingyue and Navin Varadarajan. 2018. "Single-Cell Technologies for Profiling T Cells to Enable Monitoring of Immunotherapies." *Current Opinion in Chemical Engineering* 19: 142–152.

Ancevski Hunter, Katerina, Mark A. Socinski, and Liza C. Villaruz. 2018. "PD-L1 Testing in Guiding Patient Selection for PD-1/PD-L1 Inhibitor Therapy in Lung Cancer."

Molecular Diagnosis & Therapy 22 (1): 1–10.

Anderson, Ana C., Nicole Joller, and Vijay K. Kuchroo. 2016. “Lag-3, Tim-3, and TIGIT: Co-Inhibitory Receptors with Specialized Functions in Immune Regulation.” *Immunity* 44 (5). Elsevier Inc.: 989–1004.

Aschenbrenner, Andrew, Laszlo G. Radvanyi, Yared Hailemichael, Chantale Bernatchez, Jason Roszik, Charuta Kale, Roza Nurieva, Luis M. Vence, Krit Ritthipichai, Willem W. Overwijk, Navin Varadarajan, Xiaohui Yi, Patrick Hwu, Minying Zhang, Cara L. Haymaker, and Melisa Martinez. 2017. “ Multifaceted Role of BTLA in the Control of CD8 + T-Cell Fate after Antigen Encounter .” *Clinical Cancer Research* 23 (20): 6151–6164.

Axelrod, Margaret L., Douglas B. Johnson, and Justin M. Balko. 2018. “Emerging Biomarkers for Cancer Immunotherapy in Melanoma.” *Seminars in Cancer Biology* 52 (Pt 2). Elsevier: 207–215.

“Babraham Bioinformatics - FastQC A Quality Control Tool for High Throughput Sequence Data.” 2019. Accessed February 26.

Bacher, Rhonda, Li-fang Chu, Ning Leng, Audrey P. Gasch, James A. Thomson, Ron M. Stewart, Michael Newton, and Christina Kendziorski. 2017. “SCnorm: Robust Normalization of Single-Cell RNA-Seq Data.” *Nature Methods* 14 (6). Nature Publishing Group, a division of Macmillan Publishers Limited. All Rights Reserved.: 584–586.

Bacher, Rhonda and Christina Kendziorski. 2016. “Design and Computational Analysis of Single-Cell RNA-Sequencing Experiments.” *Genome Biology* 17 (1): 63.

Baitsch, Lukas, Petra Baumgaertner, Estelle Devêvre, Sunil K Raghav, Amandine Legat, Leticia Barba, Sébastien Wieckowski, Hanifa Bouzourene, Bart Deplancke, Pedro Romero,

Nathalie Rufer, and Daniel E Speiser. 2011. “Exhaustion of Tumor-Specific CD8+ T Cells in Metastases from Melanoma Patients.” *Journal of Clinical Investigation* 121 (6): 2350–2360.

Barlogie, Barthel, Martin N. Raber, Johannes Schumann, Tod S. Johnson, Benjamin Drewinko, Douglas E Swartzendruber, Wolfgang Göhde, Michael Andreeff, and Emil J. Freireich. 1983. “Flow Cytometry in Clinical Cancer Research.” *Cancer Research* 43 (9): 3982–3997.

Baron, Maayan, Adrian Veres, Samuel L. Wolock, Aubrey L. Faust, Renaud Gaujoux, Amedeo Vetere, Jennifer Hyoje Ryu, Bridget K. Wagner, Shai S. Shen-Orr, Allon M. Klein, Douglas A. Melton, and Itai Yanai. 2016. “A Single-Cell Transcriptomic Map of the Human and Mouse Pancreas Reveals Inter- and Intra-Cell Population Structure.” *Cell Systems* 3 (4). Elsevier Inc.: 346-360.e4.

Barry, Michele and R. Chris Bleackley. 2018. “Cytotoxic T Lymphocytes: All Roads Lead to Death.” *Nature Reviews Immunology* 2 (6): 401–409.

Becker, Petra S. A., Erhard Seifried, Evelyn Ullrich, Torsten Tonn, Christian Seidl, Paulina Nowakowska, Peter Bader, and Garnet Suck. 2016. “Selection and Expansion of Natural Killer Cells for NK Cell-Based Immunotherapy.” *Cancer Immunology, Immunotherapy* 65 (4). Springer: 477–484.

Bengsch, Bertram, Takuya Ohtani, Ramin Sedaghat Herati, Niels Bovenschen, Kyong-Mi Chang, and E. John Wherry. 2017. “Deep Immune Profiling by Mass Cytometry Links Human T and NK Cell Differentiation and Cytotoxic Molecule Expression Patterns.” *Journal of Immunological Methods* 453 (February): 3–10.

Bewersdorf, Jan Philipp, Maximilian Stahl, and Amer M. Zeidan. 2019. “Immune

Checkpoint-Based Therapy in Myeloid Malignancies: A Promise yet to Be Fulfilled." *Expert Review of Anticancer Therapy*, March. Taylor & Francis, 1–12.

Bichsel, Colette A., Christoph Zechner, Christian A. Jordi, Cem Albayrak, Savaş Tay, Jing Lin, and Mustafa Khammash. 2016. "Digital Quantification of Proteins and MRNA in Single Mammalian Cells." *Molecular Cell* 61 (6): 914–924.

Blank, Christian U., John B. Haanen, Antoni Ribas, and Ton N. Schumacher. 2016. "CANCER IMMUNOLOGY. The 'Cancer Immunogram'." *Science (New York, N.Y.)* 352 (6286): 658–660.

Bock, Christoph, Matthias Farlik, and Nathan C. Sheffield. 2016. "Multi-Omics of Single Cells: Strategies and Applications." *Trends in Biotechnology* 34 (8): 605–608.

Borghaei, Hossein, Luis Paz-Ares, Leora Horn, David R. Spigel, Martin Steins, Neal E. Ready, Laura Q. Chow, Everett E. Vokes, Enriqueta Felip, Esther Holgado, Fabrice Barlesi, Martin Kohlhäufl, Oscar Arrieta, Marco Angelo Burgio, Jérôme Fayette, Hervé Lena, Elena Poddubskaya, David E. Gerber, Scott N. Gettinger, Charles M. Rudin, Naiyer Rizvi, Lucio Crinò, George R. Blumenschein, Scott J. Antonia, Cécile Dorange, Christopher T. Harbison, Friedrich Graf Finckenstein, and Julie R. Brahmer. 2015. "Nivolumab versus Docetaxel in Advanced Nonsquamous Non-Small-Cell Lung Cancer." *The New England Journal of Medicine* 373 (17): 1627–1639.

Brahmer, Julie, Karen L. Reckamp, Paul Baas, Lucio Crinò, Wilfried E.E. Eberhardt, Elena Poddubskaya, Scott Antonia, Adam Pluzanski, Everett E. Vokes, Esther Holgado, David Waterhouse, Neal Ready, Justin Gainor, Osvaldo Arén Frontera, Libor Havel, Martin Steins, Marina C. Garassino, Joachim G. Aerts, Manuel Domine, Luis Paz-Ares, Martin Reck, Christine Baudelet, Christopher T. Harbison, Brian Lestini, and David R. Spigel.

2015. “Nivolumab versus Docetaxel in Advanced Squamous-Cell Non–Small-Cell Lung Cancer.” *New England Journal of Medicine* 373 (2): 123–135.

Bray, Nicolas L., Harold Pimentel, Páll Melsted, and Lior Pachter. 2016. “Near-Optimal Probabilistic RNA-Seq Quantification.” *Nature Biotechnology* 34 (5): 525–527.

Breart, Béatrice, Fabrice Lemaître, Susanna Celli, and Philippe Bousso. 2008. “Two-Photon Imaging of Intratumoral CD8+ T Cell Cytotoxic Activity during Adoptive T Cell Therapy in Mice.” *Journal of Clinical Investigation* 118 (4): 1390–1397.

Brentjens, Renier J., Marco L. Davila, Isabelle Riviere, Jae Park, Xiuyan Wang, Lindsay G. Cowell, Shirley Bartido, Jolanta Stefanski, Clare Taylor, Malgorzata Olszewska, Oriana Borquez-Ojeda, Jinrong Qu, Teresa Wasielewska, Qing He, Yvette Bernal, Ivelise V. Rijo, Cyrus Hedvat, Rachel Kobos, Kevin Curran, Peter Steinherz, Joseph Jurcic, Todd Rosenblat, Peter Maslak, Mark Frattini, and Michel Sadelain. 2013. “CD19-Targeted T Cells Rapidly Induce Molecular Remissions in Adults with Chemotherapy-Refractory Acute Lymphoblastic Leukemia.” *Science Translational Medicine* 5 (177): 177ra38.

Butterfield, Lisa H. 2018. “The Society for Immunotherapy of Cancer Biomarkers Task Force Recommendations Review.” *Seminars in Cancer Biology* 52 (October): 12–15.

Cao, Jing, Jesse Seegmiller, Naomi Q. Hanson, Christopher Zaun, and Danni Li. 2015. “A Microfluidic Multiplex Proteomic Immunoassay Device for Translational Research.” *Clinical Proteomics* 12 (1): 28.

Chen, Lieping and Dallas B. Flies. 2013. “Molecular Mechanisms of T Cell Co-Stimulation and Co-Inhibition.” *Nature Reviews Immunology*.

Chen, Pei Ling, Whijae Roh, Alexandre Reuben, Zachary A. Cooper, Christine N. Spencer, Peter A. Prieto, John P. Miller, Roland L. Bassett, Vancheswaran Gopalakrishnan, Khalida

Wani, Mariana Petaccia De Macedo, Jacob L. Austin-Breneman, Hong Jiang, Qing Chang, Sangeetha M. Reddy, Wei Shen Chen, Michael T. Tetzlaff, Russell J. Broaddus, Michael A. Davies, Jeffrey E. Gershenwald, Lauren Haydu, Alexander J. Lazar, Sapna P. Patel, Patrick Hwu, Wen Jen Hwu, Adi Diab, Isabella C. Glitza, Scott E. Woodman, Luis M. Vence, Ignacio I. Wistuba, Rodabe N. Amaria, Lawrence N. Kwong, Victor Prieto, R. Eric Davis, Wencai Ma, Willem W. Overwijk, Arlene H. Sharpe, Jianhua Hu, P. Andrew Futreal, Jorge Blando, Padmanee Sharma, James P. Allison, Lynda Chin, and Jennifer A. Wargo. 2016. “Analysis of Immune Signatures in Longitudinal Tumor Samples Yields Insight into Biomarkers of Response and Mechanisms of Resistance to Immune Checkpoint Blockade.” *Cancer Discovery* 6 (8): 827–837.

Chevrier, Stéphane, Jacob Harrison Levine, Vito Riccardo Tomaso Zanotelli, Karina Silina, Daniel Schulz, Marina Bacac, Carola Hermine Ries, Laurie Ailles, Michael Alexander Spencer Jewett, Holger Moch, Maries van den Broek, Christian Beisel, Michael Beda Stadler, Craig Gedye, Bernhard Reis, Dana Pe’er, and Bernd Bodenmiller. 2017. “An Immune Atlas of Clear Cell Renal Cell Carcinoma.” *Cell* 169 (4): 736-749.e18.

Chiappinelli, Katherine B., Pamela L. Strissel, Alexis Desrichard, Huili Li, Christine Henke, Benjamin Akman, Alexander Hein, Neal S. Rote, Leslie M. Cope, Alexandra Snyder, Vladimir Makarov, Sadna Buhu, Dennis J. Slamon, Jedd D. Wolchok, Drew M. Pardoll, Matthias W. Beckmann, Cynthia A. Zahnow, Taha Merghoub, Timothy A. Chan, Stephen B. Baylin, and Reiner Strick. 2015. “Inhibiting DNA Methylation Causes an Interferon Response in Cancer via DsRNA Including Endogenous Retroviruses.” *Cell* 162 (5): 974–986.

Chokkalingam, Venkatachalam, Jurjen Tel, Florian Wimmers, Xin Liu, Sergey Semenov,

Julian Thiele, Carl G. Figdor, and Wilhelm T. S. Huck. 2013. “Probing Cellular Heterogeneity in Cytokine-Secreting Immune Cells Using Droplet-Based Microfluidics.” *Lab on a Chip* 13 (24): 4740.

Chowdhury, Dipanjan and Judy Lieberman. 2008. “Death by a Thousand Cuts: Granzyme Pathways of Programmed Cell Death.” *Annual Review of Immunology* 26: 389–420.

Cloughesy, Timothy F., Aaron Y. Mochizuki, Joey R. Orpilla, Willy Hugo, Alexander H. Lee, Tom B. Davidson, Anthony C. Wang, Benjamin M. Ellingson, Julie A. Rytlewski, Catherine M. Sanders, Eric S. Kawaguchi, Lin Du, Gang Li, William H. Yong, Sarah C. Gaffey, Adam L. Cohen, Ingo K. Mellinghoff, Eudocia Q. Lee, David A. Reardon, Barbara J. O’Brien, Nicholas A. Butowski, Phioanh L. Nghiemphu, Jennifer L. Clarke, Isabel C. Arrillaga-Romany, Howard Colman, Thomas J. Kaley, John F. de Groot, Linda M. Liau, Patrick Y Wen, and Robert M Prins. 2019. “Neoadjuvant Anti-PD-1 Immunotherapy Promotes a Survival Benefit with Intratumoral and Systemic Immune Responses in Recurrent Glioblastoma.” *Nature Medicine* 25 (3): 477–486.

Cohen, Cyrille J., Jared J. Gartner, Miryam Horovitz-Fried, Katerina Shamalov, Kasia Trebska-McGowan, Valery V. Bliskovsky, Maria R. Parkhurst, Chen Ankri, Todd. D. Prickett, Jessica S. Crystal, Yong F. Li, Mona El-Gamil, Steven A. Rosenberg, and Paul F. Robbins. 2015. “Isolation of Neoantigen-Specific T Cells from Tumor and Peripheral Lymphocytes.” *Journal of Clinical Investigation* 125 (10): 3981–3991.

Coral, Sandra, Luca Sigalotti, Aldo Gasparollo, Ilaria Cattarossi, Alberto Visintin, Alessandro Cattelan, Maresa Altomonte, and Michele Maio. 1999. “Prolonged Upregulation of the Expression of HLA Class I Antigens and Costimulatory Molecules on Melanoma Cells Treated with 5-Aza-2’-Deoxycytidine (5-AZA-CdR).” *Journal of*

Immunotherapy (Hagerstown, Md.: 1997) 22 (1): 16–24.

Corces, M Ryan, Howard Y. Chang, Julie L. Koenig, Beijing Wu, Jonathan K. Pritchard, William J. Greenleaf, Ravindra Majeti, Jason D Buenrostro, Steven M. Chan, Michael P. Snyder, Peyton G. Greenside, and Anshul Kundaje. 2016. “Lineage-Specific and Single-Cell Chromatin Accessibility Charts Human Hematopoiesis and Leukemia Evolution.” *Nature Genetics* 48 (10): 1193–1203.

Cristescu, Razvan, Robin Mogg, Mark Ayers, Andrew Albright, Erin Murphy, Jennifer Yearley, Xinwei Sher, Xiao Qiao Liu, Hongchao Lu, Michael Nebozhyn, Chunsheng Zhang, Jared K. Lunceford, Andrew Joe, Jonathan Cheng, Andrea L. Webber, Nageatte Ibrahim, Elizabeth R. Plimack, Patrick A. Ott, Tanguy Y. Seiwert, Antoni Ribas, Terrill K. McClanahan, Joanne E. Tomassini, Andrey Loboda, and David Kaufman. 2018. “Pan-Tumor Genomic Biomarkers for PD-1 Checkpoint Blockade–Based Immunotherapy.” *Science* 362 (6411): eaar3593.

Darmanis, Spyros, Caroline Julie Gallant, Voichita Dana Marinescu, Mia Niklasson, Anna Segerman, Georgios Flamourakis, Simon Fredriksson, Erika Assarsson, Martin Lundberg, Sven Nelander, Bengt Westermark, and Ulf Landegren. 2016. “Simultaneous Multiplexed Measurement of RNA and Proteins in Single Cells.” *Cell Reports* 14 (2): 380–389.

Daud, Adil I., Kimberly Loo, Mariela L. Pauli, Robert Sanchez-Rodriguez, Priscila Munoz Sandoval, Keyon Taravati, Katy Tsai, Adi Nosrati, Lorenzo Nardo, Michael D. Alvarado, Alain P. Algazi, Miguel H. Pampaloni, Iryna V. Lobach, Jimmy Hwang, Robert H. Pierce, Iris K. Gratz, Matthew F. Krummel, and Michael D. Rosenblum. 2016. “Tumor Immune Profiling Predicts Response to Anti-PD-1 Therapy in Human Melanoma.” *The Journal of Clinical Investigation* 126 (9): 3447–3452.

Daver, Naval, Prajwal Boddu, Guillermo Garcia-Manero, Shalini Singh Yadav, Padmanee Sharma, James Allison, and Hagop Kantarjian. 2018. “Hypomethylating Agents in Combination with Immune Checkpoint Inhibitors in Acute Myeloid Leukemia and Myelodysplastic Syndromes.” *Leukemia* 32 (5): 1094–1105.

Daver, Naval, Guillermo Garcia-Manero, Sreyashi Basu, Prajwal C. Boddu, Mansour Alfayez, Jorge E. Cortes, Marina Konopleva, Farhad Ravandi-Kashani, Elias Jabbour, Tapan Kadia, Graciela M. Nogueras-Gonzalez, Jing Ning, Naveen Pemmaraju, Courtney D. DiNardo, Michael Andreeff, Sherry A. Pierce, Tauna Gordon, Steven M. Kornblau, Wilmer Flores, Zainab Alhamal, Carlos Bueso-Ramos, Jeffrey L. Jorgensen, Keyur P. Patel, Jorge Blando, James P. Allison, Padmanee Sharma, and Hagop Kantarjian. 2018. “Efficacy, Safety, and Biomarkers of Response to Azacitidine and Nivolumab in Relapsed/Refractory Acute Myeloid Leukemia: A Nonrandomized, Open-Label, Phase II Study.” *Cancer Discovery* 9 (3): 370–383.

Decocq, J., B. Combadiere, S. N. Quoc, D. Duffy, V. Vieillard, M. Le Garff-Tavernier, V. Beziat, and P. Debre. 2011. “CD56brightCD16+ NK Cells: A Functional Intermediate Stage of NK Cell Differentiation.” *The Journal of Immunology* 186 (12): 6753–6761.

Dieu, Rifca Le, David C. Taussig, Alan G. Ramsay, Richard Mitter, Faridah Miraki-Moud, Rewas Fatah, Abigail M. Lee, T. Andrew Lister, John G. Gribben, T. A. Lister, and John G. Gribben. 2009. “Peripheral Blood T Cells in Acute Myeloid Leukemia (AML) Patients at Diagnosis Have Abnormal Phenotype and Genotype and Form Defective Immune Synapses with AML Blasts.” *Blood* 114 (18): 3909–3916.

Diggs, Laurence P. and Eddy C. Hsueh. 2017. “Utility of PD-L1 Immunohistochemistry Assays for Predicting PD-1/PD-L1 Inhibitor Response.” *Biomarker Research* 5 (1): 12.

Duncombe, Todd A., Chi-Chih Kang, Santanu Maity, Toby M. Ward, Mark D. Pegram, Niren Murthy, and Amy E. Herr. 2016. “Hydrogel Pore-Size Modulation for Enhanced Single-Cell Western Blotting.” *Advanced Materials* 28 (2): 327–334.

Dundua, Alexander, Steffen Franzka, and Mathias Ulbricht. 2016. “Improved Antifouling Properties of Polydimethylsiloxane Films via Formation of Polysiloxane/Polyzwitterion Interpenetrating Networks.” *Macromol Rapid Commun* 37 (24): 2030–2036.

Duraiswamy, Jaikumar, Chris C. Ibegbu, David Masopust, Joseph D. Miller, Koichi Araki, Gregory H. Doho, Pramila Tata, Satish Gupta, Michael J. Zilliox, Helder I. Nakaya, Bali Pulendran, W. Nicholas Haining, Gordon J. Freeman, and Rafi Ahmed. 2011. “Phenotype, Function, and Gene Expression Profiles of Programmed Death-1hi CD8 T Cells in Healthy Human Adults.” *The Journal of Immunology* 186 (7): 4200–4212.

Durinck, Steffen, Yves Moreau, Arek Kasprzyk, Sean Davis, Bart De Moor, Alvis Brazma, and Wolfgang Huber. 2005. “BioMart and Bioconductor: A Powerful Link between Biological Databases and Microarray Data Analysis.” *Bioinformatics* 21 (16): 3439–3440.

Ekins, Roger P. 1998. “Ligand Assays: From Electrophoresis to Miniaturized Microarrays.” *Clinical Chemistry* 44 (9): 2015–2030.

Elshal, Mohamed F. and J. Philip McCoy. 2006. “Multiplex Bead Array Assays: Performance Evaluation and Comparison of Sensitivity to ELISA.” *Methods (San Diego, Calif.)* 38 (4): 317–323.

Eltahla, Auda A., Simone Rizzetto, Mehdi R. Pirozyan, Brigid D. Betz-Stablein, Vanessa Venturi, Katherine Kedzierska, Andrew R. Lloyd, Rowena A. Bull, and Fabio Luciani. 2016. “Linking the T Cell Receptor to the Single Cell Transcriptome in Antigen-Specific Human T Cells.” *Immunology and Cell Biology* 94 (6): 604–611.

Eyer, Klaus, Raphaël C.L. Doineau, Carlos E. Castrillon, Luis Briseño-Roa, Vera Menrath, Guillaume Mottet, Patrick England, Alexei Godina, Elodie Brient-Litzler, Clément Nizak, Allan Jensen, Andrew D. Griffiths, Jérôme Bibette, Pierre Bruhns, and Jean Baudry. 2017. "Single-Cell Deep Phenotyping of IgG-Secreting Cells for High-Resolution Immune Monitoring." *Nature Biotechnology* 35 (10). Nature Publishing Group, a division of Macmillan Publishers Limited. All Rights Reserved.: 977–982.

Frei, Andreas P., Felice-Alessio Bava, Eli R. Zunder, Elena W. Y. Hsieh, Shih-Yu Chen, Garry P. Nolan, and Pier Federico Gherardini. 2016. "Highly Multiplexed Simultaneous Detection of RNAs and Proteins in Single Cells." *Nat Meth* 13 (3). Nature Publishing Group, a division of Macmillan Publishers Limited. All Rights Reserved.: 269–275.

Galon, Jérôme and Daniela Bruni. 2019. "Approaches to Treat Immune Hot, Altered and Cold Tumours with Combination Immunotherapies." *Nature Reviews Drug Discovery* 18 (March). Springer US: 10–13.

Gandini, Sara, Daniela Massi, and Mario Mandalà. 2016. "PD-L1 Expression in Cancer Patients Receiving Anti PD-1/PD-L1 Antibodies: A Systematic Review and Meta-Analysis." *Critical Reviews in Oncology/Hematology* 100. Elsevier Ireland Ltd: 88–98.

Gao, Jianjun, Lewis Zhichang Shi, Hao Zhao, Jianfeng Chen, Liangwen Xiong, Qiuming He, Tenghui Chen, Jason Roszik, Chantale Bernatchez, Scott E Woodman, Pei-Ling Chen, Patrick Hwu, James P. Allison, Andrew Futreal, Jennifer A. Wargo, and Padmanee Sharma. 2016. "Loss of IFN-γ Pathway Genes in Tumor Cells as a Mechanism of Resistance to Anti-CTLA-4 Therapy." *Cell* 167 (2): 397-404.e9.

Garon, Edward B., Naiyer A. Rizvi, Rina Hui, Natasha Leighl, Ani S. Balmanoukian, Joseph Paul Eder, Amita Patnaik, Charu Aggarwal, Matthew Gubens, Leora Horn, Enric

Carcereny, Myung-Ju Ahn, Enriqueta Felip, Jong-Seok Lee, Matthew D. Hellmann, Omid Hamid, Jonathan W. Goldman, Jean-Charles Soria, Marisa Dolled-Filhart, Ruth Z. Rutledge, Jin Zhang, Jared K. Lunceford, Reshma Rangwala, Gregory M. Lubiniecki, Charlotte Roach, Kenneth Emancipator, and Leena Gandhi. 2015. “Pembrolizumab for the Treatment of Non–Small-Cell Lung Cancer.” *New England Journal of Medicine* 372 (21): 2018–2028.

Genshaft, Alex S., Shuqiang Li, Caroline J. Gallant, Spyros Darmanis, Sanjay M. Prakadan, Carly G. K. Ziegler, Martin Lundberg, Simon Fredriksson, Joyce Hong, Aviv Regev, Kenneth J. Livak, Ulf Landegren, and Alex K. Shalek. 2016. “Multiplexed, Targeted Profiling of Single-Cell Proteomes and Transcriptomes in a Single Reaction.” *Genome Biology* 17 (1): 188.

Gerbitz, Armin, Madhusudhanan Sukumar, Florian Helm, Andrea Wilke, Christian Friese, Cornelia Fahrenwaldt, Frank M Lehmann, Christoph Loddenkemper, Thomas Kammertoens, Josef Mautner, Clemens A. Schmitt, Thomas Blankenstein, and Georg W. Bornkamm. 2012. “Stromal Interferon-γ Signaling and Cross-Presentation Are Required to Eliminate Antigen-Loss Variants of B Cell Lymphomas in Mice.” Edited by Zhang, Luwen. *PLoS ONE* 7 (3): e34552.

Gide, Tuba N., Camelia Quek, Alexander M. Menzies, Annie T. Tasker, Ping Shang, Jeff Holst, Jason Madore, Su Yin Lim, Rebecca Velickovic, Matthew Wongchenko, Yibing Yan, Serigne Lo, Matteo S. Carlino, Alexander Guminski, Robyn P M Saw, Angel Pang, Helen M. McGuire, Umaimainthan Palendira, John F. Thompson, Helen Rizos, Ines Pires da Silva, Marcel Batten, Richard A. Scolyer, Georgina V. Long, and James S. Wilmott. 2019. “Distinct Immune Cell Populations Define Response to Anti-PD-1 Monotherapy and

Anti-PD-1/Anti-CTLA-4 Combined Therapy." *Cancer Cell* 35 (2). Elsevier Inc.: 238-255.e6.

Gierahn, Todd M., Marc H. Wadsworth, Travis K. Hughes, Bryan D. Bryson, Andrew Butler, Rahul Satija, Sarah Fortune, J Christopher Love, and Alex K. Shalek. 2017. "Seq-Well: Portable, Low-Cost RNA Sequencing of Single Cells at High Throughput." *Nature Methods* 14 (4). Nature Publishing Group, a division of Macmillan Publishers Limited. All Rights Reserved.: 395–398.

Gong, Jun, Alexander Chehrazi-Raffle, Srikanth Reddi, and Ravi Salgia. 2018. "Development of PD-1 and PD-L1 Inhibitors as a Form of Cancer Immunotherapy: A Comprehensive Review of Registration Trials and Future Considerations." *Journal for ImmunoTherapy of Cancer* 6 (1): 1–18.

Gong, Qiang, Chao Wang, Weiwei Zhang, Javeed Iqbal, Yang Hu, Timothy C Greiner, Adam Cornish, Jo-Heon Kim, Raul Rabadan, Francesco Abate, Xin Wang, Giorgio G Inghirami, Timothy W McKeithan, and Wing C Chan. 2017. "Assessment of T-Cell Receptor Repertoire and Clonal Expansion in Peripheral T-Cell Lymphoma Using RNA-Seq Data." *Scientific Reports* 7 (1): 11301.

Goodyear, Oliver, Angelo Agathanggelou, Igor Novitzky-Basso, Shamyla Siddique, Tina McSkeane, Gordon Ryan, Paresh Vyas, Jamie Cavenagh, Tanja Stankovic, Paul Moss, and Charles Craddock. 2010. "Induction of a CD8+ T-Cell Response to the MAGE Cancer Testis Antigen by Combined Treatment with Azacitidine and Sodium Valproate in Patients with Acute Myeloid Leukemia and Myelodysplasia." *Blood* 116 (11): 1908–1918.

Gopalakrishnan, V., C. N. Spencer, L. Nezi, A. Reuben, M. C. Andrews, T V Karpinets, P A Prieto, D Vicente, K Hoffman, S C Wei, A P Cogdill, L Zhao, C W Hudgens, D S

Hutchinson, T Manzo, M. Petaccia de Macedo, T Cotechini, T Kumar, W S Chen, S M Reddy, R. Szczepaniak Sloane, J. Galloway-Pena, H Jiang, P L Chen, E J Shpall, K Rezvani, A M Alousi, R. F. Chemaly, S. Shelburne, L. M. Vence, P. C. Okhuysen, V. B. Jensen, A. G. Swennes, F. McAllister, E. Marcelo Riquelme Sanchez, Y Zhang, E. Le Chatelier, L. Zitvogel, N. Pons, J. L. Austin-Breneman, L. E. Haydu, E. M. Burton, J. M. Gardner, E. Sirmans, J. Hu, A. J. Lazar, T. Tsujikawa, A. Diab, H. Tawbi, I. C. Glitza, W J Hwu, S. P. Patel, S. E. Woodman, R. N. Amaria, M. A. Davies, J. E. Gershenwald, P. Hwu, J. E. Lee, J. Zhang, L. M. Coussens, Z. A. Cooper, P. A. Futreal, C. R. Daniel, N. J. Ajami, J. F. Petrosino, M. T. Tetzlaff, P. Sharma, J. P. Allison, R. R. Jenq, and J. A. Wargo. 2018. “Gut Microbiome Modulates Response to Anti-PD-1 Immunotherapy in Melanoma Patients.” *Science (New York, N.Y.)* 359 (6371): 97–103.

Gros, Alena, Maria R. Parkhurst, Eric Tran, Anna Pasetto, Paul F. Robbins, Sadia Ilyas, Todd D. Prickett, Jared J. Gartner, Jessica S. Crystal, Ilana M. Roberts, Kasia Trebska-McGowan, John R. Wunderlich, James C. Yang, and Steven A. Rosenberg. 2016. “Prospective Identification of Neoantigen-Specific Lymphocytes in the Peripheral Blood of Melanoma Patients.” *Nature Medicine* 22 (4): 433–438.

Hamid, Omid, Henrik Schmidt, Aviram Nissan, Laura Ridolfi, Steinar Aamdal, Johan Hansson, Michele Guida, David M. Hyams, Henry Gómez, Lars Bastholt, Scott D. Chasalow, and David Berman. 2011. “A Prospective Phase II Trial Exploring the Association between Tumor Microenvironment Biomarkers and Clinical Activity of Ipilimumab in Advanced Melanoma.” *Journal of Translational Medicine* 9 (1): 204.

Han, Qing, Neda Bagheri, Elizabeth M. Bradshaw, David A. Hafler, Douglas A. Lauffenburger, and J Christopher Love. 2012. “Polyfunctional Responses by Human T

Cells Result from Sequential Release of Cytokines." *Proceedings of the National Academy of Sciences* 109 (5): 1607–1612.

Han, Qing, Elizabeth M. Bradshaw, Björn Nilsson, David A. Hafler, and J. Christopher Love. 2010. "Multidimensional Analysis of the Frequencies and Rates of Cytokine Secretion from Single Cells by Quantitative Microengraving." *Lab on a Chip* 10 (11): 1391.

Haque, Ashraful, Jessica Engel, Sarah A. Teichmann, and Tapio Lönnberg. 2017. "A Practical Guide to Single-Cell RNA-Sequencing for Biomedical Research and Clinical Applications." *Genome Medicine* 9 (1): 75.

Haymaker, Cara L., Richard C. Wu, Krit Ritthipichai, Chantale Bernatchez, Marie-Andrée Forget, Jie Qing Chen, Hui Liu, Ena Wang, Francesco Marincola, Patrick Hwu, and Laszlo G. Radvanyi. 2015. "BTLA Marks a Less-Differentiated Tumor-Infiltrating Lymphocyte Subset in Melanoma with Enhanced Survival Properties." *OncoImmunology* 4 (8): e1014246.

Heath, James R., Antoni Ribas, and Paul S. Mischel. 2016. "Single-Cell Analysis Tools for Drug Discovery and Development." *Nat Rev Drug Discov* 15 (3): 204–216.

Hellmann, Matthew D., Claire F. Friedman, and Jedd D. Wolchok. 2016. "Combinatorial Cancer Immunotherapies." In , 251–277.

Henson, Sian M. and Arne N. Akbar. 2009. "KLRG1—More than a Marker for T Cell Senescence." *AGE* 31 (4): 285–291.

Heyes, Colin D., Jurgen Groll, Martin Moller, and G. Ulrich Nienhaus. 2007. "Synthesis, Patterning and Applications of Star-Shaped Poly(Ethylene Glycol) Biofunctionalized Surfaces." *Mol Biosyst* 3 (6). The Royal Society of Chemistry: 419–430.

Hodi, F Stephen, Steven J. O'Day, David F. McDermott, Robert W. Weber, Jeffrey A.

Sosman, John B. Haanen, Rene Gonzalez, Caroline Robert, Dirk Schadendorf, Jessica C. Hassel, Wallace Akerley, Alfons J.M. van den Eertwegh, Jose Lutzky, Paul Lorigan, Julia M. Vaubel, Gerald P. Linette, David Hogg, Christian H. Ottensmeier, Celeste Lebbé, Christian Peschel, Ian Quirt, Joseph I. Clark, Jedd D. Wolchok, Jeffrey S. Weber, Jason Tian, Michael J. Yellin, Geoffrey M. Nichol, Axel Hoos, and Walter J. Urba. 2010. "Improved Survival with Ipilimumab in Patients with Metastatic Melanoma." *New England Journal of Medicine* 363 (8): 711–723.

Hogan, Sabrina A., Anaïs Courtier, Phil F. Cheng, Nicoletta F. Jaberg-Bentele, Simone M. Goldinger, Manuarii Manuel, Solène Perez, Nadia Plantier, Jean-François Mouret, Thi Dan Linh Nguyen-Kim, Marieke I.G. Raaijmakers, Pia Kvistborg, Nicolas Pasqual, John B.A.G. Haanen, Reinhard Dummer, and Mitchell P. Levesque. 2018. "Peripheral Blood TCR Repertoire Profiling May Facilitate Patient Stratification for Immunotherapy against Melanoma." *Cancer Immunology Research* 7 (1): 77–85.

Hu, Xiaoyu, Soumya D. Chakravarty, and Lionel B. Ivashkiv. 2008. "Regulation of Interferon and Toll-like Receptor Signaling during Macrophage Activation by Opposing Feedforward and Feedback Inhibition Mechanisms." *Immunological Reviews* 226 (1): 41–56.

Huang, Alexander C., Robert J. Orlowski, Xiaowei Xu, Rosemarie Mick, Sangeeth M. George, Patrick K. Yan, Sasikanth Manne, Adam A. Kraya, Bradley Wubbenhorst, Liza Dorfman, Kurt D'Andrea, Brandon M. Wenz, Shujing Liu, Lakshmi Chilukuri, Andrew Kozlov, Mary Carberry, Lydia Giles, Melanie W. Kier, Felix Quagliarello, Suzanne McGettigan, Kristin Kreider, Lakshmanan Annamalai, Qing Zhao, Robin Mogg, Wei Xu, Wendy M. Blumenschein, Jennifer H. Yearley, Gerald P. Linette, Ravi K. Amaravadi,

Lynn M. Schuchter, Ramin S. Herati, Bertram Bengsch, Katherine L. Nathanson, Michael D. Farwell, Giorgos C. Karakousis, E. John Wherry, Tara C. Mitchell, Kurt D'Andrea, Brandon M. Wenz, Shujing Liu, Lakshmi Chilukuri, Andrew Kozlov, Mary Carberry, Lydia Giles, Melanie W. Kier, Felix Quagliarello, Suzanne McGettigan, Kristin Kreider, Lakshmanan Annamalai, Qing Zhao, Robin Mogg, Wei Xu, Wendy M. Blumenschein, Jennifer H. Yearley, Gerald P. Linette, Ravi K. Amaravadi, Lynn M. Schuchter, Ramin S. Herati, Bertram Bengsch, Katherine L. Nathanson, Michael D. Farwell, Giorgos C. Karakousis, E. John Wherry, and Tara C. Mitchell. 2019. "A Single Dose of Neoadjuvant PD-1 Blockade Predicts Clinical Outcomes in Resectable Melanoma." *Nature Medicine*, February.

Huang, Alexander C., michael A Postow, Robert J Orlowski, Rosemarie Mick, Bertram Bengsch, Sasikanth Manne, Wei Xu, Shannon Harmon, Josephine R Giles, Brandon Wenz, Matthew Adamow, Deborah Kuk, Katherine S Panageas, Cristina Carrera, Phillip Wong, Felix Quagliarello, Bradley Wubbenhorst, Kurt D'Andrea, Kristen E Pauken, Ramin S Herati, Ryan P Staupe, Jason M. Schenkel, Suzanne McGettigan, Shawn Kothari, Sangeeth M. George, Robert H Vonderheide, Ravi K Amaravadi, Giorgos C. Karakousis, Lynn M. Schuchter, Xiaowei Xu, Katherine L Nathanson, Jedd D Wolchok, Tara C. Gangadhar, E. John Wherry, Kurt D'Andrea, Kristen E Pauken, Ramin S Herati, Ryan P Staupe, Jason M. Schenkel, Suzanne McGettigan, Shawn Kothari, Sangeeth M. George, Robert H Vonderheide, Ravi K Amaravadi, Giorgos C. Karakousis, Lynn M. Schuchter, Xiaowei Xu, Katherine L Nathanson, Jedd D Wolchok, Tara C. Gangadhar, and E. John Wherry. 2017. "T-Cell Invigoration to Tumour Burden Ratio Associated with Anti-PD-1 Response." *Nature* 545 (7652). Macmillan Publishers Limited, part of Springer Nature. All rights

reserved.: 60–65.

Hughes, Alex J., Dawn P. Spelke, Zhuchen Xu, Chi-Chih Kang, David V. Schaffer, and Amy E. Herr. 2014. “Single-Cell Western Blotting.” *Nature Methods* 11 (7). Nature Publishing Group, a division of Macmillan Publishers Limited. All Rights Reserved.: 749–755.

Imai, Toshio, Kunio Hieshima, Christopher Haskell, Masataka Baba, Morio Nagira, Miyuki Nishimura, Mayumi Kakizaki, Shin Takagi, Hisayuki Nomiyama, Thomas J. Schall, and Osamu Yoshie. 1997. “Identification and Molecular Characterization of Fractalkine Receptor CX3CR1, Which Mediates Both Leukocyte Migration and Adhesion.” *Cell* 91 (4): 521–530.

Iwahori, Kota, Yasushi Shintani, Soichiro Funaki, Yoko Yamamoto, Mitsunobu Matsumoto, Tetsuya Yoshida, Akiko Morimoto-Okazawa, Atsunari Kawashima, Eiichi Sato, Stephen Gottschalk, Meinoshin Okumura, Atsushi Kumanogoh, and Hisashi Wada. 2019. “Peripheral T Cell Cytotoxicity Predicts T Cell Function in the Tumor Microenvironment.” *Scientific Reports* 9 (1): 2636.

Jiang, Tao, Caicun Zhou, and Shengxiang Ren. 2016. “Role of IL-2 in Cancer Immunotherapy.” *OncoImmunology* 5 (6): e1163462.

Kaech, Susan M., Scott Hemby, Ellen Kersh, and Rafi Ahmed. 2002. “Molecular and Functional Profiling of Memory CD8 T Cell Differentiation Systems, the Mechanisms That Determine How and When These Memory T Cells Develop Remain Largely Unknown. The Differentiation of Naı¨venaı¨ve CD8 T Cells into Effector.” *Cell* 111: 837–851.

Kakaradov, Boyko, Justine Lopez, Gene W Yeo, John T Chang, Bingfei Yu, Zhaoren He, Christella E Widjaja, Ananda W Goldrath, Janilyn Arsenio, Ellen J Wehrens, Patrick J

Metz, Stephanie H Kim, Stefan Aigner, and Elina I Zuniga. 2017. “Early Transcriptional and Epigenetic Regulation of CD8+ T Cell Differentiation Revealed by Single-Cell RNA Sequencing.” *Nature Immunology* 18 (4). Nature Publishing Group, a division of Macmillan Publishers Limited. All Rights Reserved.: 422–432.

Kalos, Michael, Bruce L. Levine, David L. Porter, Sharyn Katz, Stephan A. Grupp, Adam Bagg, and Carl H. June. 2011. “T Cells with Chimeric Antigen Receptors Have Potent Antitumor Effects and Can Establish Memory in Patients with Advanced Leukemia.” *Science Translational Medicine* 3 (95): 95ra73.

Kamphorst, Alice O., Rathi N. Pillai, Shu Yang, Tahseen H. Nasti, Rama S. Akondy, Andreas Wieland, Gabriel L. Sica, Ke Yu, Lydia Koenig, Nikita T. Patel, Madhusmita Behera, Hong Wu, Megan McCausland, Zhengjia Chen, Chao Zhang, Fadlo R. Khuri, Taofeek K. Owonikoko, Rafi Ahmed, and Suresh S. Ramalingam. 2017. “Proliferation of PD-1+ CD8 T Cells in Peripheral Blood after PD-1–Targeted Therapy in Lung Cancer Patients.” *Proceedings of the National Academy of Sciences* 114 (19). National Academy of Sciences: 4993–4998.

Kamphorst, Alice O., Andreas Wieland, Tahseen Nasti, Shu Yang, Ruan Zhang, Daniel L. Barber, Bogumila T. Konieczny, Candace Z. Daugherty, Lydia Koenig, Ke Yu, Gabriel L. Sica, Arlene H. Sharpe, Gordon J. Freeman, Bruce R. Blazar, Laurence A. Turka, Taofeek K. Owonikoko, Rathi Pillai, Suresh S Ramalingam, Koichi Araki, and Rafi Ahmed. 2017. “Rescue of Exhausted CD8 T Cells by PD-1–Targeted Therapies Is CD28-Dependent.” *Science*, March.

Kang, Chi-Chih, Jung-Ming G. Lin, Zhuchen Xu, Sanjay Kumar, and Amy E. Herr. 2014. “Single-Cell Western Blotting after Whole-Cell Imaging to Assess Cancer

Chemotherapeutic Response.” *Analytical Chemistry* 86 (20). American Chemical Society: 10429–10436.

Kang, Chi-Chih, Kevin A. Yamauchi, Julea Vlassakis, Elly Sinkala, Todd A. Duncombe, and Amy E. Herr. 2016. “Single Cell-Resolution Western Blotting.” *Nat. Protocols* 11 (8). Nature Publishing Group, a division of Macmillan Publishers Limited. All Rights Reserved.: 1508–1530.

Kato, Daiki, Tomonori Yaguchi, Takashi Iwata, Kenji Morii, Takayuki Nakagawa, Ryohei Nishimura, and Yutaka Kawakami. 2017. “Prospects for Personalized Combination Immunotherapy for Solid Tumors Based on Adoptive Cell Therapies and Immune Checkpoint Blockade Therapies.” *Nihon Rinsho Men’eki Gakkai Kaishi = Japanese Journal of Clinical Immunology* 40 (1): 68–77.

Ke, Rongqin, Marco Mignardi, Alexandra Pacureanu, Jessica Svedlund, Johan Botling, Carolina Wählby, and Mats Nilsson. 2013. “In Situ Sequencing for RNA Analysis in Preserved Tissue and Cells.” *Nature Methods* 10 (9): 857–860.

Khalil, Danny N., Eric L. Smith, Renier J. Brentjens, and Jedd D. Wolchok. 2016. “The Future of Cancer Treatment: Immunomodulation, CARs and Combination Immunotherapy.” *Nature Reviews Clinical Oncology* 13 (5): 273–290.

Kim, Daehwan, Ben Langmead, and Steven L Salzberg. 2015. “HISAT: A Fast Spliced Aligner with Low Memory Requirements.” *Nat Meth* 12 (4). Nature Publishing Group, a division of Macmillan Publishers Limited. All Rights Reserved.: 357–360.

Kim, John J., Elly Sinkala, and Amy E. Herr. 2017. “High-Selectivity Cytology via Lab-on-a-Disc Western Blotting of Individual Cells.” *Lab on a Chip* 17 (5): 855–863.

Kim, Kyung Hwan, Jinhyun Cho, Bo Mi Ku, Jiae Koh, Jong-Mu Sun, Se-Hoon Lee, Jin

Seok Ahn, Jaekyung Cheon, Young Joo Min, Su-Hyung Park, Keunchil Park, Myung-Ju Ahn, and Eui-Cheol Shin. 2019. “The First-Week Proliferative Response of Peripheral Blood PD-1 + CD8 + T Cells Predicts the Response to Anti-PD-1 Therapy in Solid Tumors.” *Clinical Cancer Research* 1: 1–12.

Kiselev, Vladimir Yu, Kristina Kirschner, Michael T Schaub, Tallulah Andrews, Andrew Yiu, Tamir Chandra, Kedar N Natarajan, Wolf Reik, Mauricio Barahona, Anthony R Green, and Martin Hemberg. 2017. “SC3: Consensus Clustering of Single-Cell RNA-Seq Data.” *Nature Methods* 14 (5): 483–486.

Knaus, Hanna A., Sofia Berglund, Hubert Hackl, Amanda L. Blackford, Joshua F. Zeidner, Raúl Montiel-Esparza, Rupkatha Mukhopadhyay, Katrina Vanura, Bruce R. Blazar, Judith E. Karp, Leo Luznik, and Ivana Gojo. 2018. “Signatures of CD8+ T Cell Dysfunction in AML Patients and Their Reversibility with Response to Chemotherapy.” *JCI Insight* 3 (21).

Konry, Tania, Alexander Golberg, and Martin Yarmush. 2013. “Live Single Cell Functional Phenotyping in Droplet Nano-Liter Reactors.” *Scientific Reports* 3 (1): 3179.

Kravchenko-Balasha, Nataly, Young Shik Shik Shin, Alex Sutherland, R D D Levine, and James R R Heath. 2016. “Intercellular Signaling through Secreted Proteins Induces Free-Energy Gradient-Directed Cell Movement.” *Proceedings of the National Academy of Sciences* 113 (20): 5520–5525.

Krieg, Carsten, Malgorzata Nowicka, Silvia Guglietta, Sabrina Schindler, Felix J Hartmann, Lukas M Weber, Reinhard Dummer, Mark D Robinson, Mitchell P Levesque, and Burkhard Becher. 2018. “High-Dimensional Single-Cell Analysis Predicts Response to Anti-PD-1 Immunotherapy.” *Nature Medicine* 24 (2). Nature Publishing Group, a division of Macmillan Publishers Limited. All Rights Reserved.: 144–153.

Krueger, Janna and Christopher E. Rudd. 2017. “Two Strings in One Bow: PD-1 Negatively Regulates via Co-Receptor CD28 on T Cells.” *Immunity* 46 (4). Elsevier Inc.: 529–531.

Kuang, Manchao, Jieyao Cheng, Chengli Zhang, Lin Feng, Xue Xu, Yajing Zhang, Ming Zu, Jianfang Cui, Hang Yu, Kaitai Zhang, Aiming Yang, and Shujun Cheng. 2017. “A Novel Signature for Stratifying the Molecular Heterogeneity of the Tissue-Infiltrating T-Cell Receptor Repertoire Reflects Gastric Cancer Prognosis.” *Scientific Reports* 7 (1): 7762.

Lanier, Lewis L. 2008. “Up on the Tightrope: Natural Killer Cell Activation and Inhibition.” *Nature Immunology* 9 (5): 495–502.

Larkin, James, Vanna Chiarion-Sileni, Rene Gonzalez, Jean Jacques Grob, C. Lance Cowey, Christopher D. Lao, Dirk Schadendorf, Reinhard Dummer, Michael Smylie, Piotr Rutkowski, Pier F. Ferrucci, Andrew Hill, John Wagstaff, Matteo S. Carlino, John B. Haanen, Michele Maio, Ivan Marquez-Rodas, Grant A. McArthur, Paolo A. Ascierto, Georgina V. Long, Margaret K. Callahan, Michael A. Postow, Kenneth Grossmann, Mario Sznol, Brigitte Dreno, Lars Bastholt, Arvin Yang, Linda M. Rollin, Christine Horak, F. Stephen Hodi, and Jedd D. Wolchok. 2015. “Combined Nivolumab and Ipilimumab or Monotherapy in Untreated Melanoma.” *New England Journal of Medicine* 373 (1): 23–34.

Larsson, Chatarina, Ida Grundberg, Ola Söderberg, and Mats Nilsson. 2010. “In Situ Detection and Genotyping of Individual MRNA Molecules.” *Nature Methods* 7 (5): 395–397.

Lavin, Yonit, Soma Kobayashi, Andrew Leader, El-Ad David Amir, Naama Elefant, Camille Bigenwald, Romain Remark, Robert Sweeney, Christian D Becker, Jacob H Levine, Klaus Meinhof, Andrew Chow, Seunghee Kim-Shulze, Andrea Wolf, Chiara

Medaglia, Hanjie Li, Julie A Rytlewski, Ryan O Emerson, Alexander Solovyov, Benjamin D Greenbaum, Catherine Sanders, Marissa Vignali, Mary Beth Beasley, Raja Flores, Sacha Gnjatic, Dana Pe'er, Adeeb Rahman, Ido Amit, and Miriam Merad. 2017. "Innate Immune Landscape in Early Lung Adenocarcinoma by Paired Single-Cell Analyses." *Cell* 169 (4): 750-765.e17.

Le, Dung T., Jennifer N. Uram, Hao Wang, Bjarne R. Bartlett, Holly Kemberling, Aleksandra D. Eyring, Andrew D. Skora, Brandon S. Luber, Nilofer S. Azad, Dan Laheru, Barbara Biedrzycki, Ross C. Donehower, Atif Zaheer, George A. Fisher, Todd S. Crocenzi, James J. Lee, Steven M. Duffy, Richard M. Goldberg, Albert de la Chapelle, Minori Koshiji, Feriyl Bhaijee, Thomas Huebner, Ralph H. Hruban, Laura D. Wood, Nathan Cuka, Drew M. Pardoll, Nickolas Papadopoulos, Kenneth W. Kinzler, Shibin Zhou, Toby C. Cornish, Janis M. Taube, Robert A. Anders, James R. Eshleman, Bert Vogelstein, and Luis A. Diaz. 2015. "PD-1 Blockade in Tumors with Mismatch-Repair Deficiency - Supplementary Appendix." *The New England Journal of Medicine* 372 (26): 2509–2520.

Lee, Chang-Han H., Gabrielle Romain, Wupeng Yan, Makiko Watanabe, Wissam Charab, Biliana Todorova, Jiwon Lee, Kendra Triplett, Moses Donkor, Oana I Lungu, Anja Lux, Nicholas Marshall, Margaret A. Lindorfer, Odile Richard-Le Goff, Bianca Balbino, Tae Hyun Kang, Hidetaka Tanno, George Delidakis, Corrine Alford, Ronald P. Taylor, Falk Nimmerjahn, Navin Varadarajan, Pierre Bruhns, Yan Jessie Zhang, and George Georgiou. 2017. "IgG Fc Domains That Bind C1q but Not Effector Fcgamma Receptors Delineate the Importance of Complement-Mediated Effector Functions." *Nat Immunol* 18 (8). Nature Publishing Group, a division of Macmillan Publishers Limited. All Rights Reserved.: 889–898.

Lee, Je Hyuk, Evan R. Daugharthy, Jonathan Scheiman, Reza Kalhor, Joyce L. Yang, Thomas C. Ferrante, Richard Terry, Sauveur S. F. Jeanty, Chao Li, Ryoji Amamoto, Derek T. Peters, Brian M. Turczyk, Adam H. Marblestone, Samuel A. Inverso, Amy Bernard, Prashant Mali, Xavier Rios, John Aach, and George M. Church. 2014. "Highly Multiplexed Subcellular RNA Sequencing in Situ." *Science (New York, N.Y.)* 343 (6177): 1360–1363.

Liadi, Ivan, Jason Roszik, Gabrielle Romain, Laurence J. N. Cooper, and Navin Varadarajan. 2013. "Quantitative High-Throughput Single-Cell Cytotoxicity Assay for T Cells." *Journal of Visualized Experiments: JoVE*, no. 72 (February): e50058.

Liadi, Ivan, Harjeet Singh, Gabrielle Romain, Nicolas Rey-Villamizar, Amine Merouane, Jay R T. Adolacion, Partow Kebriaei, Helen Huls, Peng Qiu, Badrinath Roysam, Laurence J. N. Cooper, and Navin Varadarajan. 2015. "Individual Motile CD4(+) T Cells Can Participate in Efficient Multikilling through Conjugation to Multiple Tumor Cells." *Cancer Immunology Research* 3 (5): 473–482.

Lim, Sean H., Stephen A. Beers, Ruth R. French, Peter W. M. Johnson, Martin J. Glennie, and Mark S. Cragg. 2010. "Anti-CD20 Monoclonal Antibodies: Historical and Future Perspectives." *Haematologica* 95 (1): 135–143.

Lim, Wendell A. and Carl H. June. 2017. "The Principles of Engineering Immune Cells to Treat Cancer." *Cell* 168 (4): 724–740.

Linsley, Peter S., Cate Speake, Elizabeth Whalen, and Damien Chaussabel. 2014. "Copy Number Loss of the Interferon Gene Cluster in Melanomas Is Linked to Reduced T Cell Infiltrate and Poor Patient Prognosis." *PLoS ONE* 9 (10).

Liu, Yaoping, Lingqian Zhang, Wengang Wu, Meiping Zhao, and Wei Wang. 2016. "Restraining Non-Specific Adsorption of Protein Using Parylene C-Caulked

Polydimethylsiloxane.” *Biomicrofluidics* 10 (2): 24126.

Long, Eric O., Hun Sik Kim, Dongfang Liu, Mary E. Peterson, and Sumati Rajagopalan. 2013. “Controlling Natural Killer Cell Responses: Integration of Signals for Activation and Inhibition.” *Annual Review of Immunology* 31 (1): 227–258.

Love, Michael I., Wolfgang Huber, and Simon Anders. 2014. “Moderated Estimation of Fold Change and Dispersion for RNA-Seq Data with DESeq2.” *Genome Biology* 15 (12): 1–21.

Lu, Yao, Qiong Xue, Markus R. Eisele, Endah S. Sulistijo, Kara Brower, Lin Han, El-ad David Amir, Dana Pe’er, Kathryn Miller-Jensen, and Rong Fan. 2015. “Highly Multiplexed Profiling of Single-Cell Effector Functions Reveals Deep Functional Heterogeneity in Response to Pathogenic Ligands.” *Proceedings of the National Academy of Sciences of the United States of America* 112 (7): E607-15.

Ma, Chao, Ann F. Cheung, Thinle Chodon, Richard C. Koya, Zhongqi Wu, Charles Ng, Earl Avramis, Alistair J. Cochran, Owen N. Witte, David Baltimore, Bartosz Chmielowski, James S. Economou, Begonya Comin-Anduix, Antoni Ribas, and James R. Heath. 2013. “Multifunctional T-Cell Analyses to Study Response and Progression in Adoptive Cell Transfer Immunotherapy.” *Cancer Discovery* 3 (4): 418–429.

Ma, Chao, Rong Fan, Habib Ahmad, Qihui Shi, Begonya Comin-Anduix, Thinle Chodon, Richard C. Koya, Chao-Chao Liu, Gabriel A. Kwong, Caius G. Radu, Antoni Ribas, and James R. Heath. 2011. “A Clinical Microchip for Evaluation of Single Immune Cells Reveals High Functional Heterogeneity in Phenotypically Similar T Cells.” *Nature Medicine* 17 (6): 738–743.

Ma, Weijie, Barbara M. Gilligan, Jianda Yuan, and Tianhong Li. 2016. “Current Status

and Perspectives in Translational Biomarker Research for PD-1/PD-L1 Immune Checkpoint Blockade Therapy." *Journal of Hematology & Oncology* 9 (1): 47.

Mahata, Bidesh, Xiuwei Zhang, Aleksandra A. Kolodziejczyk, Valentina Proserpio, Liora Haim-Vilmovsky, Angela E. Taylor, Daniel Hebenstreit, Felix A. Dingler, Victoria Moignard, Berthold Göttgens, Wiebke Arlt, Andrew N.J. McKenzie, and Sarah A. Teichmann. 2014. "Single-Cell RNA Sequencing Reveals T Helper Cells Synthesizing Steroids De Novo to Contribute to Immune Homeostasis." *Cell Reports* 7 (4): 1130–1142.

Mahendra, Ankit, Xingyu Yang, Shaza Abnouf, Jay R T. Adolacion, Daechan Park, Sanam Soomro, Jason Roszik, Cristian Coarfa, Gabrielle Romain, Keith Wanzeck, S. Louis Bridges, Amita Aggarwal, Peng Qiu, Sandeep K. Agarwal, Chandra Mohan, and Navin Varadarajan. 2019. "Beyond Autoantibodies: Biologic Roles of Human Autoreactive B Cells in Rheumatoid Arthritis Revealed by RNA-Sequencing." *Arthritis & Rheumatology* 71 (4): 529–541.

Maleki Vareki, Saman, Carmen Garrigós, and Ignacio Duran. 2017. "Biomarkers of Response to PD-1/PD-L1 Inhibition." *Critical Reviews in Oncology/Hematology* 116 (August): 116–124.

Manjarrez-Orduño, Nataly, Laurence C. Menard, Selena Kansal, Paul Fischer, Bijal Kakrecha, Can Jiang, Mark Cunningham, Danielle Greenawalt, Vishal Patel, Minghui Yang, Ryan Golhar, Julie A. Carman, Sergey Lezhnin, Hongyue Dai, Paul S. Kayne, Suzanne J. Suchard, Steven H. Bernstein, and Steven G. Nadler. 2018. "Circulating T Cell Subpopulations Correlate with Immune Responses at the Tumor Site and Clinical Response to PD1 Inhibition in Non-Small Cell Lung Cancer." *Frontiers in Immunology* 9 (AUG): 1–9.

Manne, Jayanthi, Michael J. Mastrangelo, Takami Sato, and David Berd. 2002. “TCR Rearrangement in Lymphocytes Infiltrating Melanoma Metastases After Administration of Autologous Dinitrophenyl-Modified Vaccine.” *The Journal of Immunology* 169 (6): 3407–3412.

Maria, Andrea De, Federica Bozzano, Claudia Cantoni, and Lorenzo Moretta. 2011. “Revisiting Human Natural Killer Cell Subset Function Revealed Cytolytic CD56(Dim)CD16+ NK Cells as Rapid Producers of Abundant IFN-Gamma on Activation.” *Proceedings of the National Academy of Sciences of the United States of America* 108 (2): 728–732.

Marie, Rodolphe, Jason P. Beech, Janos Vörös, Jonas O. Tegenfeldt, and Fredrik Höök. 2006. “Use of PLL-g-PEG in Micro-Fluidic Devices for Localizing Selective and Specific Protein Binding.” *Langmuir : The ACS Journal of Surfaces and Colloids* 22 (24): 10103–10108.

Martinelli, E., R. De Palma, M. Orditura, F. De Vita, and F. Ciardiello. 2009. “Anti-Epidermal Growth Factor Receptor Monoclonal Antibodies in Cancer Therapy.” *Clinical & Experimental Immunology* 158 (1). AIP Publishing LLC: 1–9.

Martinon, Frédéric, Katrin Kaldma, Rein Sikut, Slobodan Čulina, Gabrielle Romain, Mari Tuomela, Maarja Adojaan, Andres Männik, Urve Toots, Toomas Kivisild, Julie Morin, Patricia Brochard, Benoît Delache, Antonella Tripiciano, Fabrizio Ensoli, Ioana Stanescu, Roger Le Grand, and Mart Ustav. 2009. “Persistent Immune Responses Induced by a Human Immunodeficiency Virus DNA Vaccine Delivered in Association with Electroporation in the Skin of Nonhuman Primates.” *Human Gene Therapy* 20 (11): 1291–1307.

Matos, Tiago R., Hongye Liu, and Jerome Ritz. 2017. “Research Techniques Made Simple: Experimental Methodology for Single-Cell Mass Cytometry.” *Journal of Investigative Dermatology* 137 (4): e31–e38.

Matson, Vyara, Jessica Fessler, Riyue Bao, Tara Chongsuwat, Yuanyuan Zha, Maria-Luisa Alegre, Jason J. Luke, and Thomas F. Gajewski. 2018. “The Commensal Microbiome Is Associated with Anti–PD-1 Efficacy in Metastatic Melanoma Patients.” *Science* 359 (6371): 104 LP – 108.

Maude, Shannon L., Noelle Frey, Pamela A. Shaw, Richard Aplenc, David M. Barrett, Nancy J. Bunin, Anne Chew, Vanessa E. Gonzalez, Zhaohui Zheng, Simon F. Lacey, Yolanda D. Mahnke, Jan J. Melenhorst, Susan R. Rheingold, Angela Shen, David T. Teachey, Bruce L. Levine, Carl H. June, David L. Porter, and Stephan A. Grupp. 2014. “Chimeric Antigen Receptor T Cells for Sustained Remissions in Leukemia.” *New England Journal of Medicine* 371 (16): 1507–1517.

Maus, Marcela V. and Carl H. June. 2016. “Making Better Chimeric Antigen Receptors for Adoptive T-Cell Therapy.” *Clinical Cancer Research : An Official Journal of the American Association for Cancer Research* 22 (8): 1875–1884.

McDermott, David F., Jeffrey A. Sosman, Mario Sznol, Christophe Massard, Michael S. Gordon, Omid Hamid, John D. Powderly, Jeffrey R. Infante, Marcella Fassò, Yan V. Wang, Wei Zou, Priti S. Hegde, Gregg D. Fine, and Thomas Powles. 2016. “Atezolizumab, an Anti-Programmed Death-Ligand 1 Antibody, in Metastatic Renal Cell Carcinoma: Long-Term Safety, Clinical Activity, and Immune Correlates from a Phase Ia Study.” *Journal of Clinical Oncology* 34 (8): 833–842.

McGranahan, Nicholas, Andrew J. S. Furness, Rachel Rosenthal, Sofie Ramskov, Rikke

Lyngaa, Sunil Kumar Saini, Mariam Jamal-Hanjani, Gareth A. Wilson, Nicolai J. Birkbak, Crispin T. Hiley, Thomas B. K. Watkins, Seema Shafi, Nirupa Murugaesu, Richard Mitter, Ayse U. Akarca, Joseph Linares, Teresa Marafioti, Jake Y. Henry, Eliezer M. Van Allen, Diana Miao, Bastian Schilling, Dirk Schadendorf, Levi A. Garraway, Vladimir Makarov, Naiyer A. Rizvi, Alexandra Snyder, Matthew D. Hellmann, Taha Merghoub, Jedd D. Wolchok, Sachet A. Shukla, Catherine J. Wu, Karl S. Peggs, Timothy A. Chan, Sine R. Hadrup, Sergio A. Quezada, and Charles Swanton. 2016. “Clonal Neoantigens Elicit T Cell Immunoreactivity and Sensitivity to Immune Checkpoint Blockade.” *Science (New York, N.Y.)* 351 (6280): 1463–1469.

Mellis, Ian A., Rohit Gupte, Arjun Raj, and Sara H. Rouhanifard. 2017. “Visualizing Adenosine-to-Inosine RNA Editing in Single Mammalian Cells.” *Nature Methods* 14 (8): 801–804.

Mellman, Ira, Jeong M. Kim, Marcus J. Taylor, Dibyendu K. Sasmal, Ronald D. Vale, Jeanne Cheung, Xiaolei Su, Enfu Hui, Jun Huang, Jing Zhu, and Heidi A. Wallweber. 2017. “T Cell Costimulatory Receptor CD28 Is a Primary Target for PD-1–Mediated Inhibition.” *Science*.

Mempel, Thorsten R. 2010. “Single-Cell Analysis of Cytotoxic T Cell Function by Intravital Multiphoton Microscopy.” *Methods in Molecular Biology (Clifton, N.J.)* 616: 181–192.

Menzin, Joseph, Kathleen Lang, Craig C. Earle, Donna Kerney, and Rajiv Mallick. 2002. “The Outcomes and Costs of Acute Myeloid Leukemia Among the Elderly.” *Archives of Internal Medicine* 162 (14): 1597.

Merico, Daniele, Ruth Isserlin, Oliver Stueker, Andrew Emili, and Gary D. Bader. 2010.

"Enrichment Map: A Network-Based Method for Gene-Set Enrichment Visualization and Interpretation." *PLoS ONE* 5 (11).

Mertz, Kirsten D., Ton N. Schumacher, Marcel Trefny, Christoph Hess, Didier Lardinois, Alfred Zippelius, Vaios Karanikas, Jonathan Hanhart, Petra Herzig, Christian Klein, Daniela S. Thommen, Sarah Dimeloe, Catherine Schill, Andreas Roller, Ping-Chih Ho, Anna Kiialainen, Mark Wiese, Viktor H. Koelzer, and Spasenija Savic Prince. 2018. "A Transcriptionally and Functionally Distinct PD-1+ CD8+ T Cell Pool with Predictive Potential in Non-Small-Cell Lung Cancer Treated with PD-1 Blockade." *Nature Medicine* 24 (7): 994–1004.

Moffitt, Jeffrey R., Junjie Hao, Guiping Wang, Kok Hao Chen, Hazen P. Babcock, and Xiaowei Zhuang. 2016. "High-Throughput Single-Cell Gene-Expression Profiling with Multiplexed Error-Robust Fluorescence in Situ Hybridization." *Proceedings of the National Academy of Sciences of the United States of America* 113 (39): 11046–11051.

Mootha, Vamsi K., Cecilia M. Lindgren, Karl-Fredrik Eriksson, Aravind Subramanian, Smita Sihag, Joseph Lehar, Pere Puigserver, Emma Carlsson, Martin Ridderstrale, Esa Laurila, Nicholas Houstis, Mark J. Daly, Nick Patterson, Jill P. Mesirov, Todd R. Golub, Pablo Tamayo, Bruce Spiegelman, Eric S. Lander, Joel N. Hirschhorn, David Altshuler, and Leif C. Groop. 2003. "PGC-1[Alpha]-Responsive Genes Involved in Oxidative Phosphorylation Are Coordinately Downregulated in Human Diabetes." *Nat Genet* 34 (3): 267–273.

Mortarini, Roberta, Adriano Piris, Andrea Maurichi, Alessandra Molla, Ilaria Bersani, Aldo Bono, Cesare Bartoli, Mario Santinami, Claudia Lombardo, Fernando Ravagnani, Natale Cascinelli, Giorgio Parmiani, and Andrea Anichini. 2003. "Lack of Terminally

Differentiated Tumor-Specific CD8+ T Cells at Tumor Site in Spite of Antitumor Immunity to Self-Antigens in Human Metastatic Melanoma." *Cancer Research* 63 (10): 2535–2545.

Motzer, Robert J., Brian I. Rini, David F. McDermott, Bruce G. Redman, Timothy M. Kuzel, Michael Roger Harrison, Ulka N. Vaishampayan, Harry a Drabkin, Saby George, Theodore F. Logan, Kim Allyson Margolin, Elizabeth R. Plimack, Alexandre M. Lambert, Ian M. Waxman, and Hans J. Hammers. 2015. "Nivolumab for Metastatic Renal Cell Carcinoma: Results of a Randomized Phase II Trial." *Journal of Clinical Oncology* 33 (13): 1430–1437.

Nakai, Katsuya, Mien-Chie Hung, and Hirohito Yamaguchi. 2016. "A Perspective on Anti-EGFR Therapies Targeting Triple-Negative Breast Cancer." *American Journal of Cancer Research* 6 (8): 1609–1623.

Newman, Aaron M., Chih Long Liu, Michael R. Green, Andrew J. Gentles, Weiguo Feng, Yue Xu, Chuong D. Hoang, Maximilian Diehn, and Ash A. Alizadeh. 2015. "Robust Enumeration of Cell Subsets from Tissue Expression Profiles." *Nature Methods* 12 (5): 453–457.

Nicolet, Benoit P., Aurelie Guislain, and Monika C. Wolkers. 2016. "Combined Single-Cell Measurement of Cytokine MRNA and Protein Identifies T Cells with Persistent Effector Function." *The Journal of Immunology* 198 (2): 962–970.

Nie, Shuai, W. Hampton Henley, Scott E. Miller, Huaibin Zhang, Kathryn M. Mayer, Patty J. Dennis, Emily A. Oblath, Jean Pierre Alarie, Yue Wu, Frank G. Oppenheim, Frederic F. Little, Ahmet Z. Uluer, Peidong Wang, J. Michael Ramsey, and David R. Walt. 2014. "An Automated Integrated Platform for Rapid and Sensitive Multiplexed Protein Profiling

Using Human Saliva Samples." *Lab Chip* 14 (6). The Royal Society of Chemistry: 1087–1098.

Nishino, Mizuki, Nikhil H. Ramaiya, Hiroto Hatabu, and F. Stephen Hodi. 2017. "Monitoring Immune-Checkpoint Blockade: Response Evaluation and Biomarker Development." *Nature Reviews Clinical Oncology*, June.

Osińska, Iwona, Katarzyna Popko, and Urszula Demkow. 2014. "Perforin: An Important Player in Immune Response." *Central European Journal of Immunology* 39 (1): 109–115.

Perfetto, Stephen P., Pratip K. Chattopadhyay, and Mario Roederer. 2004. "Seventeen-Colour Flow Cytometry: Unravelling the Immune System." *Nature Reviews. Immunology* 4 (8). Nature Publishing Group: 648.

Peterson, Vanessa M., Kelvin Xi Zhang, Namit Kumar, Jerelyn Wong, Lixia Li, Douglas C. Wilson, Renee Moore, Terrill K. McClanahan, Svetlana Sadekova, and Joel A. Klappenbach. 2017. "Multiplexed Quantification of Proteins and Transcripts in Single Cells." *Nat Biotech* 35 (10): 936–939.

Phillips, Therese, Pauline Simmons, Hector D. Inzunza, John Cogswell, James Novotny, Clive Taylor, and Xiaoling Zhang. 2015. "Development of an Automated PD-L1 Immunohistochemistry (IHC) Assay for Non-Small Cell Lung Cancer." *Applied Immunohistochemistry and Molecular Morphology* 23 (8): 541–549.

Poirion, Olivier B., Xun Zhu, Travers Ching, and Lana Garmire. 2016. "Single-Cell Transcriptomics Bioinformatics and Computational Challenges." *Frontiers in Genetics*.

Poli, Aurélie, Tatiana Michel, Maud Thérésine, Emmanuel Andrès, François Hentges, and Jacques Zimmer. 2009. "CD56bright Natural Killer (NK) Cells: An Important NK Cell Subset." *Immunology* 126 (4): 458–465.

Proserpio, Valentina and Bidesh Mahata. 2016. “Single-Cell Technologies to Study the Immune System.” *Immunology* 147 (2): 133–140.

Qi, Qian, Yi Liu, Yong Cheng, Jacob Glanville, David Zhang, Ji-Yeun Lee, Richard A. Olshen, Cornelia M. Weyand, Scott D. Boyd, and Jörg J. Goronzy. 2014. “Diversity and Clonal Selection in the Human T-Cell Repertoire.” *Proceedings of the National Academy of Sciences of the United States of America* 111 (36): 13139–13144.

Qin, Zhihai, Johannes Schwartzkopff, Felicia Pradera, Thomas Kammertoens, Barbara Seliger, Hanspeter Pircher, and Thomas Blankenstein. 2003. “A Critical Requirement of Interferon Gamma-Mediated Angiostasis for Tumor Rejection by CD8+ T Cells.” *Cancer Research* 63 (14): 4095–4100.

Quandt, Dagmar, Hans Dieter Zucht, Arno Amann, Anne Wulf-Goldenberg, Carl Borrebaeck, Michael Cannarile, Diether Lambrechts, Herbert Oberacher, James Garrett, Tapan Nayak, Michael Kazinski, Charles Massie, Heidi Schwarzenbach, Michele Maio, Robert Prins, Björn Wendik, Richard Hockett, Daniel Enderle, Mikkel Noerholm, Hans Hendriks, Heinz Zwierzina, and Barbara Seliger. 2017. “Implementing Liquid Biopsies into Clinical Decision Making for Cancer Immunotherapy.” *Oncotarget* 8 (29): 48507–48520.

Redmond, David, Asaf Poran, and Olivier Elemento. 2016. “Single-Cell TCRseq: Paired Recovery of Entire T-Cell Alpha and Beta Chain Transcripts in T-Cell Receptors from Single-Cell RNAseq.” *Genome Medicine* 8 (1): 1.

Reefman, Esther, Jason G. Kay, Stephanie M. Wood, Carolin Offenhäuser, Darren L. Brown, Sandrine Roy, Amanda C. Stanley, Pei Ching Low, Anthony P. Manderson, and Jennifer L. Stow. 2010. “Cytokine Secretion Is Distinct from Secretion of Cytotoxic

Granules in NK Cells." *The Journal of Immunology* 184 (9): 4852–4862.

Reimand, Jüri, Ruth Isserlin, Veronique Voisin, Mike Kucera, Christian Tannus-Lopes, Asha Rostamianfar, Lina Wadi, Mona Meyer, Jeff Wong, Changjiang Xu, Daniele Merico, and Gary D. Bader. 2019. "Pathway Enrichment Analysis and Visualization of Omics Data Using g:Profiler, GSEA, Cytoscape and EnrichmentMap." *Nature Protocols* 14 (2): 482–517.

Restifo, Nicholas P., Mark E. Dudley, and Steven A. Rosenberg. 2012. "Adoptive Immunotherapy for Cancer: Harnessing the T Cell Response." *Nature Reviews. Immunology* 12 (4): 269–281.

Restifo, Nicholas P. and Luca Gattinoni. 2013. "Lineage Relationship of Effector and Memory T Cells." *Curr Opin Immunol* 25 (5): 556–563.

Rezvani, Katayoun and Rayne H. Rouce. 2015. "The Application of Natural Killer Cell Immunotherapy for the Treatment of Cancer." *Frontiers in Immunology* 6. Frontiers Media SA.

Rizvi, Naiyer A., Matthew D. Hellmann, Alexandra Snyder, Pia Kvistborg, Vladimir Makarov, Jonathan J. Havel, William Lee, Jianda Yuan, Phillip Wong, Teresa S. Ho, Martin L. Miller, Natasha Rekhtman, Andre L. Moreira, Fawzia Ibrahim, Cameron Bruggeman, Billel Gasmi, Roberta Zappasodi, Yuka Maeda, Chris Sander, Edward B. Garon, Taha Merghoub, Jedd D. Wolchok, Ton N. Schumacher, and Timothy A. Chan. 2015. "Mutational Landscape Determines Sensitivity to PD-1 Blockade in Non–Small Cell Lung Cancer." *Science* 348 (6230): 124–128.

Romain, Gabrielle, Vladimir Senyukov, Nicolas Rey-Villamizar, Amine Merouane, William Kelton, Ivan Liadi, Ankit Mahendra, Wissam Charab, George Georgiou,

Badrinath Roysam, Dean A. Lee, and Navin Varadarajan. 2014. “Antibody Fc Engineering Improves Frequency and Promotes Kinetic Boosting of Serial Killing Mediated by NK Cells.” Edited by Ahlenstiel, Golo. *Blood* 124 (22). Public Library of Science: 3241–3249.

Romee, Rizwan, Maximillian Rosario, Melissa M. Berrien-Elliott, Julia A. Wagner, Brea A. Jewell, Timothy Schappe, Jeffrey W. Leong, Sara Abdel-Latif, Stephanie E. Schneider, Sarah Willey, Carly C. Neal, Liyang Yu, Stephen T. Oh, Yi-Shan Shan Lee, Arend Mulder, Frans Claas, Megan A. Cooper, and Todd A. Fehniger. 2016. “Cytokine-Induced Memory-like Natural Killer Cells Exhibit Enhanced Responses against Myeloid Leukemia.” *Science Translational Medicine* 8 (357): 357ra123.

Rosenberg, Steven A. 2014. “IL-2: The First Effective Immunotherapy for Human Cancer.” *The Journal of Immunology* 192 (12): 5451–5458.

Rosenberg, Steven A., Trinh Hoc-Tran Pham, Richard M. Sherry, Eden C. Payabyab, Mark Raffeld, and Liqiang Xi. 2016. “Circulating Tumor DNA as an Early Indicator of Response to T-Cell Transfer Immunotherapy in Metastatic Melanoma.” *Clinical Cancer Research* 22 (22): 5480–5486.

Routy, Bertrand, Emmanuelle Le Chatelier, Lisa Derosa, Connie P. M. Duong, Maryam Tidjani Alou, Romain Daillère, Aurélie Fluckiger, Meriem Messaoudene, Conrad Rauber, Maria P. Roberti, Marine Fidelle, Caroline Flament, Vichnou Poirier-Colame, Paule Opolon, Christophe Klein, Kristina Iribarren, Laura Mondragón, Nicolas Jacquelot, Bo Qu, Gladys Ferrere, Céline Clémenson, Laura Mezquita, Jordi Remon Masip, Charles Naltet, Solenn Brosseau, Coureche Kaderbhai, Corentin Richard, Hira Rizvi, Florence Levenez, Nathalie Galleron, Benoit Quinquis, Nicolas Pons, Bernhard Ryffel, Véronique Minard-Colin, Patrick Gonin, Jean-Charles Soria, Eric Deutsch, Yohann Loriot, François

Ghiringhelli, Gérard Zalcman, François Goldwasser, Bernard Escudier, Matthew D. Hellmann, Alexander Eggermont, Didier Raoult, Laurence Albiges, Guido Kroemer, and Laurence Zitvogel. 2018. “Gut Microbiome Influences Efficacy of PD-1–Based Immunotherapy against Epithelial Tumors.” *Science* 359 (6371): 91–97.

Roysam, Badrinath, Ying Chen, Ena Ladi, Paul Herzmark, and Ellen Robey. 2008. “Automated 5-D Analysis of Cell Migration and Interaction in the Thymic Cortex from Time-Lapse Sequences of 3-D Multi-Channel Multi-Photon Images.” *Journal of Immunological Methods* 340 (1): 65–80.

Sade-Feldman, Moshe, Keren Yizhak, Stacey L. Bjorgaard, John P. Ray, Carl G. de Boer, Russell W. Jenkins, David J. Lieb, Jonathan H. Chen, Dennie T. Frederick, Michal Barzily-Rokni, Samuel S. Freeman, Alexandre Reuben, Paul J. Hoover, Alexandra-Chloé Villani, Elena Ivanova, Andrew Portell, Patrick H. Lizotte, Amir R. Aref, Jean-Pierre Eliane, Marc R. Hammond, Hans Vitzthum, Shauna M. Blackmon, Bo Li, Vancheswaran Gopalakrishnan, Sangeetha M. Reddy, Zachary A. Cooper, Cloud P. Paweletz, David A. Barbie, Anat Stemmer-Rachamimov, Keith T. Flaherty, Jennifer A. Wargo, Genevieve M. Boland, Ryan J. Sullivan, Gad Getz, and Nir Hacohen. 2018. “Defining T Cell States Associated with Response to Checkpoint Immunotherapy in Melanoma.” *Cell* 175 (4): 998-1013.e20.

Sakamoto, Naoyuki, Takeshi Ishikawa, Satoshi Kokura, Tetsuya Okayama, Kaname Oka, Mitsuko Ideno, Fumiyo Sakai, Akiko Kato, Masashige Tanabe, Tatsuji Enoki, Junichi Mineno, Yuji Naito, Yoshito Itoh, and Toshikazu Yoshikawa. 2015. “Phase I Clinical Trial of Autologous NK Cell Therapy Using Novel Expansion Method in Patients with Advanced Digestive Cancer.” *Journal of Translational Medicine* 13 (1): 277.

Sato, Tohru, Henrik Thorlacius, Brent Johnston, Tracy L. Staton, Wenkai Xiang, Dan R. Littman, and Eugene C. Butcher. 2005. “Role for CXCR6 in Recruitment of Activated CD8+ Lymphocytes to Inflamed Liver.” *The Journal of Immunology* 174 (1): 277–283.

Schneider, Florian, Jan Draheim, Robert Kamberger, and Ulrike Wallrabe. 2009. “Process and Material Properties of Polydimethylsiloxane (PDMS) for Optical MEMS.” *Sensors and Actuators A: Physical* 151 (2): 95–99.

Sendra, Victor G., Anthony Lie, Gabrielle Romain, Sandeep K. Agarwal, and Navin Varadarajan. 2013. “Detection and Isolation of Auto-Reactive Human Antibodies from Primary B Cells.” *Methods* 64 (2): 153–159.

Shah, Sheel, Eric Lubeck, Wen Zhou, and Long Cai. 2016. “In Situ Transcription Profiling of Single Cells Reveals Spatial Organization of Cells in the Mouse Hippocampus.” *Neuron* 92 (2): 342–357.

Shahi, Payam, Samuel C. Kim, John R. Haliburton, Zev J. Gartner, and Adam R. Abate. 2017. “Abseq: Ultrahigh-Throughput Single Cell Protein Profiling with Droplet Microfluidic Barcoding.” *Scientific Reports* 7 (March). The Author(s): 44447.

Shannon, Paul, Andrew Markiel, Owen Ozier, Nitin S. Baliga, Jonathan T. Wang, Daniel Ramage, Nada Amin, Beno Schwikowski, and Trey Ideker. 2003. “Cytoscape: A Software Environment for Integrated Models of Biomolecular Interaction Networks.” *Genome Research* 13 (11): 2498–2504.

Sharma, Padmanee and James P. Allison. 2015a. “The Future of Immune Checkpoint Therapy.” *Science* 348 (6230): 56–61.

Sharma, Padmanee and James P. Allison. 2015b. “Immune Checkpoint Targeting in Cancer Therapy: Toward Combination Strategies with Curative Potential.” *Cell* 161 (2): 205–214.

Sharma, Padmanee, Siwen Hu-Lieskovan, Jennifer A. Wargo, and Antoni Ribas. 2017. “Primary, Adaptive, and Acquired Resistance to Cancer Immunotherapy.” *Cell* 168 (4): 707–723.

Sharpe, Arlene H. and Kristen E. Pauken. 2018. “The Diverse Functions of the PD1 Inhibitory Pathway.” *Nature Reviews Immunology* 18 (3): 153–167.

Shenghui, Zhang, Han Yixiang, Wu Jianbo, Yu Kang, Bi Laixi, Zhuang Yan, and Xu Xi. 2011. “Elevated Frequencies of CD4+CD25+CD127lo Regulatory T Cells Is Associated to Poor Prognosis in Patients with Acute Myeloid Leukemia.” *International Journal of Cancer* 129 (6): 1373–1381.

Shore, Neal D. 2015. “Advances in the Understanding of Cancer Immunotherapy.” *BJU International* 116 (3): 321–329.

Simon, Sylvain and Nathalie Labarriere. 2017. “PD-1 Expression on Tumor-Specific T Cells: Friend or Foe for Immunotherapy?” *OncoImmunology* 7 (1). Taylor & Francis: 1–7.

Singh, Puneet, Paul de Souza, Kieran F. Scott, Bruce M. Hall, Nirupama D. Verma, Therese M. Becker, James W. T. Toh, Mila Sajinovic, and Kevin J. Spring. 2019. “Biomarkers in Immune Checkpoint Inhibition Therapy for Cancer Patients: What Is the Role of Lymphocyte Subsets and PD1/PD-L1?” *Translational Medicine Communications* 4 (1). Translational Medicine Communications: 1–13.

Somanchi, Srinivas S., Vladimir V. Senyukov, Cecele J. Denman, and Dean A. Lee. 2011. “Expansion, Purification, and Functional Assessment of Human Peripheral Blood NK Cells.” *J Vis Exp*, no. 48. MyJove Corporation: 2540.

Son, Kyung Jin, Ali Rahimian, Dong-Sik Shin, Christian Siltanen, Tushar Patel, and Alexander Revzin. 2016. “Microfluidic Compartments with Sensing Microbeads for

Dynamic Monitoring of Cytokine and Exosome Release from Single Cells.” *The Analyst* 141 (2): 679–688.

Spitzer, Matthew H., Yaron Carmi, Nathan E. Reticker-Flynn, Serena S. Kwek, Deepthi Madhireddy, Maria M. Martins, Pier Federico Gherardini, Tyler R. Prestwood, Jonathan Chabon, Sean C. Bendall, Lawrence Fong, Garry P. Nolan, and Edgar G. Engleman. 2017. “Systemic Immunity Is Required for Effective Cancer Immunotherapy.” *Cell* 168 (3): 487-502.e15.

Spitzer, Matthew H. and Garry P. Nolan. 2016. “Mass Cytometry: Single Cells, Many Features.” *Cell* 165 (4): 780–791.

Spranger, Stefani, Riyue Bao, and Thomas F. Gajewski. 2015. “Melanoma-Intrinsic β-Catenin Signalling Prevents Anti-Tumour Immunity.” *Nature* 523 (7559): 231–235.

Stahl, Maximilian, Michelle DeVeaux, Pau Montesinos, Raphael Itzykson, Ellen K. Ritchie, Mikkael A. Sekeres, John D. Barnard, Nikolai A. Podoltsev, Andrew M. Brunner, Rami S. Komrokji, Vijaya R. Bhatt, Aref Al-Kali, Thomas Cluzeau, Valeria Santini, Amir T. Fathi, Gail J. Roboz, Pierre Fenaux, Mark R. Litzow, Sarah Perreault, Tae Kon Kim, Thomas Prebet, Norbert Vey, Vivek Verma, Ulrich Germing, Juan Miguel Bergua, Josefina Serrano, Steven D. Gore, and Amer M. Zeidan. 2018. “Hypomethylating Agents in Relapsed and Refractory AML: Outcomes and Their Predictors in a Large International Patient Cohort.” *Blood Advances* 2 (8): 923–932.

Stoeckius, Marlon, Christoph Hafemeister, William Stephenson, Brian Houck-Loomis, Pratip K Chattopadhyay, Harold Swerdlow, Rahul Satija, and Peter Smibert. 2017. “Simultaneous Epitope and Transcriptome Measurement in Single Cells.” *Nat Meth* 14 (9). Nature Publishing Group, a division of Macmillan Publishers Limited. All Rights

Reserved.: 865–868.

Stubbington, Michael J. T., Tapio Lonnberg, Valentina Proserpio, Simon Clare, Anneliese O. Speak, Gordon Dougan, and Sarah A. Teichmann. 2016. “T Cell Fate and Clonality Inference from Single-Cell Transcriptomes.” *Nat Meth* 13 (4). Nature Publishing Group, a division of Macmillan Publishers Limited. All Rights Reserved.: 329–332.

Su, Yapeng, Qihui Shi, and Wei Wei. 2017. “Single Cell Proteomics in Biomedicine: High-Dimensional Data Acquisition, Visualization, and Analysis.” *Proteomics* 17 (3–4): 1600267.

Subramanian, Aravind, Pablo Tamayo, Vamsi K. Mootha, Sayan Mukherjee, Benjamin L. Ebert, Michael A Gillette, Amanda Paulovich, Scott L. Pomeroy, Todd R. Golub, Eric S. Lander, and Jill P. Mesirov. 2005. “Gene Set Enrichment Analysis: A Knowledge-Based Approach for Interpreting Genome-Wide Expression Profiles.” *Proceedings of the National Academy of Sciences* 102 (43): 15545–15550.

Szczepanski, Miroslaw J., Marta Szajnik, Malgorzata Czystowska, Magis Mandapathil, Laura Strauss, Ann Welsh, Kenneth A. Foon, Theresa L. Whiteside, and Michael Boyiadzis. 2009. “Increased Frequency and Suppression by Regulatory T Cells in Patients with Acute Myelogenous Leukemia.” *Clinical Cancer Research* 15 (10): 3325–3332.

Tang, J., A. Shalabi, and V. M. Hubbard-Lucey. 2018. “Comprehensive Analysis of the Clinical Immuno-Oncology Landscape.” *Annals of Oncology* 29 (1): 84–91.

Tang, Jun, Jia Xin Yu, Vanessa M. Hubbard-Lucey, Svetoslav T. Neftelinov, Jeffrey P. Hodge, and Yunqing Lin. 2018. “The Clinical Trial Landscape for PD1/PDl1 Immune Checkpoint Inhibitors.” *Nature Reviews Drug Discovery* 17 (12). Nature Publishing Group: 854–855.

Tentori, Augusto M., Kevin A. Yamauchi, and Amy E. Herr. 2016. “Detection of Isoforms Differing by a Single Charge Unit in Individual Cells.” *Angewandte Chemie International Edition* 55 (40): 12431–12435.

Thommen, Daniela S. and Ton N. Schumacher. 2018. “T Cell Dysfunction in Cancer.” *Cancer Cell* 33 (4). Elsevier Inc.: 547–562.

Tirosh, Itay, Benjamin Izar, Sanjay M. Prakadan, Marc H. Wadsworth, Daniel Treacy, John J. Trombetta, Asaf Rotem, Christopher Rodman, Christine Lian, George Murphy, Mohammad Fallahi-Sichani, Ken Dutton-Regester, Jia-Ren Lin, Ofir Cohen, Parin Shah, Diana Lu, Alex S. Genshaft, Travis K. Hughes, Carly G K. Ziegler, Samuel W. Kazer, Aleth Gaillard, Kellie E. Kolb, Alexandra-Chloé Villani, Cory M. Johannessen, Aleksandr Y. Andreev, Eliezer M. Van Allen, Monica Bertagnolli, Peter K. Sorger, Ryan J. Sullivan, Keith T. Flaherty, Dennie T. Frederick, Judit Jané-Valbuena, Charles H. Yoon, Orit Rozenblatt-Rosen, Alex K. Shalek, Aviv Regev, and Levi A. Garraway. 2016. “Dissecting the Multicellular Ecosystem of Metastatic Melanoma by Single-Cell RNA-Seq.” *Science* 352 (6282): 189 LP – 196.

Topalian, Suzanne L., Charles G. Drake, and Drew M. Pardoll. 2015. “Immune Checkpoint Blockade: A Common Denominator Approach to Cancer Therapy.” *Cancer Cell* 27 (4). Elsevier Inc.: 450–461.

Topalian, Suzanne L., F. Stephen Hodi, Julie R. Brahmer, Scott N. Gettinger, David C. Smith, David F. McDermott, John D. Powderly, Richard D. Carvajal, Jeffrey A. Sosman, Michael B. Atkins, Philip D. Leming, David R. Spigel, Scott J. Antonia, Leora Horn, Charles G. Drake, Drew M. Pardoll, Lieping Chen, William H. Sharfman, Robert A. Anders, Janis M. Taube, Tracee L. McMiller, Haiying Xu, Alan J. Korman, Maria Jure-

Kunkel, Shruti Agrawal, Daniel McDonald, Georgia D. Kollia, Ashok Gupta, Jon M. Wigginton, and Mario Sznol. 2012. “Safety, Activity, and Immune Correlates of Anti–PD-1 Antibody in Cancer.” *New England Journal of Medicine* 366 (26). Massachusetts Medical Society: 2443–2454.

Topalian, Suzanne L., Janis M. Taube, Robert A. Anders, and Drew M. Pardoll. 2016. “Mechanism-Driven Biomarkers to Guide Immune Checkpoint Blockade in Cancer Therapy.” *Nat Rev Cancer* 16 (5). Nature Publishing Group, a division of Macmillan Publishers Limited. All Rights Reserved.: 275–287.

Torres, Alexis J., Abby S. Hill, and J. Christopher Love. 2014. “Nanowell-Based Immunoassays for Measuring Single-Cell Secretion: Characterization of Transport and Surface Binding.” *Analytical Chemistry* 86 (23): 11562–11569.

Tricot, Sabine, Mickael Meyrand, Chiara Sammicheli, Jamila Elhmouzi-Younes, Aurélien Corneau, Sylvie Bertholet, Marie Malissen, Roger Le Grand, Sandra Nuti, Hervé Luche, and Antonio Cosma. 2015. “Evaluating the Efficiency of Isotope Transmission for Improved Panel Design and a Comparison of the Detection Sensitivities of Mass Cytometer Instruments.” *Cytometry Part A* 87 (4): 357–368.

Tsai, Hwei Fang and Ping Ning Hsu. 2017. “Cancer Immunotherapy by Targeting Immune Checkpoints: Mechanism of T Cell Dysfunction in Cancer Immunity and New Therapeutic Targets John T Kung.” *Journal of Biomedical Science* 24 (1): 35.

Tumeh, Paul C., Christina L. Harview, Jennifer H. Yearley, I. Peter Shintaku, Emma J.M. M Taylor, Lidia Robert, Bartosz Chmielowski, Marko Spasic, Gina Henry, Voicu Ciobanu, Alisha N. West, Manuel Carmona, Christine Kivork, Elizabeth Seja, Grace Cherry, Antonio J. Gutierrez, Tristan R. Grogan, Christine Mateus, Gorana Tomasic, John A.

Glaspy, Ryan O. Emerson, Harlan Robins, Robert H. Pierce, David A. Elashoff, Caroline Robert, and Antoni Ribas. 2014. “PD-1 Blockade Induces Responses by Inhibiting Adaptive Immune Resistance.” *Nature* 515 (7528). Nature Publishing Group, a division of Macmillan Publishers Limited. All Rights Reserved.: 568–571.

Turtle, Cameron J., Laïla-Aïcha Hanafi, Carolina Berger, Theodore A. Gooley, Sindhu Cherian, Michael Hudecek, Daniel Sommermeyer, Katherine Melville, Barbara Pender, Tanya M. Budiarto, Emily Robinson, Natalia N. Steevens, Colette Chaney, Lorinda Soma, Xueyan Chen, Cecilia Yeung, Brent Wood, Daniel Li, Jianhong Cao, Shelly Heimfeld, Michael C. Jensen, Stanley R. Riddell, and David G. Maloney. 2016. “CD19 CAR-T Cells of Defined CD4+:CD8+ Composition in Adult B Cell ALL Patients.” *The Journal of Clinical Investigation* 126 (6): 2123–2138.

Vallejos, Catalina A., Davide Risso, Antonio Scialdone, Sandrine Dudoit, and John C. Marioni. 2017. “Normalizing Single-Cell RNA Sequencing Data: Challenges and Opportunities.” *Nat Meth* 14 (6). Nature Publishing Group, a division of Macmillan Publishers Limited. All Rights Reserved.: 565–571.

Varadarajan, Navin, Douglas S. Kwon, Kenneth M. Law, Adebola O. Ogunniyi, Melis N. Anahtar, James M. Richter, Bruce D. Walker, and J. Christopher Love. 2012. “Rapid, Efficient Functional Characterization and Recovery of HIV-Specific Human CD8+ T Cells Using Microengraving.” *Proc Natl Acad Sci U S A* 109 (10): 3885–3890.

Vasaturo, Angela, Altuna Halilovic, Kalijn F. Bol, Dagmar I. Verweij, Willeke A. M. Blokx, Cornelis J. A. Punt, Patricia J. T. A. Groenen, J. Han J. M. van Krieken, Johannes Textor, I. Jolanda M. de Vries, and Carl G. Figdor. 2016. “T-Cell Landscape in a Primary Melanoma Predicts the Survival of Patients with Metastatic Disease after Their Treatment

with Dendritic Cell Vaccines." *Cancer Research* 76 (12): 3496–3506.

Vivier, Eric, David H. Raulet, Alessandro Moretta, Michael A. Caligiuri, Laurence Zitvogel, Lewis L. Lanier, Wayne M. Yokoyama, and Sophie Ugolini. 2011. "Innate or Adaptive Immunity? The Example of Natural Killer Cells." *Science (New York, N.Y.)* 331 (6013): 44–49.

Walsh, Matthew J, Jennifer E Dodd, and Guillaume M Hautbergue. 2013. "Ribosome-Inactivating Proteins: Potent Poisons and Molecular Tools." *Virulence* 4 (8). AIP Publishing LLC: 774–784.

Wang, Bo, Junjie Zhu, Emma Pierson, Daniele Ramazzotti, and Serafim Batzoglou. 2017. "Visualization and Analysis of Single-Cell RNA-Seq Data by Kernel-Based Similarity Learning." *Nature Methods* 14 (4): 414–416.

Wang, Xingbing, Jine Zheng, Jun Liu, Junxia Yao, Yanli He, Xiaoqing Li, Jingming Yu, Jing Yang, Zhongping Liu, and Shiang Huang. 2005. "Increased Population of CD4(+)CD25(High), Regulatory T Cells with Their Higher Apoptotic and Proliferating Status in Peripheral Blood of Acute Myeloid Leukemia Patients." *European Journal of Haematology* 75 (6): 468–476.

Weber, Jeffrey S., David M. Berman, F. Stephen Hodi, Caroline Robert, Tai-Tsang Chen, Omid Hamid, Kim Margolin, Jedd D. Wolchok, Dirk Schadendorf, and Debra Patt. 2015. "Pooled Analysis of Long-Term Survival Data From Phase II and Phase III Trials of Ipilimumab in Unresectable or Metastatic Melanoma." *Journal of Clinical Oncology* 33 (17): 1889–1894.

Wei, Spencer C., Colm R. Duffy, and James P. Allison. 2018. "Fundamental Mechanisms of Immune Checkpoint Blockade Therapy." *Cancer Discovery* 8 (9): 1069–1086.

Wei, Spencer C., Jacob H. Levine, Alexandria P. Cogdill, Yang Zhao, Nana Ama A.S. Anang, Miles C. Andrews, Padmanee Sharma, Jing Wang, Jennifer A. Wargo, Dana Pe'er, and James P. Allison. 2017. "Distinct Cellular Mechanisms Underlie Anti-CTLA-4 and Anti-PD-1 Checkpoint Blockade." *Cell* 170 (6): 1120-1133.e17.

Wei, Wei, Young Shik Shin, Min Xue, Tomoo Matsutani, Kenta Masui, Huijun Yang, Shiro Ikegami, Yuchao Gu, Ken Herrmann, Dazy Johnson, Xiangming Ding, Kiwook Hwang, Jungwoo Kim, Jian Zhou, Yapeng Su, Xinmin Li, Bruno Bonetti, Rajesh Chopra, C. David James, Webster K. Cavenee, Timothy F. Cloughesy, Paul S. Mischel, James R. Heath, and Beatrice Gini. 2016. "Single-Cell Phosphoproteomics Resolves Adaptive Signaling Dynamics and Informs Targeted Combination Therapy in Glioblastoma." *Cancer Cell* 29 (4): 563–573.

Willhauck, Martina, Carmen Scheibenbogen, Michael Pawlita, Thomas Möhler, Eckhard Thiel, and Ulrich Keilholz. 2003. "Restricted T-Cell Receptor Repertoire in Melanoma Metastases Regressing after Cytokine Therapy." *Cancer Research* 63 (13): 3483–3485.

Williams, Patrick, Sreyashi Basu, Guillermo Garcia-Manero, Christopher S. Hourigan, Karolyn A. Oetjen, Jorge E. Cortes, Farhad Ravandi, Elias J. Jabbour, Zainab Al-Hamal, Marina Konopleva, Jing Ning, Lianchun Xiao, Juliana Hidalgo Lopez, Steve M. Kornblau, Michael Andreeff, Wilmer Flores, Carlos Bueso-Ramos, Jorge Blando, Pallavi Galera, Katherine R. Calvo, Gheath Al-Atrash, James P. Allison, Hagop M. Kantarjian, Padmanee Sharma, and Naval G. Daver. 2018. "The Distribution of T-Cell Subsets and the Expression of Immune Checkpoint Receptors and Ligands in Patients with Newly Diagnosed and Relapsed Acute Myeloid Leukemia." *Cancer*, November, 1–4.

Wong, Ieong and Chih Ming Ho. 2009. "Surface Molecular Property Modifications for

Poly(Dimethylsiloxane) (PDMS) Based Microfluidic Devices." *Microfluidics and Nanofluidics* 7 (3): 291–306.

Wu, Angela R., Jianbin Wang, Aaron M. Streets, and Yanyi Huang. 2017. "Single-Cell Transcriptional Analysis." *Annual Review of Analytical Chemistry*, no. 0. Annual Reviews 4139 El Camino Way, PO Box 10139, Palo Alto, California 94303-0139, USA.

Wu, Peng, Thomas E. Nielsen, and Mads H. Clausen. 2015. "FDA-Approved Small-Molecule Kinase Inhibitors." *Trends in Pharmacological Sciences* 36 (7): 422–439.

Yan, Yiyi, Siyu Cao, Xin Liu, Susan M. Harrington, Wendy E. Bindeman, Alex A. Adjei, Jin Sung Jang, Jin Jen, Ying Li, Pritha Chanana, Aaron S. Mansfield, Sean S. Park, Svetomir N. Markovic, Roxana S. Dronca, and Haidong Dong. 2018. "CX3CR1 Identifies PD-1 Therapy–Responsive CD8+ T Cells That Withstand Chemotherapy during Cancer Chemoimmunotherapy." *JCI Insight* 3 (8): e97828.

Yang, Liu, Zhihua Wang, Yuliang Deng, Yan Li, Wei Wei, and Qihui Shi. 2016. "Single-Cell, Multiplexed Protein Detection of Rare Tumor Cells Based on a Beads-on-Barcode Antibody Microarray." *Analytical Chemistry* 88 (22). American Chemical Society: 11077–11083.

Yarchoan, Mark, Alexander Hopkins, and Elizabeth M. Jaffee. 2017. "Tumor Mutational Burden and Response Rate to PD-1 Inhibition." *New England Journal of Medicine* 377 (25): 2500–2501.

Yi, Ming, Shuang Qin, Weiheng Zhao, Shengnan Yu, Qian Chu, and Kongming Wu. 2018. "The Role of Neoantigen in Immune Checkpoint Blockade Therapy." *Experimental Hematology and Oncology* 7 (1). BioMed Central: 1–11.

Yu, Shengnan, Anping Li, Qian Liu, Tengfei Li, Xun Yuan, Xinwei Han, and Kongming

Wu. 2017. “Chimeric Antigen Receptor T Cells: A Novel Therapy for Solid Tumors.” *Journal of Hematology & Oncology* 10 (1): 78.

Yu, Xiaoling, Junzhu Xiao, and Fuquan Dang. 2015. “Surface Modification of Poly(Dimethylsiloxane) Using Ionic Complementary Peptides to Minimize Nonspecific Protein Adsorption.” *Langmuir* 31 (21). American Chemical Society: 5891–5898.

Zaidi, M. Raza and Glenn Merlino. 2011. “The Two Faces of Interferon-γ in Cancer.” *Clinical Cancer Research : An Official Journal of the American Association for Cancer Research* 17 (19): 6118–6124.

Zaretsky, Irina, Michal Polonsky, Eric Shifrut, Shlomit Reich-Zeliger, Yaron Antebi, Guy Aidelberg, Nir Waysbort, and Nir Friedman. 2012. “Monitoring the Dynamics of Primary T Cell Activation and Differentiation Using Long Term Live Cell Imaging in Microwell Arrays.” *Lab Chip* 12 (23): 5007–5015.

Zaretsky, J M, A Garcia-Diaz, D S Shin, H Escuin-Ordinas, W Hugo, S Hu-Lieskovan, D Y Torrejon, G Abril-Rodriguez, S Sandoval, L Barthly, J Saco, B Homet Moreno, R Mezzadra, B Chmielowski, K Ruchalski, I P Shintaku, P J Sanchez, C Puig-Saus, G Cherry, E Seja, X Kong, J Pang, B Berent-Maoz, B Comin-Anduix, T G Graeber, P C Tumeh, T N Schumacher, R S Lo, and A Ribas. 2016. “Mutations Associated with Acquired Resistance to PD-1 Blockade in Melanoma.” *N Engl J Med* 375 (9): 819–829.

Zarour, Hassane M. 2016. “Reversing T-Cell Dysfunction and Exhaustion in Cancer.” *Clinical Cancer Research* 22 (8): 1856–1864.

Zhang, Chao, Peter Hirth, Gideon Bollag, Keith Nolop, James Tsai, Jiazhong Zhang, and Prabha Ibrahim. 2012. “Vemurafenib: The First Drug Approved for BRAF-Mutant Cancer.” *Nature Reviews Drug Discovery* 11 (11): 873–886.

Zhang, Lei, Xin Yu, Liangtao Zheng, Yuanyuan Zhang, Yansen Li, Qiao Fang, Ranran Gao, Boxi Kang, Qiming Zhang, Julie Y. Huang, Hiroyasu Konno, Xinyi Guo, Yingjiang Ye, Songyuan Gao, Shan Wang, Xueda Hu, Xianwen Ren, Zhanlong Shen, Wenjun Ouyang, and Zemin Zhang. 2018. “Lineage Tracking Reveals Dynamic Relationships of T Cells in Colorectal Cancer.” *Nature* 564 (7735): 268–272.

Zhao, Junfei, Andrew X. Chen, Robyn D. Gartrell, Andrew M. Silverman, Luis Aparicio, Tim Chu, Darius Bordbar, David Shan, Jorge Samanamud, Aayushi Mahajan, Ioan Filip, Rose Orenbuch, Morgan Goetz, Jonathan T. Yamaguchi, Michael Cloney, Craig Horbinski, Rimas V. Lukas, Jeffrey Raizer, Ali I. Rae, Jinzhou Yuan, Peter Canoll, Jeffrey N. Bruce, Yvonne M. Saenger, Peter Sims, Fabio M. Iwamoto, Adam M. Sonabend, and Raul Rabadan. 2019. “Immune and Genomic Correlates of Response to Anti-PD-1 Immunotherapy in Glioblastoma.” *Nature Medicine* 25 (3): 462–469.

Zheng, Chunhong, Liangtao Zheng, Jae-Kwang Yoo, Huahu Guo, Yuanyuan Zhang, Xinyi Guo, Boxi Kang, Ruozhen Hu, Julie Y. Huang, Qiming Zhang, Zhouzerui Liu, Minghui Dong, Xueda Hu, Wenjun Ouyang, Jirun Peng, and Zemin Zhang. 2017. “Landscape of Infiltrating T Cells in Liver Cancer Revealed by Single-Cell Sequencing.” *Cell* 169 (7): 1342-1356.e16.

Zhou, Jing, Alaina Kaiser, Colin Ng, Rachel Karcher, Tim McConnell, Patrick Paczkowski, Cristina Fernandez, Min Zhang, Sean Mackay, and Moriya Tsuji. 2017. “CD8+ T-Cell Mediated Anti-Malaria Protection Induced by Malaria Vaccines; Assessment of Hepatic CD8+ T Cells by SCBC Assay.” *Human Vaccines and Immunotherapeutics* 13 (7). Taylor & Francis: 1625–1629.

Zhou, Qing, Meghan E. Munger, Rachelle G. Veenstra, Brenda J. Weigel, Mitsuomi

Hirashima, David H. Munn, William J. Murphy, Miyuki Azuma, Ana C. Anderson, Vijay K. Kuchroo, and Bruce R. Blazar. 2011. “Coexpression of Tim-3 and PD-1 Identifies a CD8+ T-Cell Exhaustion Phenotype in Mice with Disseminated Acute Myelogenous Leukemia.” *Blood* 117 (17): 4501–4510.

Zitvogel, Laurence, Lorenzo Galluzzi, Mark J. Smyth, and Guido Kroemer. 2013. “Mechanism of Action of Conventional and Targeted Anticancer Therapies: Reinstating Immunosurveillance.” *Immunity* 39 (1): 74–88.